AD-A188 792 SELF-BORING PRESSUREMETER IN PLUVIALLY DEPOSITED SANDS (U) CENTRO DI RICERCA IDRAULICA E STRUTTURALE MILAN (ITALY) R BELLOTTI ET AL. JUN 87 DAJA45-84-C-0034 1/2

UNCLASSIFIED F/G 14/2 NL

1.0
1.1
1.25
1.4
1.6
1.8
2.0

SELF-BORING PRESSUREMETER IN PLUVIALLY DEPOSITED SANDS

Final Technical Report

by

R. Bellotti, V. Crippa, V.N. Ghionna, M. Jamiolkowski

and P.K. Robertson

June 1987

United States Army

EUROPEAN RESEARCH OFFICE OF THE U.S. ARMY

London England

CONTRACT NUMBER DAJA45-84-C-0034

ENEL CRIS - MILAN (ITALY)

UNCLASSIFIED

SECURITY CLASSIFICATION OF THIS PAGE (When Data Entered)

REPORT DOCUMENTATION PAGE		READ INSTRUCTIONS BEFORE COMPLETING FORM
1. REPORT NUMBER	2. GOVT ACCESSION NO.	3. RECIPIENT'S CATALOG NUMBER
4. TITLE (and Subtitle) SELF-BORING PRESSUREMETER IN PLUVIALLY DEPOSITED SANDS		5. TYPE OF REPORT & PERIOD COVERED FINAL TECHNICAL REPORT Aug 84 - Aug 87
		6. PERFORMING ORG. REPORT NUMBER BELLOTTI
7. AUTHOR(s) R. Bellotti, V. Crippa, V.N. Ghionna, M. Jamiolkowski, and P.K. Robertson		8. CONTRACT OR GRANT NUMBER(s) DAJA 45-84-C-0034 BELLOTTI
9. PERFORMING ORGANIZATION NAME AND ADDRESS ENEL-CRIS Via Ornato, 90/14 20162 - MILANO (ITALY)		10. PROGRAM ELEMENT, PROJECT, TASK AREA & WORK UNIT NUMBERS 61102A 1L161102BH57EN-01
11. CONTROLLING OFFICE NAME AND ADDRESS USARDSG (UK) Box 65. FPO NY 09510 1500		12. REPORT DATE June 1987
		13. NUMBER OF PAGES 33
14. MONITORING AGENCY NAME & ADDRESS (if different from Controlling Office)		15. SECURITY CLASS. (of this report) UNCLASSIFIED
		15a. DECLASSIFICATION/DOWNGRADING SCHEDULE

16. DISTRIBUTION STATEMENT (of this Report)

Approved for Public Release Distribution Unlimited

17. DISTRIBUTION STATEMENT (of the abstract entered in Block 20, if different from Report)

18. SUPPLEMENTARY NOTES

19. KEY WORDS (Continue on reverse side if necessary and identify by block number)

Self-boring pressuremeter, Sands, Initial in-situ horizontal stress, Shear modulus, Shear Strength, Limit Pressure, Calibration Chamber

20. ABSTRACT (Continue on reverse side if necessary and identify by block number)

This report presents the results of 47 self-boring pressuremeter (SBP) tests performed under strictly controlled boundary conditions on pluvially deposited Ticino and Hokksund sand samples in the Calibration Chamber existing at ENEL-CRIS (Milan-Italy): N°25 tests were performed with the probe in place during sample preparation and N°22 with the probe self-bored into saturated sand.

DD FORM 1 JAN 73 1473 EDITION OF 1 NOV 65 IS OBSOLETE

Unclassified

SECURITY CLASSIFICATION OF THIS PAGE (When Data Entered)

20. The purpose of the testing was to evaluate the performance of the self-boring pressuremeter and to critically review existing interpretation methods of SBPT in sand.

Accession For		
NTIS GRA&I	☑	
DTIC TAB	☐	
Unannounced	☐	
Justification		
By		
Distribution/		
Availability Codes		
Dist	Avail and/or Special	
A-1		

TABLE OF CONTENTS

LIST OF TABLES

LIST OF FIGURES

LIST OF APPENDIXES

1. INTRODUCTION

This report presents the results of 47 self-boring pressuremeter tests (SBPT's) performed in the ENEL-CRIS(*) calibration chamber (CC). The tests were performed in dry and saturated Ticino and Hokksund sand. Pressuremeter tests were performed with the probe in-place during sample preparation ("ideal installation") and with the probe self-bored into the saturated sand.
The purpose of the testing was to evaluate the performance of the self-boring pressuremeter (SBP) probe under strictly controlled laboratory conditions and to critically review existing interpretation methods of the SBPT in sands. The SBP probe used in the study was the Camkometer Mark VIII manufactured by Cambridge In-situ Ltd., England.

2. TEST EQUIPMENT

2.1. Calibration Chamber (CC)

The ENEL-CRIS calibration chamber was designed to calibrate and evaluate different in-situ testing devices in sands under strictly controlled boundary conditions.
A complete description of the chamber is given by Bellotti et al. (1982). The equipment consists of a double wall chamber, a loading frame, a mass sand spreader for sand deposition and a saturation system. The chamber can test a cylindrical sample of sand 1.2 m (3.9 feet) in diameter and 1.5 m (4.9 feet) in height.
A schematic cross-section of the ENEL-CRIS calibration chamber is shown in Figure 1.
The sample is confined laterally with a flexible rubber membrane surrounded by water through which the horizontal stresses are applied. The bottom of the sample is supported on a water filled cushion resting on a rigid steel piston.
The vertical confining stress is applied through the water filled base cushion and vertical deflection of the sample is controlled by the movement of the base steel piston. The top of the sample is confined by a rigid top plate and fixed beam.
The double-walled chamber allows the application of a zero average lateral strain boundary condition to the test sample by maintaining the pressure in the double-wall cavity equal to the lateral pressure acting on the sample membrane.

(*) ENEL - CRIS: Italian National Electricity Board - Hydraulic and Structural Research Center.

The axial and lateral confining pressures can be varied independently so that the ratio of the applied horizontal stress (σ_h) to the vertical stress (σ_v) can be maintained at any desired value.
A schematic cross-section of the CC loading system is shown in Figure 2.

2.2. Self-boring Pressuremeter

The SBP probe used in the study was the Camkometer Mark VIII manufactured by Cambridge In-Situ Ltd., England. A schematic outline of the SBP probe is given in Figure 3.
The SBP probe is essentially a thick walled steel cylinder with a flexible membrane attached to the outside. The instrument is advanced into the ground as the soil displaced by a sharp cutting shoe is removed up the center of the probe by the action of a rotating cutter inside the shoe. The cuttings are flushed to the surface by water or drilling mud which is pumped down to the cutting head.
The cylindrical adiprene membrane used in this study was 82 mm in diameter and 490 mm in length, corresponding to a length to diameter ratio (L/D) of approximately 6. The adiprene membrane was designed to be flush with the body of the probe. An outer flexible protective membrane with stainless steel strips ("chinese lantern") can be placed over the adiprene membrane during penetration and testing in dense or abrasive soils.
Once the instrument is at the desired test depth, the membrane is expanded against the soil using pressurized N_2 gas. The radial expansion of the membrane is measured at the mid-height of the membrane by three pivoted levers, called strain arms. The strain arms are located at 120 degrees around the circumference. The strain arms are kept in light contact with the inside of the membrane by strain gauged cantilever springs (Figure 3). Individual and average readings were taken of the three strain arms. The sensitivity of the strain arms was approximately 0.02 mm/mV.
A strain gauged total pressure cell (TPC) is located inside the probe to measure the inflation gas pressure. Two strain gauged pore pressure cells (PPC) are also incorporated into the membrane. The sensitivity of the PPC and TPC was approximately 8 kPa/mV.
The data from all six transducers (3 strain, 1 total pressure, 2 pore pressure) was collected by the original data acquisition system consisting of a data capture unit, and a thermal paper printer with the addition of a cartridge equipped HP 9825 computer and a wider paper tape printer. The output was also recorded on a four channel Y-T chart recorder and an X-Y plotter for simultaneous plotting of raw data (Fig.2).

3. TEST SAND

Two natural sands have been tested; Ticino sand from Italy and Hokksund sand from Norway. Both sands have a uniform gradation and are medium to coarse grained with a mean grain size, D_{50}=0.53 mm, and 0.39 mm for Ticino and Hokksund sand, respectively.
General characteristics of the sands and grain size distributions are given in Fig.4.
A detailed description of the physical properties of the two sands is given by Baldi et al. (1985).
During the course of the testing different batches of Ticino sand were used. However, each batch was tested to ensure consistent grain size characteristics.

4. TEST PROCEDURES

4.1. Sample Formation

All test samples were prepared by pluvial deposition of dry sand in air using a gravity mass sand spreader (Jacobsen, 1976). A schematic representation of the mass sand spreader is shown in Figure 5.
The pluvial deposition method has the following advantages;

- good repeatibility
- wide range of obtainable relative densities ($20\% \le D_R \le 98\%$)
- good homogeneity of sample
- cost effectiveness.

The homogeneity of the samples is generally good although somewhat erratic for medium dense specimens ($40\% \le D_R \le 60\%$). Full details concerning sample homogeneity is given by Baldi et al. (1985).
Sample formation is performed in one operation and the sand container holds enough sand necessary for specimen preparation.

4.2. Probe Installation

4.2.1. Ideal

To evaluate and avoid the influence of the self-boring installation on the pressuremeter results a series of tests were performed with "ideal installation".
For ideal installation the probe was placed in the CC before sample formation. A schematic outline of the ideal installation procedure is shown in Figure 6.

The SBP probe was placed in the center of the CC with the mid-height of the membrane approximately 65 cm (25 inches) from the sample base. A protective cylinder was placed above the probe and extended up to the base of the sand container (see Fig.6). This was done to avoid sand falling onto the top of the probe during sample formation.

4.2.2. Self-bored

To simulate field self-boring conditions a series of tests were performed with the probe self-bored into the CC. A schematic outline of the self-bored installation procedure is given in Figure 7.
The sand samples were first formed using pluvial deposition and then saturated with de-aired water. Full details of the saturation procedures are given by Bellotti et al. (1982). The probe was self-bored into the CC using water as the flushing fluid. Drainage was generally allowed at the base of the sample. A summary of the installation conditions during self-boring is given in Table 1.
Installation was performed with various boundary conditions in order to evaluate their influence on the test results (see Table 1).
A small vacuum (5 t/m^2) was applied to the inside of the SBP probe to maintain the adiprene membrane in close contact with the body of the probe.
The cutter speed was generally maintained at a rate of about 60 revolutions per minute. The distance of the cutter from the leading edge of the cutting shoe was varied from about 1.9 cm (0.75 inch) to 5.4 cm (2.13 inches). For the tests in dense sand the adiprene membrane was generally protected by using the chinese lantern. The size of the cutting shoe was adjusted to be the same diameter as the membranes.
The probe was advanced into the CC at a rate of about 3 cm/min. (1.18 inches/min).
A flowmeter was used to monitor the flow rate of the flushing water sent to the cutter. The flow rate was generally about 9 to 12 lt/min. The flow rates from the probe and calibration drainage lines were also monitored. During the installation, the CC pore pressures and boundary stresses and strains were monitored. All the sand flushed out from the CC during installation was carefully collected and weighted (oven-dry).

4.3. Sample Stresses

Following sample formation and probe installation, the sample was subjected to one-dimensional consolidation under conditions of no average lateral strain (i.e. $\Delta\epsilon_h = 0$). Normally

consolidated (NC) and mechanically overconsolidated (OC) specimens were reproduced.
During the loading and unloading consolidation phases, changes in vertical effective stress (σ_v') and the corresponding vertical strain (ϵ_v) were recorded. This allowed the calculation of the constrained modulus (M_o) and the coefficient of earth pressure at rest (K_o).
A summary of the general CC conditions at the end of consolidation is given in Table 2.
An example of data collected during a typical sample stressing is given in Figure 8.
During the SBPT the sample boundary conditions could be controlled.
A summary of the possible boundary conditions is given in Figure 9.
The boundary conditions applied during each pressuremeter test are given in Table 2.
The most common boundary condition applied was constant vertical (σ_v = constant) and horizontal (σ_h = constant) stresses (BC1).

4.4. Pressuremeter Expansion

After sample stressing and the self-boring insertion when appropriate, the pressuremeter test was performed by expanding the membrane to a maximum cavity strain (ϵ_o) of about 10%. Cavity strain is defined in terms of circumferential strain;

$$\epsilon_o = \frac{\Delta R}{R_o} \qquad \ldots (1)$$

where:
R_o = initial cavity radius
ΔR = increment of cavity radius.

Generally, before the beginning of the expansion phase, a relaxation time ranging between:
- 30' to 60' in tests with ideal installation
- 60' to 180' in tests with self-boring installation

was allowed.
Only strain controlled tests were performed using an electronic Strain Control Unit (SCU) supplied by Cambridge In-Situ Ltd.
The SCU automatically adjusts the expansion pressure as a function of the output from the strain arms.
Constant strain rates of 0.1%/hour up to 2% per minute can be achieved. Generally, tests were performed at a strain rate of about 1%/minute.
Generally, during each expansion phase, two or three unloading-reloading (UR) loops and, during the contraction phase, one or two reloading-unloading (RU) loops were performed. The strain

amplitude for each UR or RU loop was maintained constant and in the order of 0.1 to 0.2%.

An example of a typical pressuremeter test result is shown in Figure 10.

Typical pressuremeter tests show the average strain for the three strain arms. The average strain is calculated at any instant in time as the numerical average of each strain arm measurement.

A summary of the probe and chamber conditions for the tests using self-bored installation is given in Table 3.

Data from all transducers in the SBP probe were stored on computer cassettes and printed in digital form on a paper tape printer. After each test the basic data was processed and corrected for membrane stiffness. Examples of the computer generated plots are given in Appendix I.

5. TEST RESULTS

A complete listing of all the test results is given in Appendix II.

5.1. Initial Horizontal Stress

It is generally postulated that, if the SBP probe is inserted into the ground with minimum disturbance to the surrounding soil, the total horizontal stress (σ_{ho}) existing in the soil prior to insertion can be measured. The σ_{ho} is measured by recording the corrected SBP cavity pressure (p_o) causing "lift-off" of the pressuremeter membrane. This postulation should be especially valid in the case of the "ideal-installation" used in the CC for test No.201 to 236, inclusive and No.262 and 263. Table 4 presents a summary of lift-off stresses for each strain arm. The lift-off stress was determined from a visual inspection of the early part of the expansion curve.

5.1.1. Initial Horizontal Stress: Ideal Installation

Examination of the results in Table 4, for ideal installation, shows that the measured average lift-off stress (p_o) is often significantly different than the applied boundary stress (σ_{ho}). Figure 11(a) presents a comparison of the measured average lift-off stress and the applied boundary stress for the tests with ideal-installation.

The average lift-off stress is defined as the observed "lift-off" from the cavity expansion versus average strain plot, as shown in Fig.10. This lift-off is generally very close to the first lift-off of one of the arms.

The reasons for the differences are not clear but may be caused by one or more of the following:

a. stress concentration around the rigid SBP probe during one-dimensional stressing,
b. mechanical compliance of the strain arms,
c. arching effects caused by the presence of an annulus of looser sand around the SBP probe.

In the field, the possible existance of anisotropic stress fields [Dalton and Hawkins (1982)] should also be considered, but this possibility does not exist in the triaxial CC tests.

5.1.2. Evaluation of Stress Concentration

The possibility of stress concentrations around the probe in the CC during the consolidation stage was investigated using a rigid self-boring K_o-cell manufactured by Cambridge In-Situ Ltd. The K_o-cell has the same diameter as the SBP probe and consists of a rigid steel cylinder with a K_o-cell mounted flush on one side. The K_o-cell is strain-gauged and operated on a null-indicator principle. Gas pressure on the inside of the cylinder is constantly adjusted to ensure no lateral strain of the K_o-cell.
One test was performed (Test N°226) using the K_o-cell with ideal-installation in the CC. The test was carried out using Ticino sand at a D_R = 60%. The sample was stressed under boundary conditions BC 1 up to a stress of σ_{ho} = 3.0 kg/cm^2 and σ_{vo} = 6.2 kg/cm^2. A comparison between the applied horizontal stress (σ_{ho}) and the measured stress (P_h) recorded with the K_o-cell is shown in Figure 12.
The results from this special test indicate that there is little or no stress concentration around the SBP probe after ideal-installation in sand in the CC. A comparison between the K_o-cell results and the SBP probe results is also included in Figure 11.

5.1.3. Mechanical Compliance of Strain Arms

The problem of mechanical compliance of the strain arms has been investigated in detail. The first indications of this phenomena emerged during SBP tests performed at several Italian clay and sand sites using the same SBP equipment used in this study [Ghionna et al. (1983), Jamiolkowski et al. (1985), Bruzzi et al. (1986)].

The following observations emerged from the field tests:

a. the "lift-off" pressures from each strain arm were almost always different. This occured even in soil deposits for which it was difficult to justify, based on geologic history, the presence of anisotropic horizontal in-situ stresses,

b. the differences between the three measured "lift-off" pressures tended to increase with increasing soil stiffness and ambient in-situ soil stress.

These observations indicated a possible problem due to mechanical compliance of the strain arms. These problems where further confirmed during the CC testing when the following observations were made;

- despite the "ideal installation" of the SBP probe and the simple stress history of the CC specimens, different "lift-off" pressures were recorded for each of the three strain arms. The difference was more pronounced in the stiffer samples,
- during the sample stressing with the probe installed, apparent inward movement of the strain arms was recorded when the radial chamber stress was increased and apparent outward movement when the chamber stress was decreased. An example of this phenomenon is shown in Figure 13.

Figure 14 presents the results of the initial portion of expansion curves recorded with each strain arm and with the averaged strain for a test with pronounced mechanical compliance.

The mechanical compliance of the strain arms tends to confuse the initial part of the expansion curves and makes the detection of the lift-off pressure uncertain.

The detection of the lift-off pressure becomes more difficult with increasing stiffness of the surrounding soil because the slope of the initial portion of the expansion curve becomes very steep.

In an effort to eliminate or at least reduce the mechanical compliance the three strain arms were modified.

A comparison between the original and modified strain arm designs is shown in Figure 15. The modified arms had the following major changes:

- the body of the arms were made thicker and stiffer and were machined from stainless steel instead of the original brass,
- the alignment of the pivots and arms with respect to their seats on the probe body were improved,
- the pivots were modified by using precision miniature bearings.

All the tests from N°225 onwards used a SBP probe with the modified strain arms.

Figure 11(b) shows a comparison between the measured average lift-off stress (with modified arms) and the applied chamber stress for the remaining CC tests with ideal-installation. The results indicate that the modifications to the strain arms have minimised to some extent the mechanical compliance but have not completely removed the problem.

At pesent, based on the CC results using ideal installation it appears that the strain measuring system in the existing version of the Cambridge In-Situ Ltd., Camkometer (Mark VIII) requires radical changes in order to improve the precision of the measured lift-off pressures, especially in stiffer soils.

5.1.4. Evaluation of Arching Effects

The possible problem of arching around the SBP probe has not been directly investigated. The experience gained in the evaluation of sample homogeneity of pluvially deposited CC samples [Baldi et al., (1985)] indicates that D_R tends to increase slightly towards the center of the sample. However, this experience refers to samples formed without the SBP probe installed inside the CC.

5.1.5. Initial Horizontal Stress: Self-Bored Installation

Figure 16 compares the measured average lift-off pressures against the applied boundary stress (σ_{ho}) for the CC tests with self-boring installation. In almost all cases the measured average lift-off stress is less than the applied stress and often close to the water pressure in the CC. This indicates significant sample disturbance during the installation, especially in loose and medium dense samples.
The ratio between the average lift-off stress (p_o (AV)) and the applied boundary stress (σ_{ho}) for the self-bored installation is:

$$\frac{p_o\ (AV)}{\sigma_{ho}} = 0.47 \pm 0.28 \qquad \ldots (2)$$

Table 4 presents a summary of the individual lift-off pressures for each strain arm. Examination of Table 4 shows that, for the self-bored installation, the variation between lift-off pressures from the individual arms in extremely large.

Because sands are generally stiff in comparison to soft clays, the measurement of in-situ stress in sands is extremely difficult.
A slight outward disturbance during self-boring will tend to produce an overestimate of σ_{ho}. A slight inward disturbance during self-boring can cause the sand around the probe to arch and produce a significant underestimate of σ_{ho}.

Based on the CC results, it appears that the measurement of in-situ stresses in sands using the self-boring pressuremeter is extremelly sensitive to disturbance.

5.2. Shear Modulus

The evaluation of deformation characteristics of soils from the results of a SBPT is usually linked to the assumption that the probe is expanded in a linear, isotropic, elastic, perfectly plastic soil. With this assumption the soil surrounding the probe is subjected to pure shear only. This holds true provided the applied pressuremeter cavity effective stress (p') stays below the yield stress (p'_y) of the soil element adjacent to the cavity wall. The values of p'_y in a purely frictional Coulomb material is given by the formula [Baguelin et al. (1978):

$$p'_y = p'_o \ (1 + \sin \phi) \qquad \ldots (3)$$

For the range of effective cavity stress $p'_o < p' \leq p'_y$, the expansion curve should have a constant slope $d_p/d\epsilon_o = 2\ G_i$ [Baguelin et al. (1972, 1978)
where:
G_i = initial shear modulus of tested soil, see Fig.17

The above is true for SBPT's performed in an infinite medium (i.e. in-situ). However Fahey (1980) demonstrated that because of the limited dimensions of a CC the initial slope of expansion curves obtained in the CC tend to be sligthly too small. In this study, the effect of the limited dimensions of the ENEL CRIS CC has only a minor effect, resulting in a reduction of less than 3% on the measured values of G.
The definition of G_i given above implicity incorporates the following simplified assumptions:

a. The length (L) to diameter (D) ratio of the probe is sufficiently large to ensure deformations of the surrounding soil occur in plane strain conditions ($\epsilon_z = 0$).
b. The expansion proceeds with no volume change in the surrounding soil mass (i.e. linear, isotropic elastic material).
c. All soil elements surrounding the expanding cavity have the same stress strain characteristics.

The first assumption (a) appears reasonable for the Camkometer probe used in this research, where the L/D=6. The other assumptions (b) and (c) are both strictly linked to the hypothesis made about the stress-strain relationship of soil. Both assumptions require that the effective stress path (ESP) projected on the horizontal plane should have a shape as shown schematically in Fig.18. In reality because of, the strain non-linearity, elastic anisotropy, and work hardening plasticity, etc., the behavour of sands deviates from that of the isotropic-elastic perfectly plastic material so that volume

changes occur even during the early stage of the expansion. A more realistic ESP, as obtained by Manassero (1987), is qualitatively also shown in Fig.18. Comparison of the two stress paths shown in Fig.18 clearly indicates that beyond the initial elastic stage (point 1') the mean effective stress (σ_0') in the soil surrounding the expanding pressuremeter probe is not constant and consequently the volumetric strain cannot be equal to zero.

Since the modulus (G_i) can only be determined with validity from the very early part of the expansion curve the value is very sensitive to disturbance.
An alternative to the assessment of G_i from the initial part of the expansion curve is to evaluate G from correctly performed unloading-reloading (G_{UR}) and reloading-unloading (G_{RU}) loops as illustrated in Fig.17. According to Wroth (1982) the amplitude of the unloading should be performed in such a manner as to avoid the failure of the soil at the cavity wall in extension. For an isotropic-elastic, perfectly plastic material the magnitude of the effective cavity stress change ($\Delta p'$) during an elastic unloading should therefore not exceed the following:

$$\Delta p' = \frac{2 \sin \phi^{PS}}{1 + \sin \phi^{PS}} \; p_c' \qquad \ldots (4)$$

where:

ϕ^{PS} = friction angle under conditions of plain strain
p_c' = effective cavity stress at which unloading loop starts.

The slope of the secant within the loop, (see Fig.17) is again equal to 2 G_{UR} or 2 G_{RU}. Both G_{UR} and G_{RU} represent an "elastic" shear stiffness of the tested sand. Within the framework of elasto-plasticity it can be demonstrated that during a drained test any unloading of the expanding cavity wall will bring the surrounding soil below the current yield surface. Inside this yield surface, (see Fig.19) the strains are small and to a large extent recoverable.
In addition to the above mentioned moduli (G_i, G_{UR}, G_{RU}) it is also possible to evaluate directly from the expansion curve the secant pressuremeter modulus G_s, as shown in Figure 17. The assessment of G_s is also based on the assumption of an elastic soil behaviour which, except for the very early part of the expansion curve where $G_s \approx G_i$, and during unloading-reloading cycles, is conceptually not true.
Despite the lack of a clear physical meaning, G_s is frequently incorporated in the empirical design rules for shallow and deep foundations in France [Baguelin et al. (1978)].
Table 5 reports the values of G_s computed at cavity strains equal to 0.5%, 1.0% and 1.5%.

Values of G_{UR} for the different unloading-reloading cycles are given in Tables 6 to 9. Values of G_{RU} for the reloading-unloading cycle are given in Table 10.

In all soils, and especially in sands, the early part of the self-bored pressuremeter curve is strongly influenced by disturbance due to the installation. Therefore, G_i and G_s are also strongly influenced by disturbance. On the other hand, G_{UR} and G_{RU} are almost completely independent from the initial shape of the expansion curve and hence, independent from disturbance.
Despite this advantage, there is still the problem of how to apply the measured G_{UR} and G_{RU} values in engineering design. This requires some assessment of the average stress and shear strain levels relevant to the measured moduli [Robertson (1982). As with all boundary value problems this is difficult to assess and requires a number of simplifying assumptions.

Concerning the relevant stress level, existing pratice has been to refer G_{UR} to the average stress existing around the expanding pressuremeter probe. This average stress may be either the mean octahedral effective stress [Robertson (1982)] or the mean value of the plane strain effective stress [Fahey and Randolph (1984)].
In this study the latter stress will be adopted.
When a value of the reference stress has been selected, the following tentative procedure can be used to relate the measured G_{UR} and G_{RU} values to any level of effective stress:

- Consider the value of G_{UR} corresponding to a given value of the double shear strain amplitude of the cycle ($\Delta\gamma = \gamma_B - \gamma_A$) and to the effective cavity stress from which the cycle starts (p'_c), see Fig.19 and Tables 6 through 10.

- Compute the weighted average of the current effective stress (p'_{AV}) existing around the SBP probe at p'_c, adopting an appropriate constitutive equation:

$$p'_{AV} = \chi \, p'_c \qquad \ldots (5)$$

For elastic perfectly plastic material, referring to the average stress on the horizontal plane existing in the plastic zone ($r_c \le r \le R_p$), the parameter χ can be computed from the following equation, see also Appendix III:

$$\chi = \frac{1}{(1-\sin\phi^{PS})} \cdot \frac{\left[\dfrac{p'_c}{\sigma'_{ho}\,(1+\sin\phi^{PS})}\right]^{\omega_1} - 1}{\left[\dfrac{p'_c}{\sigma'_{ho}\,(1+\sin\phi^{PS})}\right]^{\omega_2} - 1} \quad \ldots (6)$$

where:

σ'_{ho} = initial effective horizontal stress. In a high quality SBPT σ'_{ho} should be closed to the measured effective lift-off pressure p'_o

$$\omega_1 = \frac{1 - \sin\phi^{PS}}{2\sin\phi^{PS}} \quad \ldots (7)$$

$$\omega_2 = \frac{2\sin\phi^{PS}}{1 + \sin\phi^{PS}} \quad \ldots (8)$$

r = radial distance from center of cavity
R_p = radius of plastic zone
r_c = radius of cavity when cavity pressure = p'_c

In practice the true value of σ'_{ho} is generally unknown, therefore, the assessment of χ is made by introducing into the above formula the measured value of p'_o.
The values of χ computed for each SBPT performed in the CC are given in Tables 6 through 10 together with the corresponding values of p'_{AV}.
The use of the relationship, $p'_{AV} = \chi\, p'_c$, is correct provided the following condition is satisfied:

$$p'_c > \sigma'_{ho}\,(1 + \sin\phi^{PS}) \quad \ldots (9)$$

If this condition is not fulfilled the p'_{AV} should be assumed equal to $\sigma'_{ho} \approx p'_o$.

- Once the p'_{AV} is assessed it is possible to compute the modulus number K_G from the following empirical formula proposed by Janbu (1963):

$$G_{UR} = K_G\, p_a \left(\frac{p'_{AV}}{p_a}\right)^n \quad \ldots (10)$$

where:

K_G = modulus number
n = modulus exponent
p_a = reference stress, usually p_a = 98.1 kPa
p'_{AV} = average effective stress around the probe

For sand, the modulus exponent is generally within the range of 0.4 to 0.5, with a slight tendency to increase with increasing level of strain [Wroth et al. (1979). Knowing the value of K_G it is possible to compute the shear modulus G for any desired stress level.

Following the procedure outlined above, the measured G_{UR} and G_{RU} values for each cycle have been referred to the effective horizontal stress σ'_{ho} applied to the boundary of the CC specimen, assuming n=0.43 as obtained by Lo Presti (1987). The corresponding values of G_{URo} and G_{RUo} are given in Tables 6 through 10.

The same tables also show the values of maximum dynamic shear modulus (G_o) obtained from resonant column tests performed by Lo Presti (1987) on pluvially deposited Ticino sand. The value of G_o corresponding to each SBPT has been computed using the following empirical equation based on the experimental data obtained by Lo Presti (1987):

$$G_o = 647.0 \cdot p_a \left(\frac{\sigma'_{ho}}{p_a} \right)^{0.43} \frac{(2.27 - e)^2}{1+e} \qquad \ldots(11)$$

where:
e = void ratio of the sand in the CC (*)
p_a = reference stress = 98.1 kPa

In order to make a meaningful comparison between the G_{URo} and G_o values it is necessary to consider other factors influencing the deformation characteristics of sand. Among them, the most relevant is the strain level. Each cycle is characterized by the double shear strain amplitude ($\Delta\gamma$) at the cavity wall where:

$$\Delta\gamma = \gamma_B - \gamma_A = 2\ (\epsilon_{oB} - \epsilon_{oA}) \qquad \ldots(12)$$

Values of $\Delta\gamma$ are reported in Tables 6 through 10.
The maximum shear modulus G_o corresponds to a shear strain level less than 10^{-4}%, which is two orders of magnitude smaller than the strains at which G_{UR} and G_{RU} have been measured. In order to be able to compare G_o against G_{UR}, at the same strain level, it is necessary to use a relationship which can match the decay of G with increasing γ. The simplest solution is offered by the well known hyperbolic stress-strain relation in the form proposed by Hardin and Drnevich (1972):

(*) Computed assuming the specific weight of the tested sands 26.35 kN/m^3 and 26.72 kN/m^3 for Ticino and Hokksund sands, respectively.

$$\frac{G}{G_o} = \frac{1}{1 + \frac{\gamma}{\gamma_r}} = \frac{1}{1 + \frac{G_o\ \gamma}{\tau_{max}}} \qquad \ldots(13)$$

where:
G = shear modulus
γ = shear strain
τ_{max} = maximum shear stress
γ_r = reference strain = $\frac{G_o}{\tau_{max}}$

Referring to the SBP unloading-reloading cycle and relating the above given hyperbolic formula directly to the modulus number (K_G), one gets:

$$\frac{G_{UR}}{G_o} = \frac{1}{1 + \frac{G_o\ \Delta\ \gamma_{AV}}{2\ \sigma'_{ho}\ \sin\ \phi^{PS}}} \qquad \ldots(14)$$

and therefore:

$$K_{G_o} = K_{G_{UR}} (\sigma'_{ho})^{n_{UR}-n_o} \cdot \left[1 + \frac{K_{G_o} \left(\sigma'_{ho}\right)^{n_o} \cdot \Delta\gamma_{AV}}{2\ \sigma'_{ho}\ \sin\ \phi^{PS}}\right] \qquad \ldots(15)$$

where:
K_{G_o} = modulus number related to the maximum dynamic shear modulus
$K_{G_{UR}}$ = modulus number as computed from G_{UR}, see equation ...(10)
$\Delta\gamma_{AV}$ = average strain in the plastic zone around the expanding probe
n_o = modulus exponent related to the maximum dynamic shear modulus, G_o
n_{UR} = modulus exponent related to G_{UR}, see equation ...(10)

Referring to the data given in Tables 6 through 10 and assuming:

- $\Delta\gamma_{AV} \approx 0.45\ \Delta\gamma$, see Robertson (1982)
- $n_o = n_{UR} = 0.43$
- σ'_{ho} = boundary stress applied to the CC specimen,

one can assess, extrapolating using the hyperbolic stress strain relation, the value of K_{G_o} and hence compute;

$$G_o^{SBP} = f\ (G_{UR},\ \Delta\gamma,\ \sigma'_{ho}) \qquad \ldots(16)$$

For the available tests in this study this approach gives, for the 1st and 2nd unloading-reloading cycles, the following:

$$1.3 \le \frac{G_o}{G_o^{SBP}} \le 1.8 \qquad \ldots(17)$$

where:

G_o = maximum dynamic shear modulus as measured in the resonant column tests

G_o^{SBP} = maximum dynamic shear modulus assessed from G_{UR}.

The lack of coincidence between G_o and G_o^{SBP} may be due to the following:

- The oversimplified and approximate nature of the procedure used to obtain G_o^{SBP} from G_{UR}.

- The influence of the number of unload-reload cycles on the shear stiffness of sands. Values of G_{UR} have been measured during a single unloading-reloading cycle. Therefore the extrapolated G_o^{SBP} values should be referred to the 1st unload-reload cycle while the resonant column G_o has been measured after thousands of unload-reload cycles. For the given level of shear strain amplitude this factor can be expected to be responsible for differences between G_o and G_o^{SBP} of up to about 10 to 20 percent.

- The pluvially deposited sand tends to exhibit an anisotropic behaviour. Within the framework of the theory of elasticity for transverally isotropic soils, the available shear moduli can be defined as follows:

  G_{UR} = G_{HH} = shear modulus for shearing in horizontal direction

  G_o = G_{VH} = shear modulus for shearing in vertical direction

  However this factor does little to justify the observed differences between G_o and G_o^{SBP}. The results of large scale tests performed by Stokoe and co-workers [Knox (1982, Stokoe and Ni (1985), Lee (1986)] indicate that, in sand the velocity of the horizontally polarized shear wave (v_s^{HH}) is 1.1 to 1.15 higher than the vertically polarized shear wave velocity (v_s^{VH}). This data indicates a G_{HH}/G_{VH} ratio ranging between 1.2 and 1.3, therefore suggesting $G_o^{SBP} > G_o$.

5.3. Shear Strength

Theoretical methods for the determination of the peak friction angle (ϕ) of sands from pressuremeter test data have been proposed by several authors; i.e. Gibson and Anderson (1961), Ladanyi (1963), Vésic (1972), Hughes et al. (1977), Robertson (1982) and Manassero (1987). Each method relies on a model for the sand behaviour. Most of the above methods consider that sand has a constant friction angle at failure. However, not all methods allow for the fact that sand changes in volume during shearing.
In Ladanyi's method the volume change is considered to be constant at the point the failure stress ratio is reached. This volume change is introduced into the assessment of the friction angle by a trial and error method.

Vésic's solution uses the results of laboratory tests directly to determine volume change. However, the problem of determining the appropriate laboratory density to perform the tests, is not easy to resolve. Also, the laboratory tests may not produce reliable volume change behaviour because the in-situ structure and fabric cannot be reproduced in the laboratory.

The solution developed by Hughes et al. (1977) relies on the fact that the volume changes are occurring during the expansion of the cavity and the amount of volume change (dilation) is closely related to the current friction angle developed. This approach brings together the stress dilatancy concept of Rowe (1962) and the observed behaviour of sand in simple shear, as for example, observed by Stroud (1971).

Figure 20 shows typical results of simple shear tests on sand conducted by Stroud (1971) and the ideal soil model assumed in the method by Hughes et al. (1977).
In the method proposed by Hughes et al. (1977), it was shown that:

$$\log\left(\frac{\Delta R}{R_o} + \frac{c}{2}\right) = \frac{n+1}{1-N} \cdot \log(p-u_o) + \text{constant} \qquad \ldots (18)$$

where:

R_o = initial radius of pressuremeter
ΔR = change in radius of pressuremeter
$\Delta R/R_o$ = cavity strain, ϵ_o
c = intercept shown on Fig.20 (c) and (d)
p = total pressuremeter cavity stress
u_o = pore water pressure

$$\frac{1-N}{n+1} = \frac{(1+\sin\nu)}{(1+\sin\phi)} \cdot \sin\phi = \text{slope } S$$

$\sin\nu$ = maximum dilation rate

In the above method the intercept "c" is assumed zero and a plot of the pressuremeter data in terms of log $(p-u_o)$ (effective cavity stress) against log $(\Delta R/R_o)$ will tend towards a straight line with a slope S. This slope is related to the in-situ friction angle (ϕ) and the maximum dilation rate (sin ν).

For very dense sands the intercept "c" is essentially negligible and for all practical purposes can be ignored. The results of the laboratory studies conducted by Jewel et al. (1980) in very dense sands (D_R = 90%) using the self-boring pressuremeter probe show that the above technique appears to work very successfully. In loose materials the method is not so convenient as the pressuremeter does not expand sufficiently for the sand around the probe to reach the linear portion of its volumetric strain/shear strain curve.

The method by Robertson (1982) expands on the method by Hughes et al. (1977) but incorporates an empirical correction to account for the non-linear nature of the volume change - shear strain relationship (see Figure 20).

The method developed by Manassero (1987) is also a further development of the Hughes et al. (1977) method but incorporates the full non-linear nature of the stress-strain curves. The method assumes that Rowes stress dilatancy concept is valid and solves the shear-volume coupling in a unique manner by using a finite difference numerical solution.

The method by Manassero (1987) allows the complete stress strain and stress path to be calculated for each pressuremeter test. Figures 21 and 22 show typical examples of the calculated stress strain and stress paths for pressuremeter tests with ideal installation. From the stress path plots (d) in Figures 21 and 22 it is clear that the soil surrounding the probe is initially strain hardening up to the point of peak strength $(\sigma_r'/\sigma_\theta')_{max}$, and then strain softening.

The deviation of the soil behaviour from the simple isotropic elastic behaviour can be represented by the angle β (see Fig.23), which is the angle between the point of peak strength $(\sigma_r/\sigma_\theta)_{max}$ and the initial mean normal stress, p_o. Values of β are given in Table 11 for each pressuremeter test analysed using the method by Manassero (1987). In order to avoid numerical instability in the calculation of the stress strain curves and stress paths using the method by Manassero (1987) a 7th order polynominal function was made to fit the measured curve.

Full details of the method by Manassero (1987) is given in Appendix IV.

The methods by Hughes et al. (1977), Robertson (1982) and Manassero (1987) have been evaluated using the results from the SBPT's performed in the CC, and results are presented in Table 11.

All three methods require a knowledge of the friction angle at constant volume (ϕ_{cv}). Values of ϕ_{cv} were determined for Ticino and Hokksund sand using a ring shear apparatus. A summary of the ring shear results are shown in Figure 24. An average value of ϕ_{cv} = 34° was used in the analyses.
A summary of the calculated angles of friction and dilatancy obtained from the pressuremeter tests performed in the CC are presented in Table 11.
Peak friction angles have also been determined from triaxial tests on Ticino sand at various stress levels and densities. Triaxial specimens were formed using the same pluvial deposition technique as used to form the CC specimens.
The peak friction angles (ϕ_p^{PS}) and dilation angles (ν^{PS}) determined from the pressuremeter are obtained under approximately plain strain conditions and are related to the average effective stress around the probe during the test. Therefore, to compare the calculated peak friction angles from the pressuremeter (ϕ_p^{PS}) with those obtained from triaxial tests (ϕ_p^{TX}) requires some corrections to account for stress level at failure (σ_{ff}) and boundary conditions (plain strain-triaxial).

The peak friction angles obtained from the laboratory triaxial compression tests (ϕ_p^{TX}) where corrected to the equivalent stress level at failure (σ'_{ff}) occurring in each pressuremeter test and then corrected to an equivalent plain strain value (ϕ_p^{PS}).

The stress level at failure (σ'_{ff}) for each pressuremeter test was calculated assuming a linear elastic isotropic soil behaviour, where:

$$\sigma'_{ff} = \sigma'_{ho} \left[1 - \sin^2 \phi_p^{PS} \right] \qquad \ldots(19)$$

The values of ϕ_p^{TX} were then determined at the σ'_{ff} stress level using the curved strength envelope equation developed by Baligh (1975), where:

$$\tan \phi_p^{TX} = \tan \phi_o^{TX} + \tan \alpha \left(\frac{1}{2.3} - \log \cdot \frac{\sigma'_{ff}}{p_a} \right) \qquad \ldots(20)$$

where:

ϕ^{TX} = secant friction angle from triaxial compression test at $\sigma'_{ff}=2.72\ p_a$

p_a = reference stress = 98.1 kPa

α = angle which describes the curvature of the failure envelope

Values for ϕ_o^{TX} and α for Ticino sand are given by Baldi et al. (1986).

The triaxial friction angle values were then converted to equivalent ϕ_p^{PS} using the following equation by Lade and Lee (1976);

$$\phi_p^{PS} = \phi_p^{TX} \cdot 1.5 - 17^\circ$$

The calculated equivalent ϕ_p^{PS} values determined from the laboratory triaxial results are also shown in Table 11.

Comparisons between the calculated ϕ_p^{PS} from the SBPT results using the methods by Hughes et al. (1977), Robertson (1982) and Manassero (1987) and the equivalent ϕ_p^{PS} obtained from triaxial results are shown in Figure 25. The following comments can be made about the results presented in Figure 25.

1. No method provides a reliable estimate of ϕ_p^{PS} for sands from the SBPT.
2. The method by Robertson (1982) appears to produce less scatter.
3. Generally the scatter in calculated ϕ_p^{PS} is slightly larger for the test results where the probe was self-bored into the CC.

It is interesting to note that, although most of the self-bored results gave very poor values of σ_{ho} due to disturbance, the self-bored data gave reasonable values of ϕ_p^{PS}. This is consistent with observations made in the field (Ghionna et al., 1983; Jamiolkowski et al., 1985; Bruzzi et al., 1986).
Based on the CC results, it appears that the determination of peak friction angle (ϕ_p^{PS}) in sands using the self-boring pressuremeter is not very reliable and depends on the method of analyses.

Table 11 also provides the values of the state parameter (ψ), as defined by Been and Jefferies (1985). The ψ combines the influence of both mean effective stress level and void ratio on the dilatancy of sand and may correlate to the parameters reflecting the behaviour at failure, i.e. ϕ, ν.

5.4. Limit Pressure

Table 5 presents the calculated limit pressures (P_{lim}) from each SBPT using two existing methods. The two methods evaluated were:

P_{lim}^{WW} : Method by Windle and Wroth (1977)

P_{lim}^{AA} : Method by Al Awkati (1975)

Examples of the plots to calculate P_{lim} are given in Appendix I.

Unfortunately, the concept of a limit pressure is not applicable to pressuremeter tests in sand, especially with a maximum cavity strain of only 10%. Because there is no fundamental concept to support the values of P_{lim}, their application to design is related to empirical correlations. This is further complicated by the fact that different values of P_{lim} are obtained from the different methods (see Table 5).

5.5. Boundary Conditions

The laboratory studies by Fahey (1980) showed that the condition of a constant horizontal stress boundary at some finite distance from the expanding pressuremeter had the effect of producing an apparent strain softening in the pressure expansion curve. This situation was not observed in any of the pressuremeter tests performed for this study. The reasons for this apparent lack of boundary effect could be the following:

- The ENEL-CRIS CC is 1.2 m in diameter, compared to the 0.9 m diameter CC used by Fahey (1980).

- Fahey studied only very dense sand (D_R = 92%) in which the plastic zone expands rapidly during the pressuremeter test. For the tests in this study where D_R < 90% there was no strain softening observed.

No influence of boundary effects could be observed for the interpreted values of σ_{ho}, G and ϕ.

6. SUMMARY AND CONCLUSIONS

A series of 47 self-boring pressuremeter tests have been performed in the ENEL-CRIS calibration chamber. 25 tests were performed with the probe in-place during sample preparation (i.e. ideal installation) and 22 tests were performed with the probe self-bored into saturated sand. 1 test was not completed due to a ruptured membrane during probe installation (Test No. 14)).

The purpose of the testing was to evaluate the performance of the self-boring pressuremeter probe under strictly controlled laboratory conditions and to critically review existing interpretation methods of SBPT in sands.
The SBP probe used in the study was the Camkometer Mark VIII manufactured by Cambridge In-Situ Ltd., England.
The results of the testing can be summarized as follows:

1. Assessment of in-situ stress (σ_{ho})

- Ideal installation:

  Large scatter exists in the experimental data because of mechanical compliance of the strain measurement system. The precision required (approximately 0.005 mm) is probably beyond the limits of a mechanical system. There is, therefore, a need for improvement in the measurement system of lift-off pressure, possibly by adding non-contact precision transducers.
  The existing strain arm design is sufficiently reliable to measure radial displacement during the main expansion phase.

- Self-bored installation:

  The disturbance caused by the self-boring process generally rendered the measured lift-off pressure too low, highly scattered and generally unrealiable.
  However, the soil tested in this study (i.e. freshly deposited, unaged, uncemented, clean sand) creates particularly unfavourable conditions with respect to the reliable assessment of in-situ stress. More reliable assessment of σ_{ho} may be possible in natural sand deposits.

2. Assessment of Shear Modulus, G

- Even for the same sand (grain size, fabric, stress history, etc.) the shear stiffness is a complex function of; void ratio (e), effective stress (p'), shear strain (γ), number of cycles (N_c) and anisotropy and plasticity.

- There is a need to improve the link between the measured G and the stiffness required for specific design problems.

- The initial shear moduli (G_i) and the secant shear moduli (G_s) are both sensitive to disturbance and are very complex to locate within the framework of elasto-plastic theory.
  Therefore, G_i and G_s are almost impossible to link to other laboratory and in-situ tests and to design problems.

- The shear moduli determined from unload-reload cycles (G_{UR} or G_{RU}) are "elastic" but non-linear and are much less sensitive to disturbance due to installation. G_{UR} or G_{RU} should be linked to the relevant design problems via appropriate corrections accounting for stress (p') and strain (γ) level. Soil anisotropy should also be considered, since SBPT G_{UR} = G_{HH}, while in many practical problems the value G_{VH} is appropriate.

- Because G_{UR} and G_{RU} reflects the shear stiffness of sands inside the current yield surface they implicity refer only to overconsolidated (OC) materials.

- When relating G_{UR} to the dynamic shear modulus (G_o) the influence of number of cycles (N_c) should also be considered.

- Further theoretical work is required concerning the application of G_{UR} to engineering design practice.

- At present G_{UR} represents a rather unique method to assess directly some kind of shear stiffness for natural sands in-situ, with the exception of the dynamic shear moduli from in-situ shear wave velocity measurements.

3. **Assessment of peak friction angle ϕ_p^{PS}**

- A large scatter exists between the calculated ϕ_p^{PS} from the SBPT results and the equivalent values of ϕ_p^{PS} obtained from triaxial compression tests.

- None of the existing methods evaluated (Hughes et al., 1977; Robertson, 1982; Manassero, 1987) provided consistently reliable values of the peak friction angle under plane strain conditions (ϕ_p^{PS}).

- Evaluation of the reference friction angle from laboratory triaxial testing is complicated by the curvature of the failure envelope, the variation in stress level at failure (σ_{ff}) in the pressuremeter test and the strain conditions (plain strain-triaxial).

- The calculation of ϕ_p^{PS} from the self-bored pressuremeter tests appear to be less sensitive to initial disturbance than the measurement of in-situ stress (σ_{ho}).

- The method by Robertson (1982) appears to produce less scatter.

- Because of the relatively high densities (D_R > 40%) and low stresses (max 500 kPa) the sand tested had $\phi_p^{PS} \geq 41°$. Therefore, the high friction angles creates particularly unfavourable conditions for the ϕ methods evaluated.

The objective of this study has been to verify the performance of the SBPT in sand and to critically review existing approaches to interpretation of the data for geotechnical design.

The objectives of this study have been reached. However, the study has produced extensive data concerning the SBPT in sand and not all the information has been fully studied and discussed in this report. Further research can be performed to fully evaluate all the available data resulting from this study.

LITERATURE CITED

AL AWKATI A., (1975). "On Problems of Soil Bearing Capacity at Depth". Ph. D. Thesis, Duke Univ., Durham, N.C.

BAGUELIN F., JEZEQUEL J.F., LE MEE H. and LE MEHAUTE A., (1972). "Expansion of Cylindrical Probes in Cohesive Soils". JSMFD, ASCE, SM11.

BAGUELIN F., JEZEQUEL J.F. and SHIELDS D.H., (1978). "The Pressuremeter and Foundation Engineering". Trans. Tech. Publications, Clausthall.

BALDI G. et al. (1985). "Laboratory Validation of In-Situ Tests". AGI, Jubilee Volume, XI ICSMFE, San Francisco.

BALDI G. et al., (1986). "Interpretation of CPT's and CPTU's. II Part: Drained Penetration on Sands". Proc. IV Int. Geotech. Seminar NTI on Field Instrumentation and in Situ Measurements, Singapore.

BALIGH M.M., (1975). "Theory of Deep Site Static Cone Penetration Resistance". Res. Rep. R75-56, N.517, MIT Cambridge Mass.

BELLOTTI R., BIZZI G., GHIONNA V.N., (1982). "Design Construction and Use of a Calibration Chamber". Proc. ESOPT II, Amsterdam, V.2.

BEEN K. and JEFFERIES M.G., (1985). "A State Parameter for Sand". Geotechnique, N.2.

BRUZZI D. et al. (1986). "Self-Boring Pressuremeter in Po River Sand". Proc. II Int. Symp. on the Pressuremeter and Its Marine Applications. Texas A&M Univ., ASTM STP 950.

DALTON J.P.C., HAWKINS P.G., (1982). "Some Measurements of the In-Situ Stress in a Meadow in Cambridge Shire Country Side". Gr. Engng. N.5.

FAHEY M., (1980). "A Study of the Pressuremeter Test in Dense Sand". Ph. D. Thesis, Cambridge Univ., U.K.

FAHEY M., RANDOLPH M.F., (1984). "Effect of Disturbance on Parameters Derived from Self-Boring Pressuremeter Tests in Sand", Geotechnique, N.1

GHIONNA V.N., JAMIOLKOWSKI M., LACASSE S., LADD C.C., LANCELLOTTA R. and LUNNE T., (1983). "Evaluation of Self-Boring Pressuremeter". Proc. Int. Symp. on Soil and Rock Investigation by In-Situ Testing, Paris, V.2

GIBSON R.E. and ANDERSON W.F., (1961). "In-Situ Measurement of Soil Properties with the Pressuremeter". Civ. Eng. & Publ. Works, Rev., May.

HARDIN B.O. and DRNEVICH V.P., (1972). "Shear Modulus and Damping in Soils: Design Equations and Curves", JSMFED, ASCE SM7.

HUGHES J.M.O., WROTH C.P. & WINDLE D., (1977). "Pressuremeter Tests in Sands". Geotechnique, N.4.

JACOBSEN M., (1976). "On Pluvial Compaction of Sand". Rep. N.9. Laboratoiert for fundering. Aalborg Univ., Denmark.

JAMIOLKOWSKI M., LADD C.C., GERMAINE J.T., LANCELLOTTA R., (1985). "New Developments in Field and Laboratory Testing of Soils". Proc. XI ICSMFE, San Francisco, Theme Lectures, V.1.

JANBU N., (1963). "Soil Compressibility as Determined by Oedometer and Triaxial Tests". Proc. III ECSMFE, S.1, Wiesbaden.

KNOX D.P., (1982). "Effect of State of Stress on Velocity of Low Amplitude Shear Wave Propagating Along Principal Stress Direction in Dry Sand". Ph. D. Thesis Texas Univ., Austin.

LADANYI B., (1963). "Evaluation of Pressuremeter Tests in Granular Soils". Proc. of the II Pan American Conf. SMFE São Paulo, V.1.

LADE P.V. & LEE K.L., (1976). "Engineering properties of Soil", Report UCLA-ENG-7652, California Univ., Los Angeles.

LEE S.H.H., (1986). "Investigation on Low Amplitude Shear Wave Velocity in Anisotropic Material". Ph. D. Thesis, Texas Univ., Austin.

LO PRESTI D., (1987). "Mechanical Behaviour of Ticino Sand from Resonant Column Test". Ph. D. Thesis, Politecnico di Torino, Torino.

MANASSERO M., (1987). "Stress-Strain Relationship of Sands from Self-Boring Pressuremeter Tests". Atti del Dipartimento di Ingegneria Strutturale, Politecnico di Torino, Torino.

ROBERTSON P.K., (1982). "In-Situ Testing of Soil With Emphasis on Its Application to Liquefaction Assessment", Ph.D., Thesis, Univ. British Columbia, Vancouver.

ROWE P.W., (1962). "The Stress-Dilatancy Relation for Static Equilibrium of An Assembly of Particles in Contact". Proc. Royal Soc.

STROUD M.A., (1971). "Sand at Low Stress Levels in the Simple Shear Apparatus", Ph. D. Thesis, Cambridge Univ., U.K.

STOKOE K.H. & NI F.H., (1985). "Effects of Stress State and Strain Amplitude on Shear Modulus of Dry Sand". Proc. II Symp. on Interaction of Non-Nuclear Munitions with Structures, Panama City Beach, Florida.

VESIC A.S., (1972). "Expansion of Cavities in Infinite Soil Masses", JSMFED, ASCE, SM3.

WINDLE D., WROTH C.P., (1977). "In-Situ Measurement of the Properties of Stiff Clays". Proc. IX ICSMFE, Tokyo, V.1

WROTH C.P., (1982). "British Experience with the Self-Boring Pressuremeter". Proc. Symp. on the Pressuremeter and Its Marine Applications, Paris.

WROTH C.P., RANDOLPH M.F., HOULSBY G.T. & FAHEY M., (1979). "A Review of the Engineering Properties of Soils with Particular Reference to the Shear Modulus", Cambridge Univ., CUED/D Soils TR75.

NOTATIONS

BC	= Boundary condition
L	= Length of pressuremeter membrane (490 mm)
D	= Diameter of pressuremeter (82 mm)
σ_h, σ_h'	= Horizontal stress; total and effective
σ_v, σ_v'	= Vertical stress; total and effective
D_R	= Relative density (after consolidation)
K_o	= Coefficient of earth pressure at rest
OCR	= Overconsolidation ratio
ϵ_v	= Vertical strain
M_o^t	= Tangent constrained modulus
M_o^s	= Secant constrained Modulus
ϵ_o	= Pressuremeter cavity strain
R_o	= Initial radius of cavity
ΔR	= Change in radius of cavity
P_o	= Lift-off stress
P_o (AV)	= Average lift-off stress (3 Arms)
p'	= Effective cavity stress
P_y	= Yield stress
P_c'	= Effective cavity stress at start of unloading cycle
ϕ^{PS}	= Friction angle under plain strain conditions
ϕ^{TX}	= Friction angle under triaxial conditions
G	= Shear modulus

G_i	= Initial shear modulus
$G_s^{1.5}$	= Secant shear modulus at cavity strain of 1.5%
G_{UR}, G_{RU}	= Shear modulus for unload-reload and reload-unload cycle
G_{URo}, G_{RUo}	= Shear modulus from unload-reload and reload-unload cycle normalized to the stress level σ'_{ho}
G_o	= Maximum dynamic shear modulus obtained from resonant column test
γ_d	= Bulk density
u_o	= Pore pressure at center of CC
p'^{AA}_{lim}	= Effective limit pressure using method by Al Awkati (1975)
p'^{WW}_{lim}	= Effective limit pressure using method by Windle and Wroth (1977)
$\Delta\gamma_{AB}$	= Shear strain increment during unload-reload or reload-unload cycle
p'_{AV}	= Calculated average effective stress around cavity
ν	= Maximum dilation angle
β	= Angle of straight line connecting p'_o and the point of peak strength $(\sigma'_r/\sigma_\theta)_{max}$
ψ	= State parameter (Been and Jefferies, 1985)

TABLE 1

SUMMARY OF INSTALLATION CONDITIONS DURING SELF-BORING

Test No.	BC	Membrane Type	Chamber Drainage	Cutter Setting cm	Advancement Rate cm/min	Cutter Speed rev/min	Water Flow ℓ/min	Vacuum Inside Membrane t/m^2	Notes
237	B-1	Not protected	Open at top and base	2.5	3.0	50÷60	11÷14	5	25 cm before end of installation stopped for 3 mins
238	B-1	Not protected	Open at base	2.5	2.4	50÷60	10	5	Instrument rotated 180° with respect to Test No.237•10 cm from end of installation stopped for 3 mins. At end of installation piping in CC
239	B-1	Not protected	Open at base	2.5	2.4	50÷60	9	5	10 cm from end of installation probe started to lift
240	B-1	Not protected	Open at base	2.5	3.0	50÷60	10	5	Failed test due to ruptured membrane during installation
241	B-1	Protected	Open at base	2.0	3.0	50÷60	10	5	
242	B-1	Not protected	Open at base	1.9	3.0	50÷60	10	5	
243	B-1	Not protected	Open at base	2.5	4.2	50÷60	9	5	
244	B-1	Not protected	Open at base	3.5	3.0	50÷60	8.5	5	
245	B-1	Not protected	Open at base	5.4	3.0	60	8÷9	5	After 22 cm of penetration installation stopped for 5 mins
246	B-3	Not protected	Open at base	4.5	3.0	60	9	5	
247	B-3	Not protected	Open at base	3.4	3.0	60	9÷10	5	
250	B-4	Not protected	Open at base	3.4	3.0	60	9÷10	5	
251	B-4	Not protected	Open at base	3.4	3.0	60	11	5	
252	B-4	Not protected	Open at base	3.3	3.0	60	11	5	
253	B-4	Not protected	Open at base	3.3	3.0	60	10÷11	5	
254	B-1	Not protected	Open at base	3.3	3.0	60	11	5	
255	B-4	Protected	Open at base	2.4	3.0	60	11	5	
256	B-4	Protected	Open at base	2.4	3.0	60	11	5	
257	B-4	Protected	Open at base	1.9	3.0	60	11	5	
258	B-4	Protected	Open at base	1.9	3.0	60	12	5	Probably disturbed due to drilling vibrations
259	B-4	Protected	Open at base	1.9	3.0	60	11	5	Probably disturbed due to drilling vibrations
260	B-4	Protected	Open at base	1.9	3.0	60	11	5	
261	B-4	Protected	Open at base	1.9	3.0	60	11	5	
TESTS FROM 237 TO 261 SAMPLES FULLY SATURATED									

TABLE 2

SUMMARY OF GENERAL CALIBRATION CHAMBER CONDITIONS AFTER SAMPLE CONSOLIDATION

	Test	Sand	γ_d	D_{RC}	OCR	σ'_{vo}	σ'_{ho}	K_o	u_o	M_o	Number of cycles		BC
	No.	-	kN/m^3	%	-	kPa	kPa	-	kPa	MPa	UR	RU	
	201	HS	16.08	67.0	2.77	112.8	74.56	0.662	0	192.18	2	1	1
	207	HS	15.22	43.9	3.29	109.9	64.75	0.586	0	185.51	2	1	1
I	208	TS-4	14.82	43.2	1.00	112.8	45.13	0.400	0	34.14	2	1	1
D	209	TS-4	15.01	49.2	1.00	116.7	51.99	0.441	0	43.56	3	1	1
E	210	TS-4	15.13	53.3	1.00	511.1	244.27	0.479	0	100.06	3	1	1
A	211	TS-4	15.57	67.4	1.00	512.1	242.31	0.473	0	114.88	3	2	1
L	212	TS-4	15.49	64.6	2.86	110.9	82.40	0.747	0	189.82	3	1	1
	213	TS-4	14.96	47.5	2.78	112.8	83.39	0.740	0	168.63	3	1	1
I	214	TS-4	14.80	42.4	1.00	113.8	53.96	0.476	0	50.82	3	1	4
N	215	TS-4	16.42	92.3	1.00	514.6	225.63	0.439	0	143.72	3	1	1
S	216	TS-4	14.92	46.3	7.57	60.8	56.90	0.927	0	156.76	3	1	1
T	218	TS-4	15.51	65.4	7.66	59.8	59.84	0.980	0	169.62	3	1	1
A	219	TS-4	15.52	65.9	5.46	112.9	101.04	0.902	0	207.48	3	1	1
L	220	TS-4	14.95	47.2	1.00	313.3	150.09	0.481	0	80.15	3	1	1
L	221	TS-4	14.87	44.6	2.88	108.9	81.42	0.751	0	167.36	3	1	1
A	222	TS-4	14.92	46.2	5.50	111.8	95.16	0.850	0	199.05	3	1	1
T	224	TS-4	15.81	74.6	5.38	113.8	93.20	0.816	0	222.39	3	1	1
I	225	TS-4	15.81	74.6	5.46	111.8	87.31	0.775	0	218.27	3	-	1
O	228	TS-4	15.89	77.0	1.00	518.0	215.82	0.417	0	120.27	3	1	1
N	233	TS-4	15.98	79.6	1.00	512.1	224.65	0.439	0	121.25	3	1	1
	234	TS-4	15.93	76.1	5.34	115.8	103.99	0.904	0	216.21	3	1	1
	235	TS-4	14.99	48.5	1.00	516.0	239.36	0.465	0	80.54	3	-	1
	236	TS-4	15.83	75.2	2.72	114.8	78.48	0.686	0	190.41	3	1	1
	237	TS-4	15.79	74.6	2.90	96.1	81.42	0.850	6.87	178.35	3	1	1
	238	TS-4	15.79	74.8	2.83	101.0	83.39	0.828	5.89	171.28	3	1	1
	239	TS-4	15.79	74.8	2.84	101.0	86.33	0.856	5.89	169.32	3	1	1
	240	TS-4	16.47	94.1	2.84	101.0	90.25	0.892	5.89	195.22	3	1	1
	241	TS-4	16.38	91.8	2.76	104.0	86.33	0.829	5.89	192.37	3	1	1
	242	TS-4	14.72	40.1	1.00	103.0	49.05	0.475	6.87	32.67	3	1	1
S	243	TS-4	14.79	42.7	3.10	95.2	74.56	0.785	6.87	141.46	4	-	1
E	244	TS-4	14.80	42.8	6.12	97.1	94.18	0.970	5.89	172.36	4	-	1
L	245	TS-4	14.72	40.0	1.00	102.0	54.94	0.539	6.87	41.40	4	-	1
F	246	TS-5	14.72	43.0	1.00	102.0	52.97	0.523	6.87	45.32	4	-	3
	247	TS-5	14.80	43.0	4.19	190.3	147.15	0.776	6.87	212.58	4	-	3
B	250	TS-5	14.81	43.0	1.00	480.7	219.74	0.457	6.87	93.20	4	-	4
O	251	TS-5	14.74	41.0	1.00	100.1	51.01	0.508	6.87	36.30	4	-	4
R	252	TS-6	15.79	75.0	1.00	101.0	52.97	0.518	6.87	58.27	4	-	1
E	253	TS-6	15.68	71.0	1.00	103.0	52.97	0.517	6.87	58.99	4	-	3
D	254	TS-6	15.69	71.0	6.16	97.1	88.29	0.912	6.87	194.43	3	-	1
	255	TS-6	15.49	65.0	1.00	108.9	55.92	0.514	6.87	56.70	2	-	1
	256	TS-7	15.46	65.0	1.73	345.3	277.62	0.690	6.87	263.69	4	-	1
	257	TS-7	16.22	87.0	1.00	130.5	77.50	0.597	6.87	69.16	4	-	1
	258	TS-7	16.18	86.0	1.00	495.4	226.61	0.458	6.87	125.47	4	-	1
	259	TS-8	16.39	92.0	4.63	138.3	139.30	1.008	6.87	215.62	4	-	1
	260	TS-8	16.29	89.0	1.00	131.5	78.48	0.595	6.87	70.53	4	-	3
	261	TS-8	16.37	91.5	3.99	199.1	157.94	0.797	6.87	261.44	4	-	1
	262	TS-9	16.28	88.7	1.00	113.8	45.10	0.398	0	73.77	4	-	1
IDEAL	263	TS-9	16.29	89.1	1.00	112.8	103.00	0.913	0	229.46	4	-	1

TABLE 3

SUMMARY OF PROBE AND CC CONDITIONS DURING SELF-BORED TESTS

Test No.	BC	Membrane Type	Notes
237	B-1	Not protected	Modified arms + bushings
238	B-1	Not protected	Modified arms + bearings
239	B-1	Not protected	Arms + bushings
240	B-1	Not protected	Arms + bushings
241	B-1	Protected	Arms + bushings
242	B-1	Not protected	Arms trimed and rounded + bushings
243	B-1	Not protected	Arms + bushings
244	B-1	Not protected	Arms + bushings
245	B-1	Not protected	Arms + bushings
246	B-3	Not protected	Arms + bushings
247	B-3	Not protected	Arms + bushings
250	B-4	Not protected	Arms+bushings.5 lift-offs. Relaxation time=96 hrs
251	B-4	Not protected	Arms + bushings
252	B-1	Not protected	Arms+bushings. Relaxation time=71 hrs
253	B-3	Not protected	Arms+bushings. At 5 bar total pressure and 4% strain membrane ruptured
254	B-1	Not protected	Arms+bushings. At 5.5 bar total pressure membrane ruptured
255	B-1	Protected	Arms + bushings
256	B-1	Protected	Arms + bushings
257	B-1	Protected	Arms + bushings
258	B-1	Protected	Arms + bushings
259	B-1	Protected	Arms+bushings. After 1st loop manual expansion due to problems with SCU
260	B-3	Protected	Arms+bushings. After 3rd loop manual expansion due to problems with SCU
261	B-1	Protected	Arms+bushings. After 1st loop manual expansion due to problems with SCU

TABLE 4

SUMMARY OF LIFT-OFF PRESSURES OF INDIVIDUAL ARMS

	Test No.	σ_{ho} kPa	ARM 1 kPa	ARM 2 kPa	ARM 3 kPa	Average (p_o) kPa	
IDEAL INSTALLATION	201	74.56	82.06	84.07	71.06	76.06	ORIGINAL STRAIN ARMS
	207	64.75	150.53	69.05	65.05	65.05	
	208	45.13	28.02	34.03	34.03	28.02	
	209	51.99	42.03	49.04	43.03	45.04	
	210	244.27	87.08	61.10	136.12	81.06	
	211	242.31	65.02	65.02	90.03	56.04	
	212	82.40	108.95	114.45	104.25	104.27	
	213	83.39	129.25	164.26	165.15	120.23	
	214	53.96	49.23	61.19	63.25	49.21	
	215	225.63	347.36	379.52	256.25	254.27	
	216	56.90	139.26	97.28	80.22	73.23	
	218	59.84	85.22	117.29	165.64	80.22	
	219	101.04	179.27	173.29	145.24	131.28	
	220	150.09	171.32	122.29	190.35	139.28	
	221	81.42	68.26	93.26	152.30	68.26	
	222	95.16	119.25	163.28	146.32	141.28	
	224	93.20	116.70	162.30	136.02	124.84	
	225	87.31	98.44	105.54	115.67	96.41	
	228	215.82	200.81	274.79	222.09	207.90	
	233	224.65	227.67	237.19	217.36	217.36	
	234	103.99	134.07	124.56	144.39	117.42	
	235	239.36	115.04	109.48	70.62	142.80	
	236	78.48	95.22	90.52	115.92	88.12	
SELF BORED	237	88.29	88.26	148.18	86.10	86.05	MODIFIED STRAIN ARMS
	238	89.28	177.50	309.01	50.01	50.01	
	239	92.22	86.78	146.42	300.68	67.15	
	241	92.22	80.39	80.39	356.82	80.39	
	242	55.92	30.99	30.99	27.26	30.33	
	243	81.43	25.20	27.56	23.14	25.15	
	244	100.07	37.27	24.71	22.07	24.58	
	245	61.81	59.82	46.78	44.62	40.95	
	246	59.84	70.81	18.53	97.58	19.81	
	247	154.02	26.53	18.53	78.65	18.53	
	250	226.61	82.06	84.07	71.06	76.06	
	251	57.88	13.15	8.49	18.33	15.09	
	252	59.84	90.79	68.44	114.35	74.51	
	253	59.84	12.47	13.94	29.12	10.85	
	254	95.16	34.94	31.28	36.88	34.94	
	255	62.79	36.47	57.51	62.38	36.47	
	256	284.49	137.17	81.83	73.14	71.83	
	257	84.37	62.98	47.64	79.05	47.64	
	258	233.48	122.34	122.34	53.53	50.67	
	259	146.17	64.34	37.34	32.46	43.17	
	260	85.35	45.00	32.65	42.90	27.40	
	261	164.81	79.79	88.16	67.02	63.65	
	262	45.10	46.93	57.12	57.81	54.54	
IDEAL	263	103.00	134.38	125.64	129.64	125.64	

IDEAL INSTALLATION: $\dfrac{p_o\ (AV)}{\sigma_{ho}} = 1.07 \pm 0.29$; **SELF-BORED INSTALLATION:** $\dfrac{p_o\ (AV)}{\sigma_{ho}} = 0.47 \pm 0.28$

TABLE 5

SUMMARY OF LIMIT PRESSURE AND SECANT SHEAR MODULUS

Test No.	p'_o kPa	p'^{WW}_{lim} kPa	p'^{AA}_{lim} kPa	$G_s(0.5\%)$ MPa	G_s [illegible] MPa	G_s [illegible] MPa
201	76.06	1471.50	1177.20	14.81	[illegible]	[illegible]
207	65.05	882.90	784.80	13.73	[illegible]	[illegible]
208	28.02	529.74	412.02	9.71	[illegible]	[illegible]
209	45.04	686.70	637.65	9.52	[illegible]	[illegible]
210	81.06	2648.70	2158.20	70.02	[illegible]	[illegible]
211	56.04	2844.90	2158.20	58.25	[illegible]	[illegible]
212	104.27	1402.83	1226.25	15.79	[illegible]	[illegible]
213	120.23	1098.72	1079.00	17.16	[illegible]	[illegible]
214	49.21	804.42	784.80	10.40	[illegible]	[illegible]
215	254.27	3678.75	2943.00	45.42	32.57	[illegible]
216	73.23	725.94	588.60	16.97	11.67	9.32
218	80.22	971.19	784.80	18.25	13.44	11.09
219	131.28	1599.03	1373.40	27.57	[illegible]	[illegible]
220	139.28	1236.06	981.00	20.01	14.22	11.48
221	68.26	1059.48	833.85	20.11	13.64	11.09
222	141.28	1206.63	981.00	17.46	12.95	10.79
224	124.84	1716.75	1373.40	21.48	16.97	14.42
225	96.41	1579.41	1275.30	20.70	15.99	13.93
228	207.90	2992.05	2305.35	33.45	24.13	21.58
233	217.36	2943.00	2207.25	26.68	22.17	20.21
234	117.42	1765.80	1373.40	24.72	18.54	15.60
235	142.80	1955.13	1373.40	33.54	25.89	21.38
236	88.12	1402.83	1079.10	19.03	14.72	12.46
237	79.18	1464.63	1170.33	25.31	19.72	15.70
238	44.12	1220.36	975.11	39.34	27.37	20.99
239	61.26	1396.94	1073.21	32.57	23.54	18.93
241	74.50	1818.77	1416.56	35.81	28.84	23.25
242	23.46	454.20	336.48	4.71	4.22	3.73
243	18.28	365.91	287.43	5.59	4.71	3.92
244	18.69	680.81	455.18	8.73	7.65	6.97
245	34.08	513.06	434.58	7.11	6.07	3.60
246	12.94	689.64	532.68	12.75	9.26	7.51
247	11.66	1611.78	1170.33	9.11	8.81	8.22
250	69.19	2494.68	1906.08	53.06	32.03	24.08
251	8.22	326.67	238.38	4.28	3.58	3.12
252	67.64	1037.90	807.36	18.14	13.57	10.93
253	3.98	985.91	651.38	10.31	11.21	10.64
254	28.07	1248.81	630.78	11.60	13.33	13.30
255	29.60	1219.38	812.27	18.28	14.77	13.20
256	64.96	1629.34	1269.32	28.93	24.23	19.85
257	40.77	1098.62	822.96	21.72	17.37	14.41
258	43.80	3918.02	2667.24	38.98	33.59	30.65
259	36.30	2065.89	1269.32	37.32	31.38	26.26
260	20.93	1833.39	1254.60	22.57	17.62	15.03
261	56.78	3231.32	2262.09	42.59	37.04	32.25
262	54.54	1149.7	826.0	13.00	10.88	9.64
263	125.64	2047.3	1500.9	25.56	19.99	17.15

TABLE 6

SUMMARY OF 1ST UNLOADING RELOADING CYCLE

Test No	P'_A kPa	P'_B kPa	P'_C kPa	ε_A %	ε_B %	ε_C %	$\Delta\varepsilon_{AB}$ %	e	P'_{av} kPa	$\Delta\varepsilon_{av}$ %	G_{UR} MPa	G_{URo} MPa	G_o MPa
201	243 20	258 [illegible]	288 83	[illegible]	[illegible]	[illegible]	0 244	0 [illegible]	[illegible]	[illegible]	[illegible]	[illegible]	[illegible]
207	179 50	250 [illegible]	256 38	1 [illegible]	1 973	1 943	0 212	0 [illegible]	84 [illegible]	[illegible]	16 [illegible]	[illegible]	[illegible]
208	60 55	[illegible]	120 51	[illegible]	[illegible]	[illegible]	0 212	0 448	[illegible] 56	[illegible]	[illegible]	[illegible]	[illegible]
209	87 13	135 95	143 23	[illegible]	[illegible]	[illegible] 422	0 144	0 455	55 23	[illegible]	[illegible]	[illegible]	[illegible]
210	[illegible]	136 [illegible]	[illegible] 53	[illegible]	[illegible]	[illegible]	0 130	0 316	278 [illegible]	[illegible]	[illegible]	[illegible]	[illegible]
211	401 50	485 28	503 25	0 [illegible]	0 862	[illegible]	0 132	0 520	288 [illegible]	[illegible]	[illegible]	[illegible]	[illegible]
212	207 50	272 58	278 68	[illegible]	[illegible]	[illegible]	0 138	0 403	112 [illegible]	[illegible]	[illegible]	[illegible]	[illegible]
213	182 80	262 [illegible]	208 79	0 525	[illegible]	[illegible]	[illegible]	0 418	112 [illegible]	[illegible]	[illegible]	[illegible]	[illegible]
214	49 79	[illegible]	144 21	0 446	[illegible]	[illegible]	[illegible]	0 485	47 [illegible]	[illegible]	[illegible]	[illegible]	[illegible]
215	[illegible]	[illegible]	[illegible] 30	0 432	[illegible]	[illegible]	0 156	0 4[illegible]	[illegible]	[illegible]	[illegible]	[illegible]	[illegible]
216	151 83	216 [illegible]	215 42	0 735	[illegible]	[illegible]	0 156	0 402	41 [illegible]	[illegible]	[illegible]	[illegible]	[illegible]
[illegible]	197 91	257 [illegible]	263 90	0 432	[illegible]	[illegible]	0 156	0 463	[illegible]	[illegible]	[illegible]	[illegible]	[illegible]
[illegible]	260 24	[illegible]	351 20	[illegible]	[illegible]	[illegible]	0 144	0 386	[illegible]	[illegible]	[illegible]	[illegible]	[illegible]
220	263 38	[illegible]	330 63	[illegible]	[illegible]	[illegible]	0 128	0 [illegible]	113 [illegible]	[illegible]	[illegible]	[illegible]	[illegible]
221	206 72	264 65	273 70	1 [illegible]	1 261	1 233	0 120	0 408	[illegible] 44	[illegible]	[illegible]	39 [illegible]	[illegible]
222	267 90	316 96	321 77	0 382	[illegible]	0 337	0 126	0 407	132 80	[illegible]	53 857	44 [illegible]	[illegible]
224	237 80	316 40	320 44	0 520	0 600	0 600	0 130	0 301	120 45	0 [illegible]	91 116	53 241	65 [illegible]
225	220 46	318 27	325 59	0 004	0 987	0 983	0 180	0 378	123 18	0 [illegible]	48 558	41 384	43 [illegible]
228	352 67	462 36	458 17	0 506	0 573	0 483	0 134	0 520	237 17	0 188	67 287	84 421	138 [illegible]
233	335 01	433 35	443 41	0 517	0 580	0 518	0 146	0 530	238 57	0 246	56 884	85 197	144 [illegible]
234	243 77	317 28	322 75	0 530	0 508	0 507	0 140	0 428	135 64	0 143	73 563	67 778	172 [illegible]
235	327 88	414 52	422 81	0 [illegible]	0 556	0 476	0 136	0 583	246 42	0 181	43 861	63 [illegible]	[illegible]
236	151 24	231 81	233 48	0 451	0 522	0 517	0 162	0 430	100 32	0 384	57 300	51 930	90 302
237	252 12	305 32	316 30	0 732	0 787	0 750	0 110	0 370	118 58	0 150	48 539	42 540	40 [illegible]
238	323 73	376 [illegible]	383 57	0 320	0 670	0 364	0 116	0 334	128 13	0 152	45 420	37 [illegible]	41 [illegible]
239	302 15	362 97	368 84	0 884	0 841	0 829	0 116	0 348	128 83	0 251	53 874	44 581	[illegible]
241	361 01	454 20	464 98	0 977	1 342	0 888	0 130	0 382	148 28	0 250	72 888	58 155	123 [illegible]
242	84 37	107 31	100 80	1 710	1 770	1 770	0 132	0 518	58 17	0 350	17 852	16 836	[illegible]
243	52 87	73 58	78 52	0 600	0 762	0 765	0 144	0 751	57 48	0 385	14 813	14 813	70 228
244	68 67	87 12	88 08	0 467	0 544	0 544	0 154	0 744	73 73	0 388	18 148	18 148	77 828
245	72 38	98 83	105 75	0 478	0 557	0 779	0 182	0 548	57 13	0 373	15 107	14 855	98 838
246	87 98	128 38	132 14	0 882	0 782	1 328	0 188	0 483	63 88	0 381	18 618	17 188	58 858
247	128 88	161 77	188 54	0 955	1 334	0 881	0 158	0 718	121 18	0 371	28 732	28 732	84 281
250	481 28	587 31	681 84	0 828	1 288	1 138	0 142	0 482	278 28	0 384	61 588	55 588	112 281
251	48 18	83 38	88 08	1 044	1 135	0 881	0 182	0 872	44 82	0 388	12 714	12 714	58 488
252	182 58	237 58	242 83	0 838	0 918	1 388	0 188	0 334	81 18	0 372	34 618	28 918	74 883
253	148 82	281 38	288 71	0 885	1 378	0 758	0 188	0 388	78 38	0 378	31 478	28 887	73 288
254	181 88	222 78	228 02	0 688	0 781	0 882	0 181	0 465	188 47	0 372	38 475	35 488	81 488
255	158 78	214 54	218 33	0 784	0 872	0 882	0 178	0 388	88 62	0 378	36 415	31 116	72 215
256	258 48	342 87	351 38	0 811	0 888	0 885	0 171	0 878	237 35	0 377	48 188	48 188	142 848
257	138 68	218 88	222 83	0 483	0 552	0 544	0 178	0 435	88 88	0 378	37 748	34 288	85 488
258	382 84	483 38	488 88	0 474	0 557	0 555	0 188	0 582	228 88	0 878	88 388	88 883	158 885
259	323 44	418 88	432 58	0 828	0 776	0 776	0 183	0 417	188 48	0 888	51 858	46 476	128 888
260	188 84	254 47	281 88	0 771	0 881	0 867	0 178	0 488	184 78	0 888	28 878	22 888	87 458
261	332 18	434 78	438 78	0 447	0 528	0 538	0 183	0 444	184 88	0 873	43 388	37 872	133 554
262	183 88	188 18	171 88	0 488	0 588	0 571	0 178	0 371	83 48	0 878	35 888	24 948	88 523
263	228 18	348 88	343 84	0 482	0 588	0 585	0 1[illegible]	0 381	134 38	0 888	57 118	42 728	113 888

G_{UR} = measured unload-reload modulus

G_{URo} = unload-reload modulus corrected for stress level (σ'_{mo})

G_o = maximum dynamic shear modulus from resonant column tests

TABLE 7

SUMMARY OF 2ND UNLOADING RELOADING CYCLE

Test No	p_A kPa	p_B kPa	p_C kPa	ε_A %	ε_B %	ε_C %	$\Delta\varepsilon_{AB}$ %	e	p_{AV} kPa	$\Delta\varepsilon_{AV}$ %	G_{UR} MPa	G_{URn} MPa	G_0 MPa
[illegible]	[illegible]	420 90	438 51	[illegible]	[illegible]	[illegible]	0 230	[illegible]	126 22	[illegible]	[illegible]	[illegible]	[illegible]
[illegible]	216 76	359 72	308 32	2 403	[illegible]	3 103	0 200	0 331	[illegible]	[illegible]	16 149	[illegible]	[illegible]
208	[illegible]	[illegible]	156 32	[illegible]	[illegible]	[illegible]	0 100	[illegible]	[illegible]	[illegible]	[illegible]	[illegible]	[illegible]
[illegible]	123 76	[illegible]	176 42	[illegible]	[illegible]	1 416	0 134	[illegible]	[illegible]	[illegible]	16 446	[illegible]	[illegible]
[illegible]	152 26	[illegible]	460 21	[illegible]	[illegible]	1 233	0 124	0 463	[illegible]	[illegible]	[illegible]	[illegible]	[illegible]
211	[illegible]	592 32	665 12	[illegible]	[illegible]	1 646	0 130	0 455	322 57	0 350	[illegible]	[illegible]	[illegible]
212	265 23	[illegible]	377 80	[illegible]	[illegible]	1 703	0 146	0 334	[illegible]	[illegible]	[illegible]	[illegible]	[illegible]
213	140 37	347 37	357 20	[illegible]	[illegible]	[illegible]	0 120	[illegible]	[illegible]	[illegible]	49 456	[illegible]	[illegible]
[illegible]	[illegible]	[illegible]	194 24	[illegible]	[illegible]	1 440	[illegible]	[illegible]	[illegible]	[illegible]	[illegible]	[illegible]	[illegible]
[illegible]	[illegible]	22 83	[illegible]	[illegible]	[illegible]	[illegible]	0 142	[illegible]	[illegible]	[illegible]	[illegible]	[illegible]	[illegible]
[illegible]	[illegible]	[illegible]	[illegible]	[illegible]	[illegible]	[illegible]	[illegible]	[illegible]	[illegible]	[illegible]	[illegible]	[illegible]	[illegible]
[illegible]	[illegible]	[illegible]	[illegible]	[illegible]	[illegible]	[illegible]	[illegible]	[illegible]	[illegible]	[illegible]	[illegible]	[illegible]	[illegible]
[illegible]	[illegible]	[illegible]	[illegible]	[illegible]	[illegible]	[illegible]	[illegible]	[illegible]	[illegible]	[illegible]	[illegible]	[illegible]	[illegible]
220	[illegible]	[illegible]	[illegible]	[illegible]	[illegible]	2 350	0 122	[illegible]	[illegible]	[illegible]	[illegible]	[illegible]	[illegible]
221	[illegible]	[illegible]	330 60	[illegible]	[illegible]	2 104	0 126	0 365	[illegible]	[illegible]	[illegible]	[illegible]	[illegible]
222	[illegible]	[illegible]	430 13	[illegible]	[illegible]	[illegible]	0 132	0 354	[illegible]	[illegible]	[illegible]	[illegible]	[illegible]
224	[illegible]	411 38	427 72	1 201	[illegible]	1 336	0 134	0 335	163 16	[illegible]	52 440	[illegible]	[illegible]
225	162 18	415 50	426 77	1 645	1 717	1 710	0 144	0 323	137 18	0 65	52 385	[illegible]	[illegible]
228	443 55	537 55	555 25	3 070	[illegible]	0 845	0 130	0 450	250 90	0 160	70 420	[illegible]	[illegible]
233	448 38	560 28	597 21	3 980	[illegible]	3 801	0 120	0 677	265 84	0 157	[illegible]	70 162	[illegible]
234	437 65	510 65	533 66	1 404	2 558	2 744	0 120	0 313	160 96	[illegible]	[illegible]	51 472	[illegible]
235	557 93	446 51	670 22	2 128	[illegible]	2 875	0 134	[illegible]	[illegible]	0 160	48 456	[illegible]	[illegible]
236	202 30	105 21	407 12	1 820	[illegible]	2 144	0 150	0 313	126 34	0 270	61 795	50 181	[illegible]
237	404 83	436 70	449 30	1 931	1 962	1 963	0 142	0 200	134 26	0 164	48 935	60 191	[illegible]
238	434 17	478 71	480 35	2 193	2 257	2 127	0 140	0 204	141 69	0 167	51 393	61 [illegible]	[illegible]
239	413 87	525 22	520 91	2 230	2 326	2 282	0 100	0 203	147 23	0 81	48 756	38 [illegible]	[illegible]
241	544 46	535 50	650 23	2 360	2 441	2 301	0 150	0 262	150 90	0 360	62 800	48 330	[illegible]
242	118 85	144 21	153 04	3 634	3 727	3 675	0 108	0 427	65 35	0 704	10 541	10 380	57 71
243	88 25	115 76	122 63	2 340	2 431	2 412	0 108	0 602	73 05	0 375	15 598	15 662	70 22
244	136 60	167 75	176 62	1 370	1 445	1 437	0 150	0 580	80 12	0 360	22 857	22 350	77 92
245	118 35	156 32	165 40	1 100	1 200	1 280	0 210	0 420	70 44	0 200	17 71	15 821	60 65
246	162 54	170 72	180 40	2 214	2 338	2 228	0 172	0 305	75 73	0 377	22 112	18 362	58 65
247	230 46	300 60	310 08	2 280	2 300	2 300	0 180	0 532	165 28	0 304	33 056	32 206	64 29
250	654 72	750 27	788 28	2 433	2 512	2 670	0 150	0 305	311 93	0 971	42 380	38 481	112 29
251	78 56	82 70	88 96	2 805	2 761	2 737	0 152	0 553	54 74	0 068	14 900	14 514	58 06
252	271 06	320 16	341 27	2 130	2 210	2 172	0 106	0 271	82 61	0 076	35 051	27 592	76 30
253	267 31	288 71	312 71	2 050	2 176	2 135	0 156	0 286	88 57	0 360	34 051	27 167	73 28
254	271 86	328 16	425 00	1 905	2 371	2 000	0 172	0 325	138 43	0 077	42 380	34 335	91 48
255	240 06	300 52	321 10	2 127	2 207	2 193	0 160	0 282	83 77	0 072	37 553	30 307	72 21
256	400 25	488 56	504 44	1 718	1 788	1 700	0 108	0 507	205 00	0 372	56 103	53 400	142 34
257	288 71	395 22	370 08	1 861	2 821	1 808	0 100	0 320	128 33	0 072	42 380	35 050	85 68
258	550 36	670 02	685 02	1 161	1 223	1 218	0 104	0 428	288 21	0 074	73 701	88 140	150 66
259	408 61	588 05	588 05	1 681	1 731	1 847	0 280	0 348	285 00	0 088	53 047	45 452	120 90
260	284 58	372 67	382 58	1 873	1 871	1 815	0 186	0 321	122 04	0 008	48 862	35 580	87 45
261	588 08	710 26	715 95	1 280	1 370	1 370	0 176	0 338	240 38	0 070	70 671	58 886	133 55
262	222 88	308 23	311 27	1 730	1 866	1 808	0 210	0 257	88 00	0 005	38 888	23 034	88 52
263	380 18	507 77	517 15	1 480	1 580	1 580	0 282	0 313	182 17	0 901	88 010	41 407	113 81

G_{UR} = measured unload-reload modulus

G_{URn} = unload-reload modulus corrected for stress level (σ'_{mo})

G_o = maximum dynamic shear modulus from resonant column tests

TABLE 8

SUMMARY OF 3RD UNLOADING-RELOADING CYCLE

Test No	P'_A kPa	P'_B kPa	P'_C kPa	ϵ_A %	ϵ_B %	ϵ_C %	$\Delta\gamma_{AB}$ %	ϵ -	P'_{AV} kPa	$\Delta\gamma_{AV}$ %	G_{UR} MPa	G_{URo} MPa	G_e MPa
201	-		-	-	-	-	-	-					91.[illegible]
207	-		-	-	-	-	-	-		-			72.691
208	-	-	-	-	-	-	-	-					[illegible]
209	158.98	223.68	225.63	2.550	2.613	2.600	0.138	0.343	[illegible]	[illegible]	[illegible]	[illegible]	[illegible]
210	559.36	761.30	779.30	2.332	2.398	1.973	0.132	0.421	[illegible]	[illegible]	73.[illegible]	69.[illegible]	[illegible]
211	705.25	810.42	827.36	2.982	2.949	2.815	0.134	0.412	332.68	0.160	81.[illegible]	[illegible]	[illegible]
212	433.54	313.46	493.44	3.124	3.138	3.177	0.148	0.285	142.53	0.[illegible]	52.287	41.[illegible]	[illegible]
213	399.54	406.49	421.33	2.[illegible]	2.971	2.829	0.136	[illegible]	136.34	0.161	51.[illegible]	41.[illegible]	[illegible]
214	179.28	234.75	244.27	2.[illegible]	2.492	2.426	0.[illegible]	[illegible]	[illegible]	[illegible]	[illegible]	[illegible]	[illegible]
215	[illegible]46.61	383.55	311.35	1.628	1.634	1.594	0.136	[illegible]	[illegible]	[illegible]	[illegible]	[illegible]	[illegible]
216	251.22	303.56	314.92	2.623	2.699	2.667	[illegible]	[illegible]	[illegible]	[illegible]	[illegible]	[illegible]	[illegible]
[illegible]	[illegible]	367.18	375.57	2.[illegible]	2.429	2.[illegible]	0.126	[illegible]	[illegible]	[illegible]	[illegible]	[illegible]	[illegible]
219	433.93	536.65	554.27	2.[illegible]	2.258	2.[illegible]	0.162	[illegible]	[illegible]	[illegible]	[illegible]	[illegible]	[illegible]
220	[illegible]95.21	455.[illegible]	474.[illegible]	3.354	3.431	3.364	0.134	0.424	[illegible].12	0.[illegible]	54.[illegible]	47.[illegible]	[illegible]
221	312.97	371.59	389.46	3.[illegible]	3.321	3.293	0.124	[illegible]	128.60	0.156	44.[illegible]	[illegible]	74.[illegible]
222	423.[illegible]	468.14	487.[illegible]	3.254	3.329	3.117	0.130	[illegible]	154.14	0.[illegible]	51.[illegible]	41.[illegible]	[illegible]
224	357.96	459.21	423.79	2.[illegible]	2.154	2.218	0.228	0.337	142.62	0.103	58.564	49.[illegible]	95.[illegible]
225	427.07	498.52	513.26	2.569	2.537	2.638	0.136	0.287	142.45	0.161	54.249	43.[illegible]	93.[illegible]
228	537.44	629.58	655.31	1.309	1.307	1.281	0.122	0.427	292.20	0.255	77.[illegible]	69.[illegible]	139.[illegible]
233	546.16	653.40	676.99	1.373	1.442	1.363	0.138	0.429	250.18	0.262	75.676	70.[illegible]	146.[illegible]
234	578.41	561.43	684.74	3.546	3.611	3.587	0.130	0.267	193.14	0.159	67.100	52.[illegible]	172.454
235	739.56	907.58	947.58	3.795	3.865	3.559	0.140	0.237	325.97	0.163	72.[illegible]	62.544	121.[illegible]
236	435.99	515.58	535.63	3.564	3.552	3.623	0.136	0.261	139.93	0.088	64.550	50.338	99.[illegible]
237	453.22	536.61	554.27	2.977	3.261	3.031	0.168	0.242	145.28	0.275	51.305	40.122	93.[illegible]
238	448.32	545.44	579.77	3.250	3.350	3.276	0.200	0.259	149.[illegible]	0.190	52.420	39.357	91.[illegible]
239	497.37	603.32	629.80	3.672	3.790	3.737	0.236	0.[illegible]	157.67	0.106	46.734	36.[illegible]	42.[illegible]
241	569.04	778.91	813.25	3.862	3.956	3.891	0.188	0.211	271.99	0.165	61.507	45.915	123.199
242	133.42	173.64	186.39	5.805	5.922	5.881	0.234	0.380	70.99	0.105	18.443	15.742	57.716
243	118.70	145.19	154.02	4.394	4.477	4.404	0.166	0.536	92.54	0.075	16.775	16.157	70.229
244	198.16	237.40	249.17	3.398	3.483	3.452	0.168	0.469	116.95	0.076	24.231	22.076	77.828
245	149.31	204.83	224.18	2.398	2.561	2.558	0.330	0.358	90.21	0.149	17.285	14.589	50.600
246	170.98	224.06	245.54	4.390	4.214	4.151	0.248	0.336	92.66	0.112	22.279	18.159	53.656
247	364.64	432.91	450.28	4.134	4.226	4.162	0.184	0.433	195.07	0.093	38.799	34.369	94.291
250	825.22	928.28	978.45	4.432	4.516	4.468	0.168	0.346	339.01	0.076	63.128	52.390	112.291
251	97.61	123.31	129.03	5.125	5.209	5.218	0.168	0.480	51.35	0.076	16.079	14.780	58.369
252	358.07	413.20	436.94	3.951	4.029	3.963	0.158	0.231	100.89	0.070	36.719	27.934	74.903
253	333.64	398.72	416.92	3.473	3.562	3.550	0.178	0.236	98.32	0.060	36.650	27.370	73.229
254	-	-	-	-	-	-	-	-	-	-	-	-	91.489
255	339.23	403.39	421.22	3.868	3.952	3.924	0.168	0.245	133.35	0.076	39.652	30.447	72.210
256	536.31	633.04	657.06	3.356	3.443	3.357	0.174	0.434	324.36	0.078	57.428	53.711	142.340
257	398.58	471.96	493.23	4.081	4.171	4.152	0.180	0.272	134.32	0.081	42.408	33.478	95.696
258	798.83	931.95	950.75	2.114	2.201	2.205	0.174	0.351	337.00	0.078	78.029	65.798	150.685
259	630.98	739.97	754.21	2.837	2.932	2.908	0.198	0.301	227.23	0.086	58.958	47.771	126.988
260	402.98	481.08	503.57	3.184	3.278	3.243	0.188	0.271	136.35	0.085	42.840	33.782	97.450
261	983.67	982.86	1012.51	2.667	2.752	2.747	0.170	0.271	274.84	0.077	71.956	56.734	133.554
262	354.43	437.62	450.97	3.615	3.723	3.680	0.216	0.202	91.11	0.097	39.890	23.200	80.523
263	536.31	677.48	692.97	2.656	2.771	2.764	0.230	0.282	181.35	0.103	62.970	40.492	113.808

G_{UR} = measured unload-reload modulus

G_{URo} = unload-reload modulus corrected for stress level (σ'_{ho})

G_e = maximum dynamic shear modulus from resonant column tests

TABLE 9

SUMMARY OF 4TH UNLOADING-RELOADING CYCLE

Test No	P'_A kPa	P'_B kPa	P'_C kPa	ϵ_A %	ϵ_B %	ϵ_C %	$\Delta\tau_{AB}$ %	x -	P'_{AV} kPa	$\Delta\tau_{AV}$ %	G_{UR} MPa	G_{URo} MPa	G_o MPa
243	144.13	178.56	191.30	7.878	7.975	7.779	0.194	0.477	91.22	0.087	17.462	16.011	70.229
244	284.87	304.11	319.81	6.625	6.709	6.647	0.168	0.437	130.14	0.076	25.114	21.853	77.828
245	188.65	252.51	270.07	5.798	5.997	5.953	0.138	0.320	86.47	0.179	17.020	14.004	60.600
246	244.07	288.32	303.91	7.317	7.411	7.256	0.188	0.294	89.39	0.085	25.437	20.312	59.556
247	489.62	489.62	592.03	6.476	6.573	6.496	0.134	0.358	218.08	0.087	42.615	35.383	94.291
250	1013.08	1112.65	1163.56	6.989	7.069	6.900	0.160	0.3[illegible]	361.26	0.072	66.286	53.536	112.291
251	121.84	150.30	154.82	7.907	7.995	7.999	0.176	0.433	67.11	0.079	17.432	15.493	58.369
252	445.47	504.33	529.70	6.541	6.626	6.508	0.17[illegible]	0.2[illegible]	107.51	0.077	36.[illegible]	27.[illegible]	74.903
253	-	-	-	-	-	-	-	-	-	-	-	-	73.299
254	-	-	-	-	-	-	-	-	-	-		-	91.433
255	437.33	500.90	525.49	6.128	6.205	6.150	0.154	0.212	111.29	0.159	43.[illegible]92	32.573	72.210
256	674.34	774.01	845.43	5.612	5.702	6.213	0.1[illegible]	0.4[illegible]	363.11	0.[illegible]91	[illegible]	52.[illegible]	142.340
257	501.39	570.35	598.92	6.385	7.076	7.020	0.132	0.241	144.14	0.[illegible]92	40.525	31.[illegible]	95.[illegible]
258	1052.81	1192.60	1240.01	3.421	3.504	3.489	0.166	[illegible]	372.65	0.075	87.054	70.291	150.685
259	786.76	887.91	923.61	4.344	4.434	4.424	0.130	0.266	245.26	0.081	58.546	45.304	126.388
260	520.71	600.47	625.91	4.764	4.554	4.807	0.130	0.236	147.54	0.081	46.401	35.370	97.450
261	1132.98	1246.75	1336.83	4.437	4.517	4.755	0.160	0.227	303.41	0.072	74.252	56.078	133.554
262	498.64	566.63	584.68	6.531	6.618	6.543	0.174	0.170	99.13	0.078	41.460	24.297	80.523
263	716.03	842.88	857.98	4.206	4.311	4.313	0.210	0.228	195.81	0.095	62.910	40.049	113.8[illegible]

G_{UR} = measured unload-reload modulus

G_{URo} = unload-reload modulus corrected for stress level (σ'_{ho})

G_o = maximum dynamic shear modulus from resonant column tests

TABLE 10

SUMMARY OF 1ST RELOADING UNLOADING CYCLE

Test No.	P'_A kPa	P'_B kPa	P'_C kPa	ϵ_A %	ϵ_B %	ϵ_C %	$\Delta\gamma_{AB}$ %	[illegible] -	P'_{AV} kPa	$\Delta\gamma_{AV}$ %	G_{RU} MPa	G_{RUo} MPa	G_o MPa
201	446.36	582.71	575.85	13.604	13.731	13.731	0.254	0.241	139.03	0.114	[illegible]	[illegible]	[illegible]
207	206.01	306.07	306.07	9.376	9.502	9.502	0.252	0.333	101.78	0.113	[illegible]	[illegible]	[illegible]
208	77.50	127.53	127.53	9.238	9.340	9.340	[illegible]	0.451	57.46	0.132	[illegible]	[illegible]	[illegible]
209	104.97	152.06	152.06	9.232	9.299	9.299	0.134	0.449	56.97	[illegible]	[illegible]	[illegible]	[illegible]
210	605.28	671.00	671.00	9.177	9.218	9.218	[illegible]	0.459	337.89	[illegible]	[illegible]	[illegible]	[illegible]
211*	1164.45	1287.07	1287.07	9.638	9.705	9.705	0.134	[illegible]	336.24	[illegible]	[illegible]	[illegible]	[illegible]
211**	554.27	658.25	658.25	9.089	9.155	9.155	0.132	0.458	331.17	[illegible]	[illegible]	[illegible]	[illegible]
212	577.81	652.37	552.37	9.626	9.696	9.636	[illegible]	0.238	[illegible]	[illegible]	[illegible]	[illegible]	[illegible]
213	464.99	556.23	533.28	9.555	9.641	9.641	[illegible]	0.267	[illegible]	[illegible]	[illegible]	[illegible]	[illegible]
214	312.34	380.63	380.63	9.910	[illegible]	[illegible]	[illegible]	[illegible]	[illegible]	[illegible]	[illegible]	[illegible]	[illegible]
215	1422.45	1579.41	1580.39	9.643	[illegible]	[illegible]	[illegible]	[illegible]	[illegible]	[illegible]	[illegible]	[illegible]	[illegible]
216	336.48	401.23	401.23	9.515	[illegible]	[illegible]	[illegible]	[illegible]	[illegible]	[illegible]	[illegible]	[illegible]	[illegible]
218	441.45	[illegible]	[illegible]	10.095	10.161	[illegible]	[illegible]	[illegible]	[illegible]	[illegible]	[illegible]	[illegible]	[illegible]
219	507.18	619.39	619.39	[illegible]	[illegible]	[illegible]	[illegible]	[illegible]	[illegible]	[illegible]	[illegible]	[illegible]	[illegible]
220	368.86	439.49	439.49	9.398	[illegible]	[illegible]	[illegible]	[illegible]	[illegible]	[illegible]	[illegible]	[illegible]	[illegible]
221	273.70	335.50	335.50	9.311	[illegible]	[illegible]	[illegible]	0.362	[illegible]	[illegible]	[illegible]	[illegible]	[illegible]
222	460.09	534.65	534.65	10.028	[illegible]	[illegible]	[illegible]	[illegible]	[illegible]	[illegible]	[illegible]	[illegible]	[illegible]
224	658.25	752.43	750.47	10.315	10.382	10.382	0.134	0.235	176.16	[illegible]	[illegible]	[illegible]	[illegible]
225	-	-	-	-	-	-							[illegible]
228	1186.03	1320.43	1320.43	10.405	10.474	10.474	0.138	0.281	370.72	0.262	[illegible]	[illegible]	[illegible]
233	1189.95	1319.45	1319.45	8.619	8.684	8.684	0.130	0.288	[illegible]	[illegible]	[illegible]	[illegible]	[illegible]
234	552.30	663.17	663.16	8.221	[illegible]	[illegible]	[illegible]	[illegible]	[illegible]	[illegible]	[illegible]	[illegible]	[illegible]
235	-	-	-	-	-		-						[illegible]
236	470.88	[illegible]	571.92	7.110	7.176	7.176	0.132	0.250	143.24	[illegible]	[illegible]	[illegible]	[illegible]
237	526.80	596.45	594.49	7.655	7.719	7.719	0.126	0.250	168.74	[illegible]	[illegible]	[illegible]	[illegible]
238	470.88	527.78	526.90	7.544	[illegible]	[illegible]	[illegible]	0.275	144.62	[illegible]	[illegible]	[illegible]	[illegible]
239	475.79	589.58	587.62	8.101	8.217	8.217	0.232	0.262	153.93	[illegible]	[illegible]	[illegible]	[illegible]
240	-	-	-	-	-	-							[illegible]
241	771.07	863.28	863.28	9.201	9.272	9.272	0.142	0.203	175.37	0.064	71.221	52.511	[illegible]
242	137.34	174.62	174.62	9.810	9.892	9.892	0.164	0.395	69.04	0.076	24.721	21.362	[illegible]

* 1st Reloading-Unloading Cycle; ** 2nd Reloading Unloading Cycle

G_{RU} = measured reload-unload modulus

G_{RUo} = reload-unload modulus corrected for stress level (σ'_{ho})

G_o = maximum dynamic shear modulus from resonant column tests

TABLE 11

SUMMARY OF CALCULATED ANGLES OF FRICTION AND DILATANCY

(ϕ_{cv} = 34°)

	Test No	S	$\phi^{PS}_{P(1)}$ °	$\phi^{PS}_{P(2)}$ °	$\phi^{PS}_{P(3)}$ °	$\nu_{(1)}$ °	$\nu_{(2)}$ °	$\nu_{(3)}$ °	β °	ψ	ϕ_P
	201	[illegible]	[illegible]	49.1		[illegible]	19.0			[illegible]	[illegible]
	207	0.46	41.2	44.0		[illegible]	13.0			[illegible]	[illegible]
I	208	0.43	39.1	[illegible]	[illegible]	[illegible]	11.0	[illegible]	[illegible]	[illegible]	[illegible]
D	209	[illegible]	[illegible]	43.8	[illegible]	[illegible]	13.0	[illegible]	[illegible]	[illegible]	[illegible]
E	210	0.43	39.1	[illegible]	[illegible]	[illegible]	10.3	[illegible]	[illegible]	[illegible]	[illegible]
A	[illegible]		[illegible]	[illegible]	[illegible]	[illegible]	[illegible]	18.[illegible]		[illegible]	[illegible]
L	[illegible]	[illegible]	[illegible]	[illegible]	[illegible]	[illegible]	[illegible]	[illegible]		[illegible]	[illegible]
	213	[illegible]	[illegible]	[illegible]	[illegible]			[illegible]	[illegible]	[illegible]	[illegible]
I	214	0.48	42.0	44.3	[illegible]	[illegible]	[illegible]	11.6	[illegible]	0.101	43.1
N	215	[illegible]	41.9	44.3	[illegible]	[illegible]	[illegible]	13.1	[illegible]	0.242	[illegible]
S	216	0.32	31.1	[illegible]	[illegible]	[illegible]	3.5	3.0	[illegible]	0.122	[illegible]
T	218	0.38	35.6	39.5	[illegible]	[illegible]	7.5	4.4	[illegible]	0.188	48.2
A	219	0.41	[illegible]	[illegible]	[illegible]	[illegible]	9.5	6.1	46.8	0.176	[illegible]
L	220	0.40	37.0	40.5	[illegible]	[illegible]	8.8	[illegible]	[illegible]	[illegible]	[illegible]
L	221	0.42	38.4	41.6	[illegible]	[illegible]	10.2	[illegible]	[illegible]	0.105	[illegible]
A	222	0.39	36.3	40.0	[illegible]	[illegible]	8.0	2.6	[illegible]	0.109	[illegible]
T	224	0.46	41.2	43.8	[illegible]	[illegible]	13.0	[illegible]	[illegible]	0.208	[illegible]
I	225	0.47	41.9	44.3	[illegible]	[illegible]	13.5	10.9	[illegible]	0.209	49.3
O	228	0.47	41.9	44.3	43.9	10.0	13.5	12.7	52.2	0.188	48.2
N	233	0.49	43.3	45.5	[illegible]	11.8	14.8	[illegible]	62.2	-0.198	48.3
	234	0.45	40.5	43.3	[illegible]	9.2	12.0	11.3	[illegible]	0.219	48.9
	235	0.42	38.4	41.5	39.3	[illegible]	9.5	6.6	[illegible]	0.088	41.7
	236	0.48	42.6	45.0	44.8	10.9	14.2	13.9	47.9	0.212	49.6
	237	0.45	40.5	43.1	43.4	8.2	11.9	12.0	43.3	0.210	49.4
	238	0.34	32.6	37.6	[illegible]	[illegible]	4.8	1.6	35.3	0.209	49.3
	239	0.38	35.6	39.4	36.0	1.9	7.1	2.4	43.0	0.208	49.3
	241	0.40	37.0	40.5	40.9	3.7	8.4	8.7	39.5	-0.268	50.2
	242	0.40	37.1	40.5	43.8	3.7	8.4	12.5	46.6	0.095	41.9
S	243	0.37	34.8	38.9	33.2	1.0	6.5	1.0	72.6	-0.098	42.0
E	244	0.40	37.0	40.5	38.1	3.7	8.4	5.1	45.4	-0.095	41.9
L	245	0.52	45.3	47.4		14.6	16.6			0.093	42.0
F	246	0.39	36.3	39.9	-	2.8	7.8			0.094	42.7
	247	0.67	55.3	55.3	48.6	29.0		19.2	9.1	-0.082	41.4
B	250	0.43	39.1	42.0	43.0	6.4	10.5	11.4	46.1	0.068	41.0
O	251	0.47	41.9	44.3	42.0	10.0	13.5	10.1	62.1	0.097	42.2
R	252	0.42	38.4	41.6	39.0	5.5	10.2	6.2	39.3	-0.215	50.3
E	253	0.59	50.0	51.8	44.7	21.2	21.9	15.0	45.0	0.203	50.0
D	254	0.56	48.0	49.8	51.3	18.3	19.3	23.1	54.4	0.197	48.7
	255	0.47	41.9	44.3	47.0	10.0	13.5	16.9	42.4	-0.181	48.5
	256	0.42	38.4	41.6	38.4	5.5	10.2	5.4	65.8	0.147	[illegible]
	257	0.48	42.6	44.3	36.9	10.9	14.2	3.6	39.9	0.251	52.5
	258	0.76	61.4	61.4	52.7	38.7		25.2	83.3	0.218	49.0
	259	0.48	42.6	44.3	44.2	10.9	14.2	13.1	45.0	0.259	49.1
	260	0.46	41.2	44.0	53.0	9.1	13.0	25.6	46.1	0.262	50.4
	261	0.51	44.6	46.7	43.8	13.7	16.0	12.5	42.6	-0.252	49.1
	262	0.53	46.0	48.1	49.4	15.5	17.2	20.3	46.0	-0.271	52.3
IDEAL	263	0.55	47.3	49.1	46.8	17.4	19.0	16.7	44.2	-0.256	50.0

Methods: 1: **Hughes et al. (1977)**
2: **Robertson (1982)**
3: **Manassero (1987)**

FIG 1 SCHEMATIC CROSS-SECTION OF ENEL CRIS CALIBRATION CHAMBER

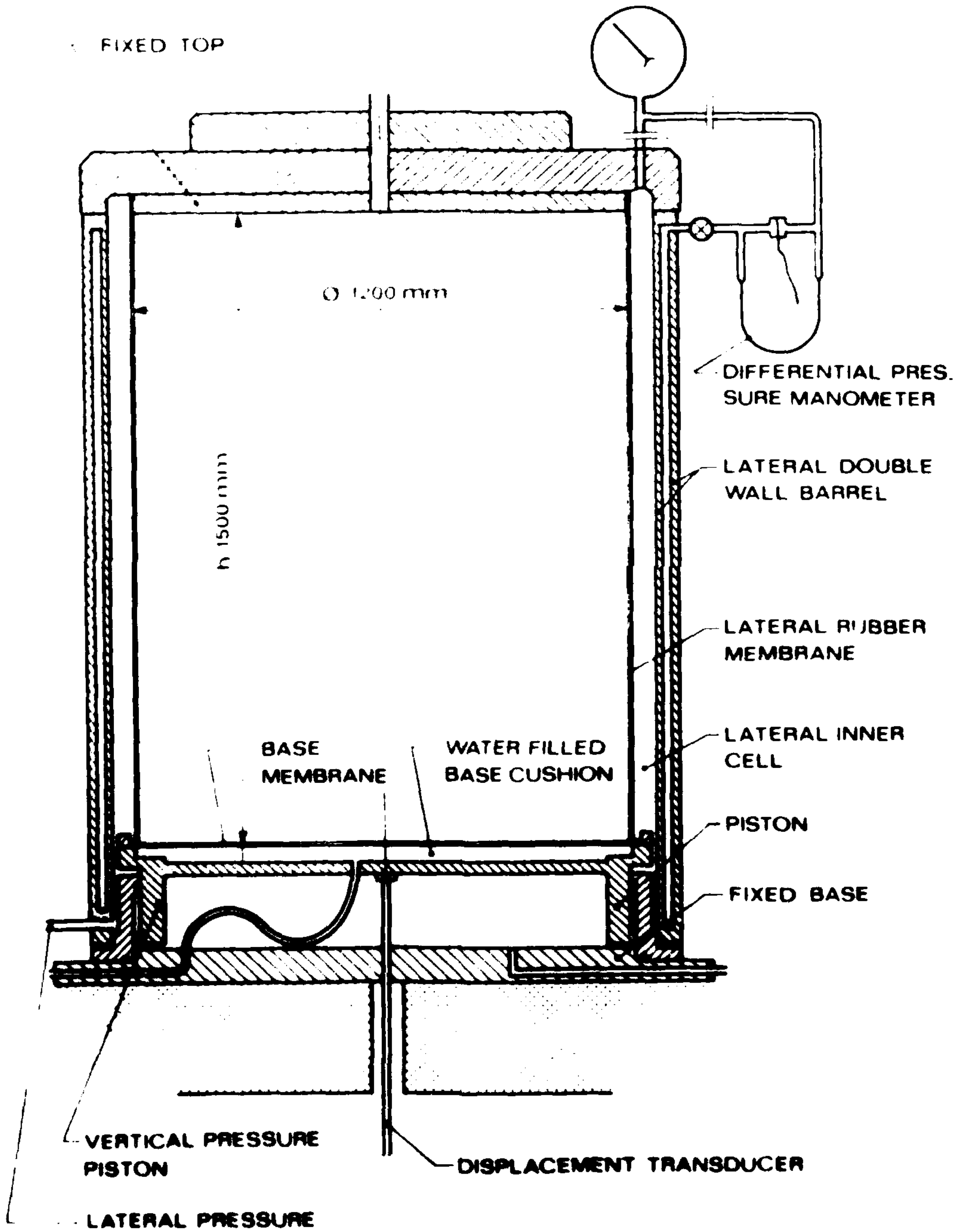

FIG. 2: SCHEMATIC OUTLINE OF CC LOADING SYSTEM AND OF DATA ACQUISITION SYSTEM FOR SBPT IN SAND

CC LOADING SYSTEM

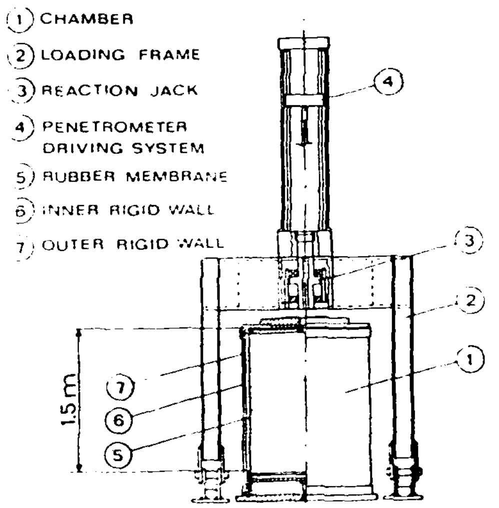

DATA ACQUISITION SYSTEM

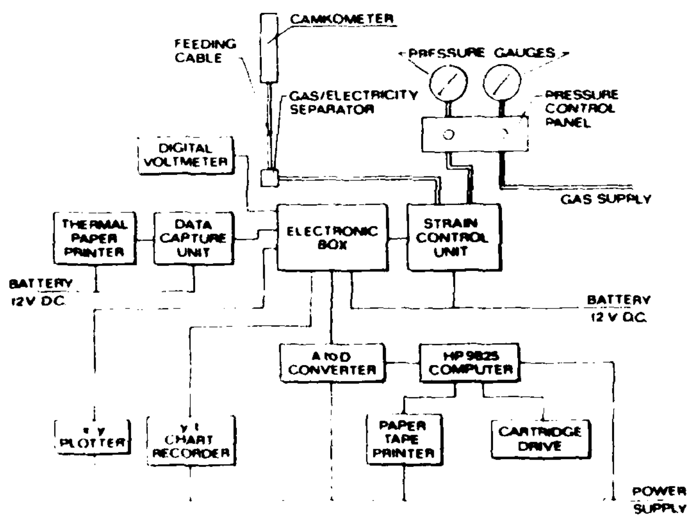

FIG. 3: SCHEMATIC OUTLINE OF SELF BORING PRESSUREMETER PROBE - CAMKOMETER MARK VIII

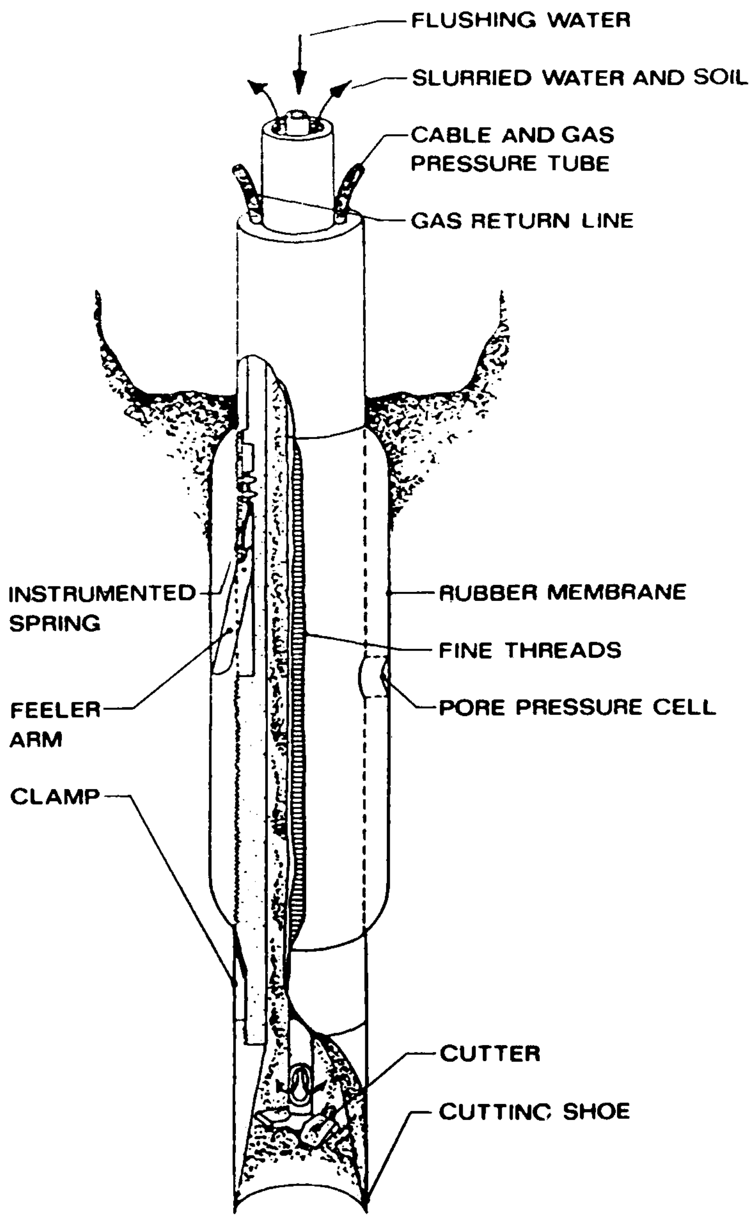

SAND	1 - TICINO	2-HOKKSUND
DOMINANT MINERAL	QUARTZ (30%)	QUARTZ (35%)
ANGULARITY (LEES' CHART)	8 ÷ 9	6 ÷ 8
MICA	~5%	~10%
γ_{max} (t/m^3)	1700	1.759
γ_{min} (t/m^3)	1391	1.438

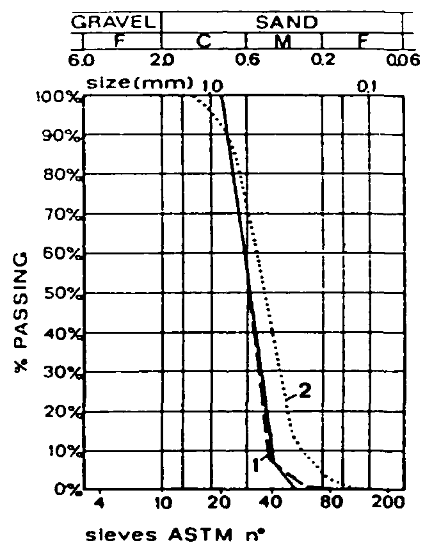

FIG.4 : CHARACTERISTICS OF THE TESTED SANDS

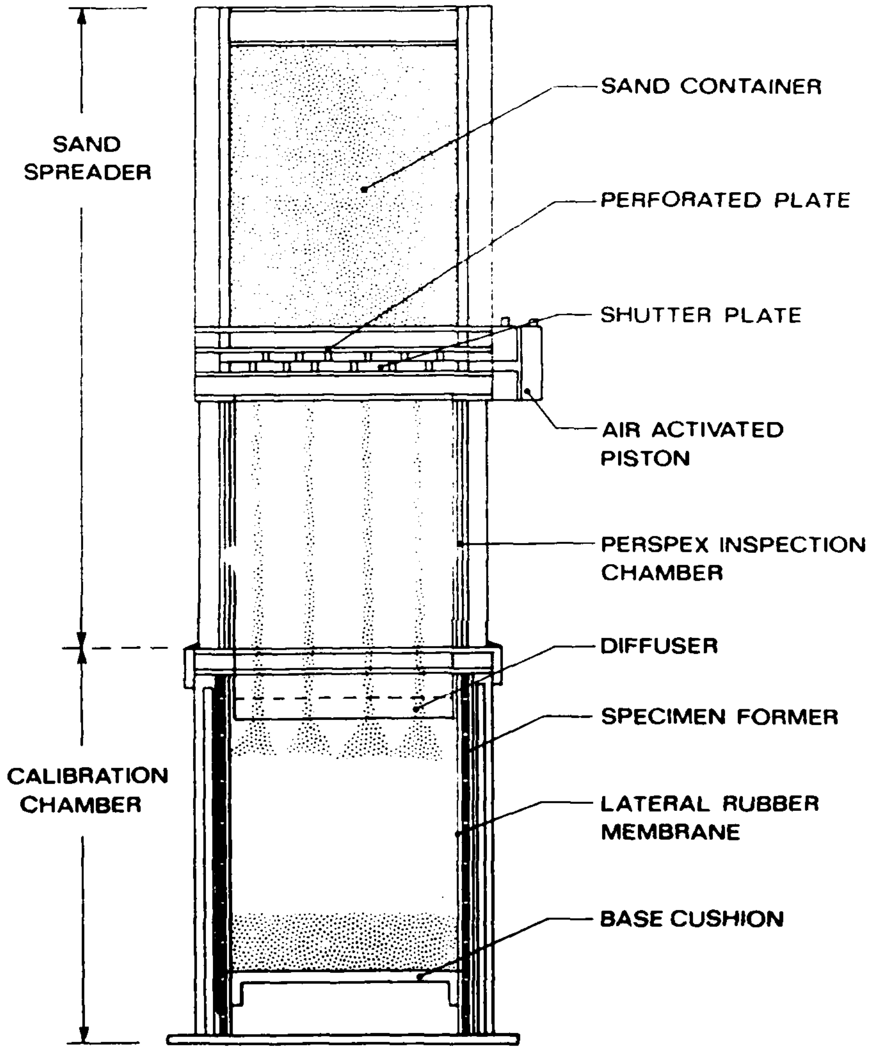

FIG.5 : SCHEMATIC OUTLINE OF SAND SPREADER

FIG.6: SCHEMATIC OUTLINE OF IDEAL INSTALLATION IN CC

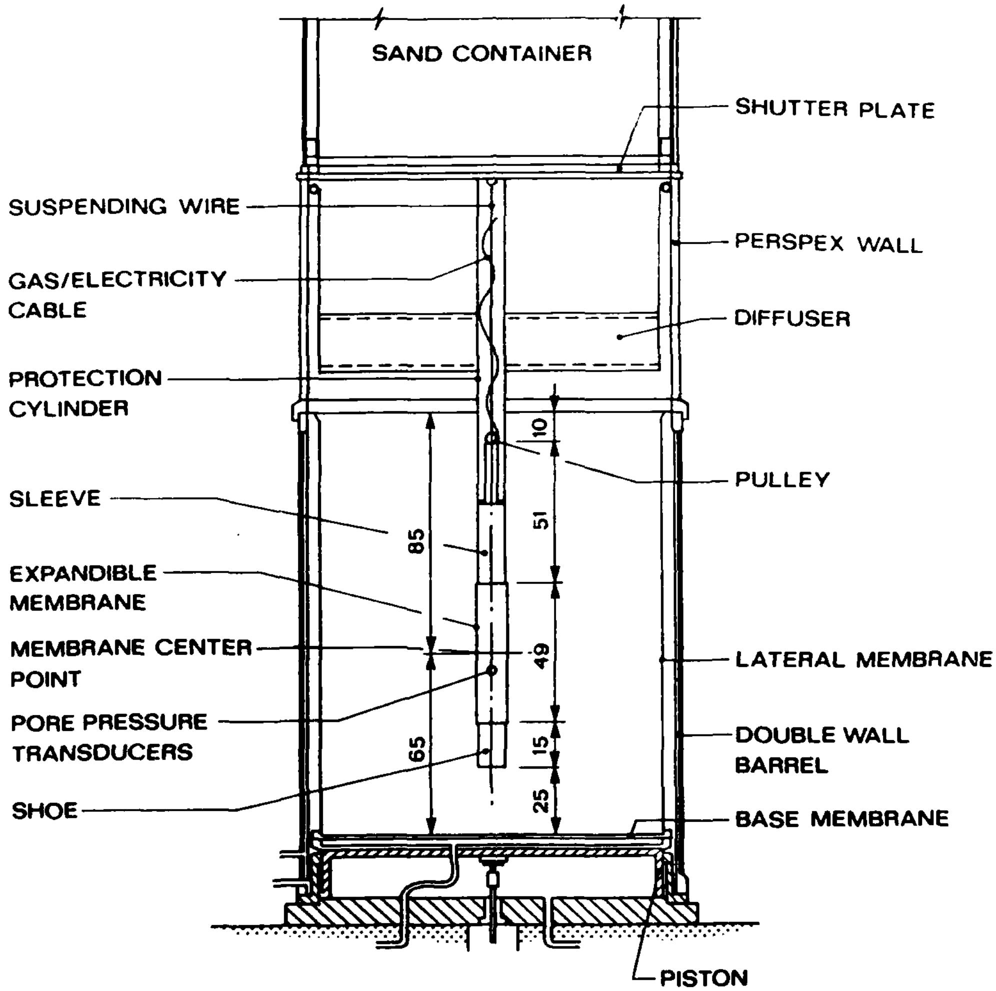

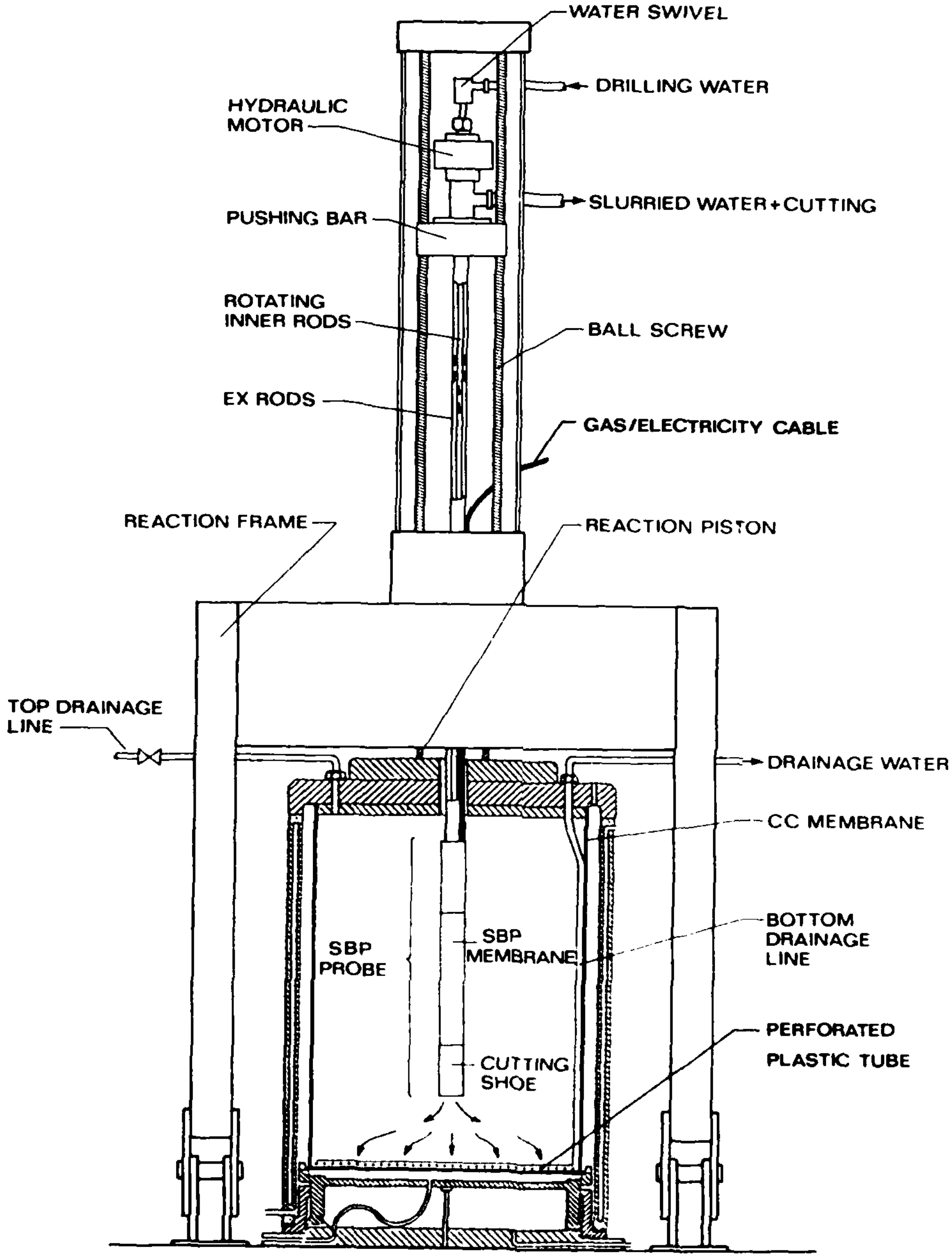

FIG. 7: SCHEMATIC OUTLINE OF SELF-BORING INSTALLATION PROCEDURE IN CC

FIG. 8: EXAMPLE OF SAMPLE CONSOLIDATION

CC TEST 234 - SBP

TICINO SAND TS-4; D_R = 76.1%; OCR = 5.34

CONSOLIDATION PHASE, BC3

Vertical Stress σ'_v [kg/cm^2]	Radial Stress σ'_h [kg/cm^2]	K_o [-]	Tangent Constrained Modulus M_o^t [kg/cm^2]
0.12	0.08	0.613	
0.34	0.15	0.445	346.7
0.68	0.30	0.441	524.8
1.19	0.52	0.433	676.1
1.71	0.75	0.433	794.3
2.20	0.97	0.439	891.3
2.71	1.19	0.440	912.0
3.19	1.40	0.439	1047.1
3.70	1.62	0.439	1122.0
4.21	1.82	0.439	1202.3
4.73	2.08	0.439	1225.9
5.24	2.30	0.439	1318.3
5.76	2.53	0.439	1349.0
6.28	2.76	0.439	1412.5

PRIMARY LOADING

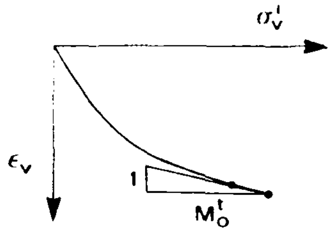

Vertical Stress σ'_v [kg/cm^2]	Radial Stress σ'_h [kg/cm^2]	K_o [-]	Secant Constrained Modulus M_o^s [kg/cm^2]
6.05	2.71	0.448	2884.0
5.84	2.66	0.456	3890.5
5.63	2.61	0.464	3890.5
5.43	2.56	0.473	3630.8
5.22	2.52	0.482	3388.4
4.72	2.39	0.507	3162.3
4.18	2.25	0.538	2818.4
3.69	2.11	0.572	2630.3
3.18	1.95	0.611	2290.9
2.70	1.78	0.657	2089.3
2.16	1.56	0.722	1862.1
1.60	1.30	0.812	1513.6
1.18	1.06	0.904	1174.9

UNLOADING

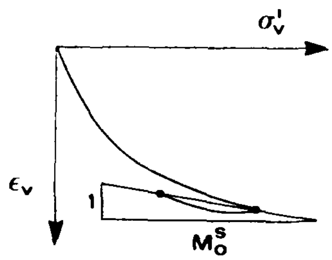

1. Stresses at mid-height of sample (75 cm)
2. No lateral strain $\Delta\epsilon_h = 0$

FIG. 9 : AVAILABLE BOUNDARY CONDITIONS IN CC

BC1 $\sigma_v = \text{const}$ $\quad \sigma_h = \text{const}$

BC2 $\Delta\epsilon_v = \Delta\epsilon_h = 0$

BC3 $\sigma_v = \text{const}$ $\quad \Delta\epsilon_h = 0$

BC4 $\Delta\epsilon_v = 0$ $\quad \sigma_h = \text{const}$

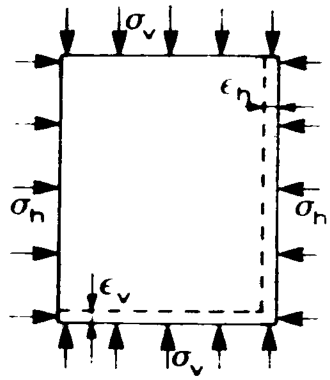

FIG 10 TYPICAL TEST RESULT FROM SBPT IN CC

CC TEST N° 234 SBP
TICINO SAND TS 4, D_R = 76.1 %, OCR = 5.34
PRESSUREMETER TEST, BC1

*All data referred to the average strain of the three strain arms, corrected for membrane stiffness

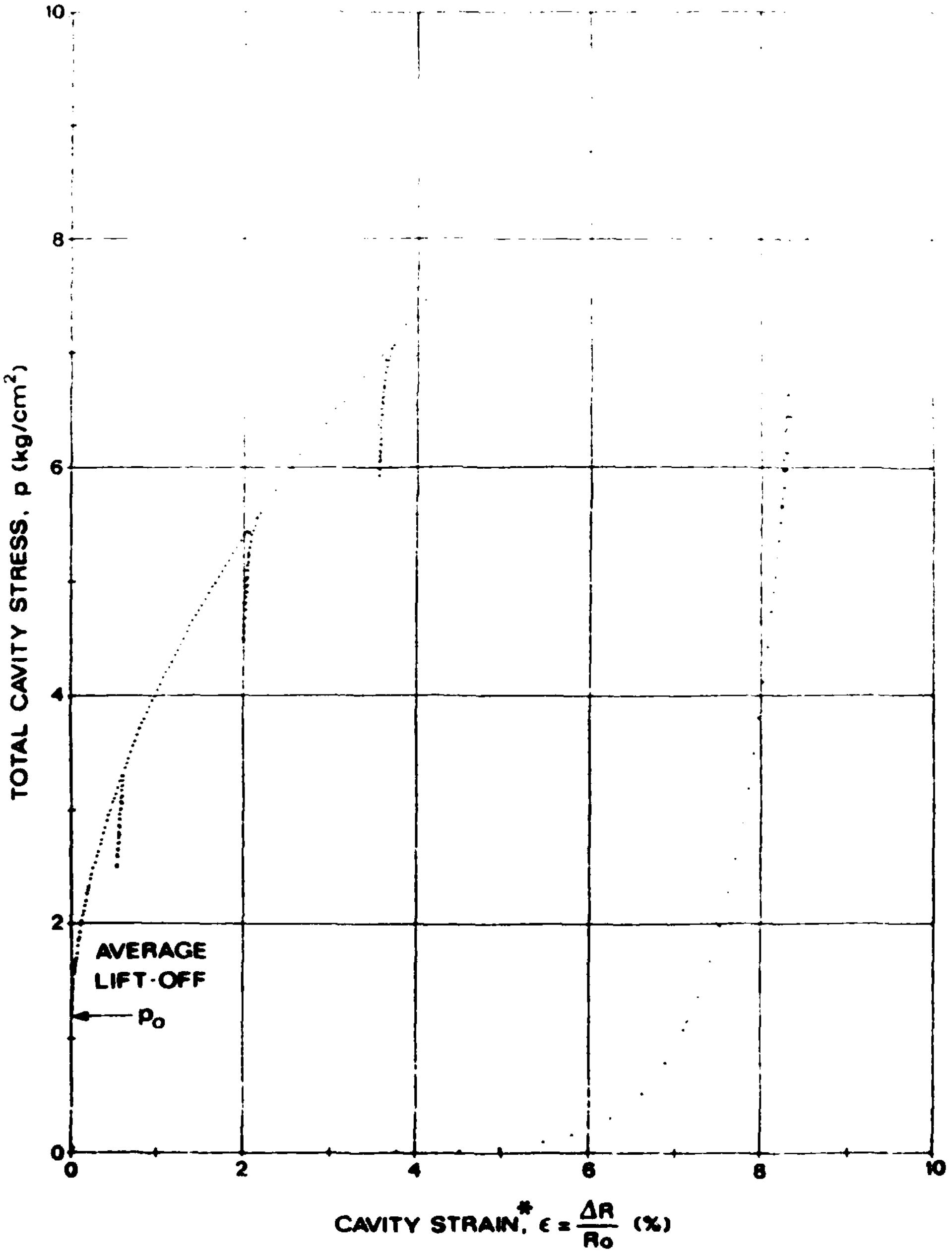

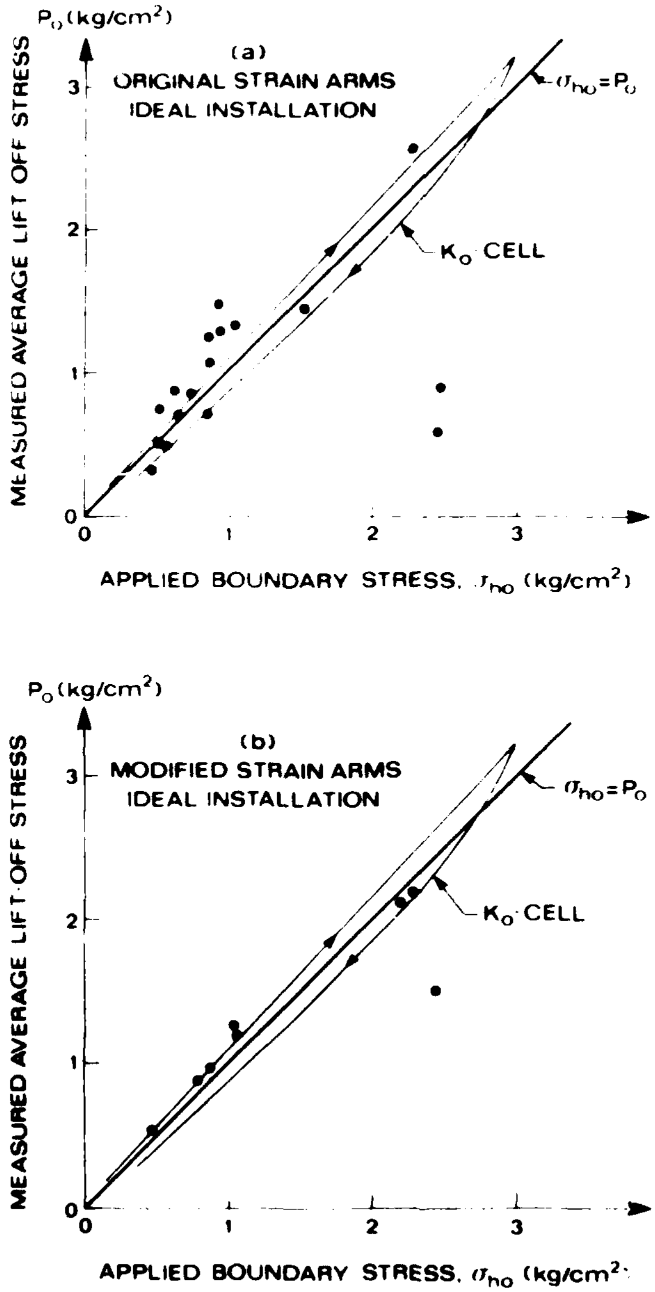

FIG. 11: COMPARISON OF MEASURED LIFT-OFF STRESS AND APPLIED HORIZONTAL STRESS FOR IDEAL INSTALLATION IN CC

FIG. 12

1-D STRESSING OF THE CAMBRIDGE K_0 CELL IN CC

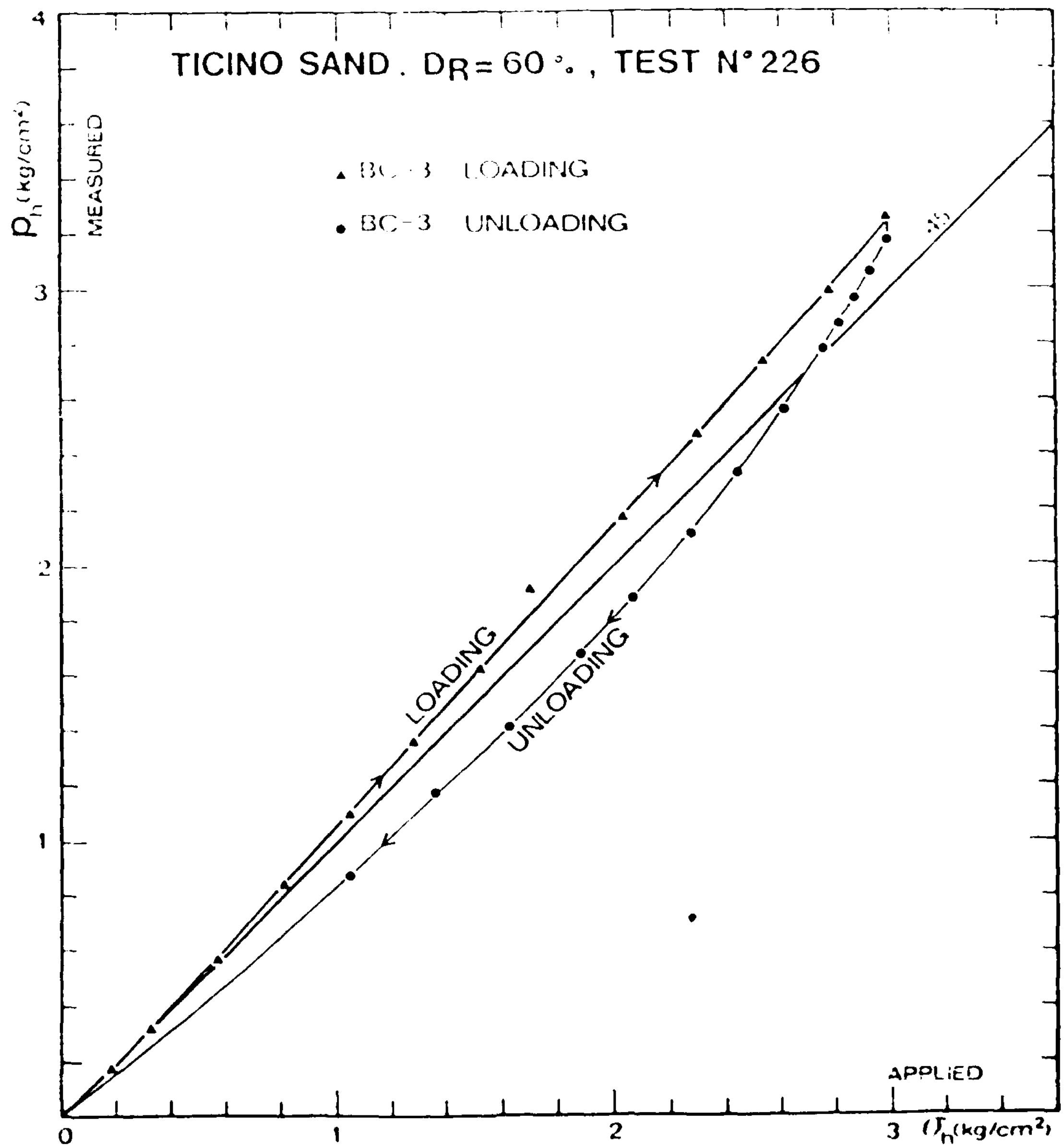

FEELER ARM COMPLIANCE
DURING COMPRESSION PHASE

IDEAL INSTALLATION TEST N 213

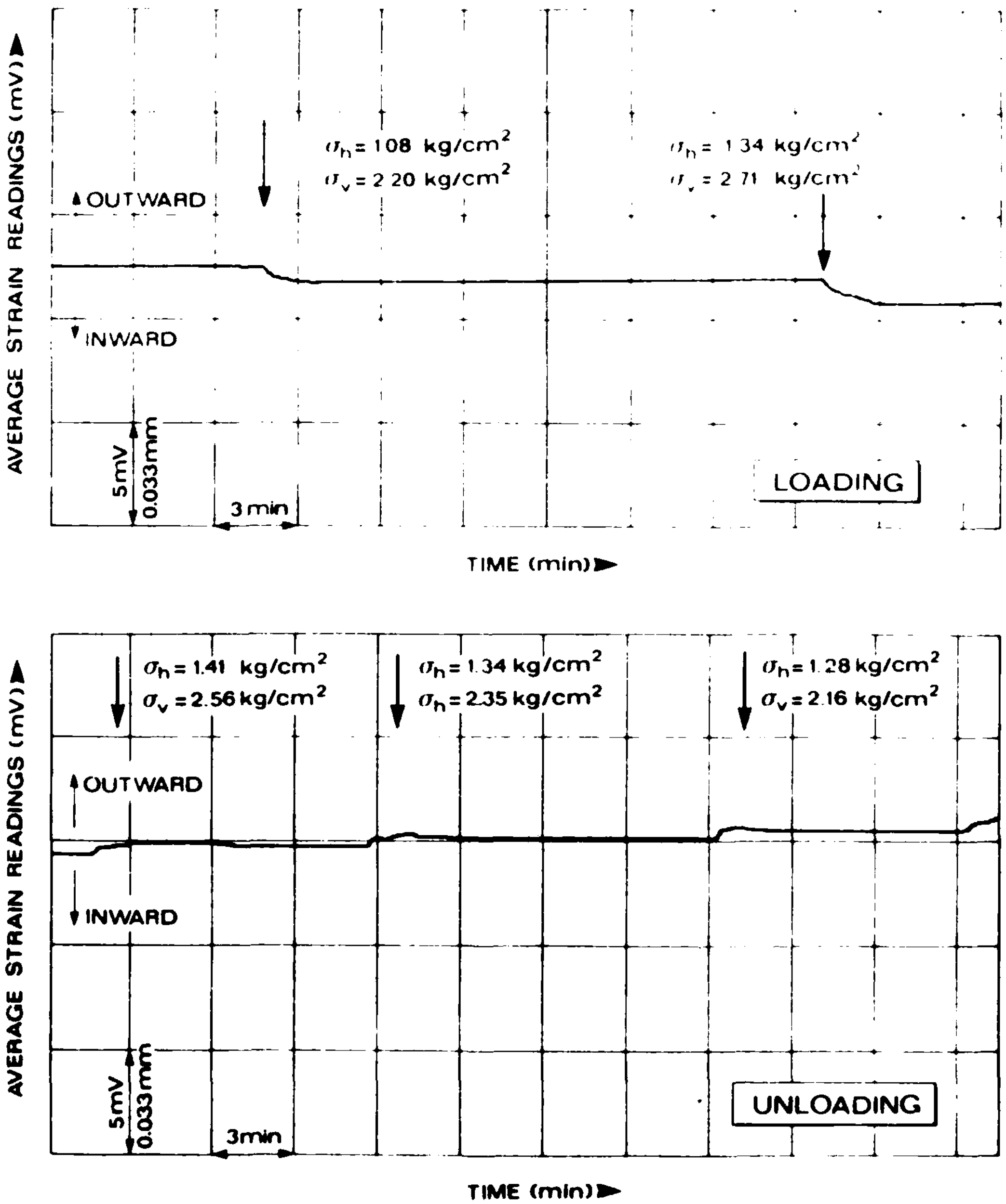

FIG. 13

FIG. 14: EXAMPLE OF PRONUNCED MECHANICAL COMPLIANCE DURING EXPANSION

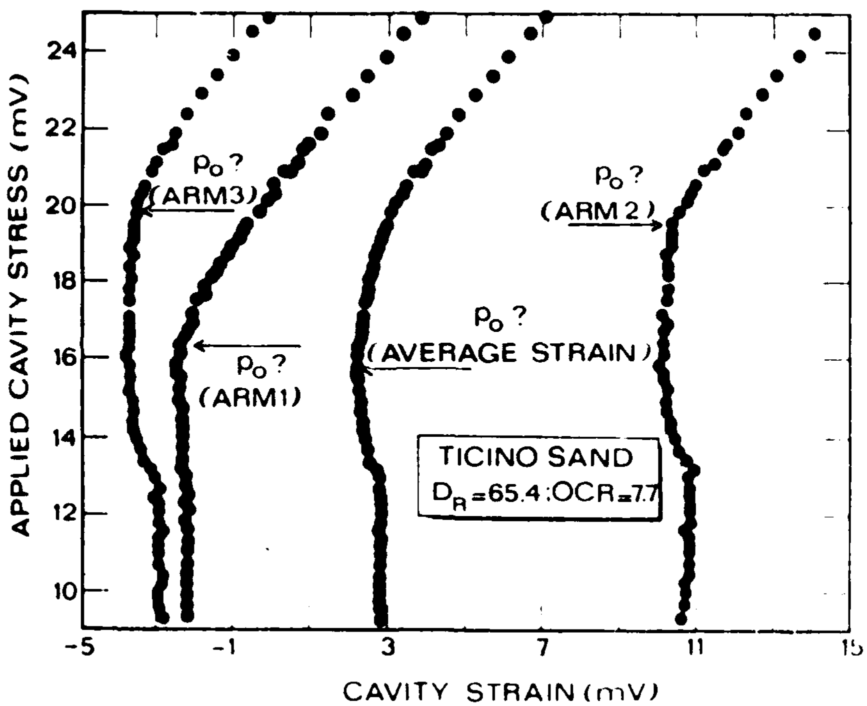

STRAIN OF	"LIFT OFF" p_o (kPa)
TOTAL	80.3
ARM 1	85.3
ARM 2	117.5
ARM 3	120.9

APPLIED LATERAL BOUNDARY STRESS

$\sigma_h = 67.3$ kPa

AVERAGE STRAIN: $1 mV = 6.9 \cdot 10^{-3}$ mm

SINGLE ARM: $1 mV = 2.1 \cdot 10^{-2}$ mm

CAVITY STRESS: $1 mV = 10.02$ kPa

FIG 15: DETAILS OF ORIGINAL AND MODIFIED SBP STRAIN ARMS

ORIGINAL DESIGN

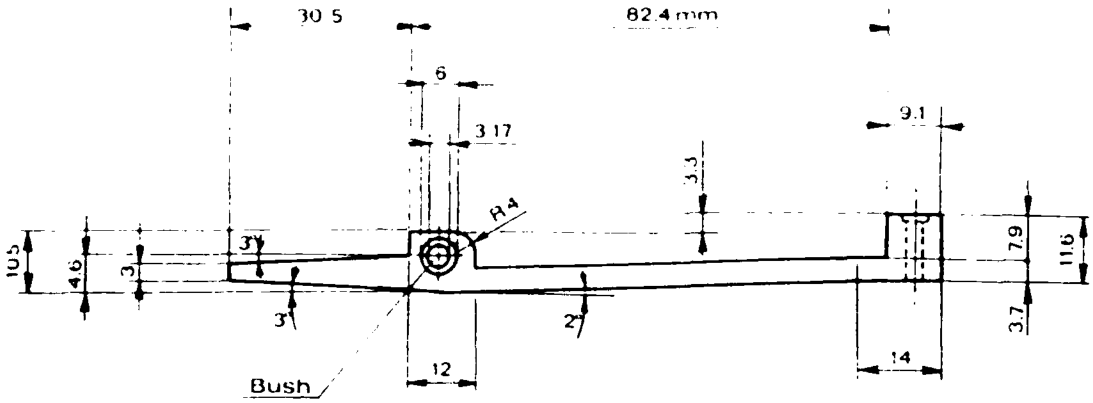

Material:
Brass

MODIFIED DESIGN

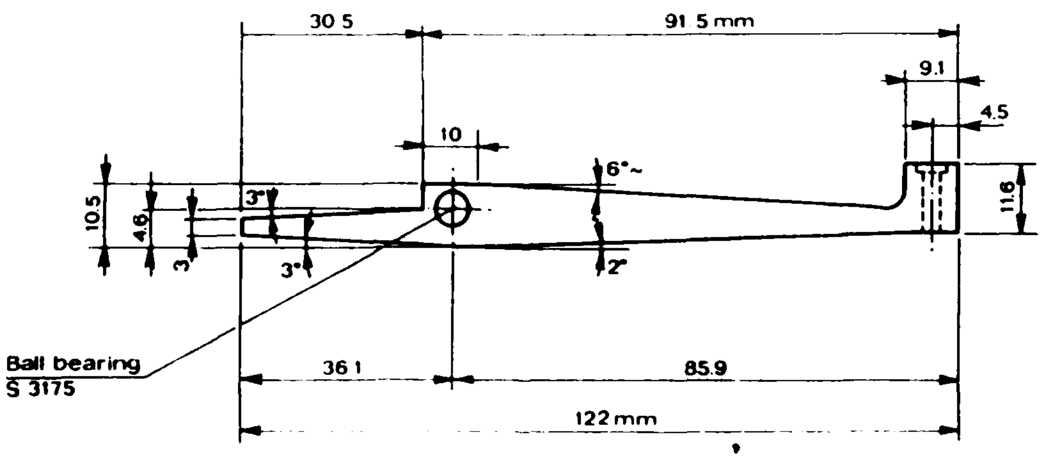

Material:
Stainless steel
AISI 420 F

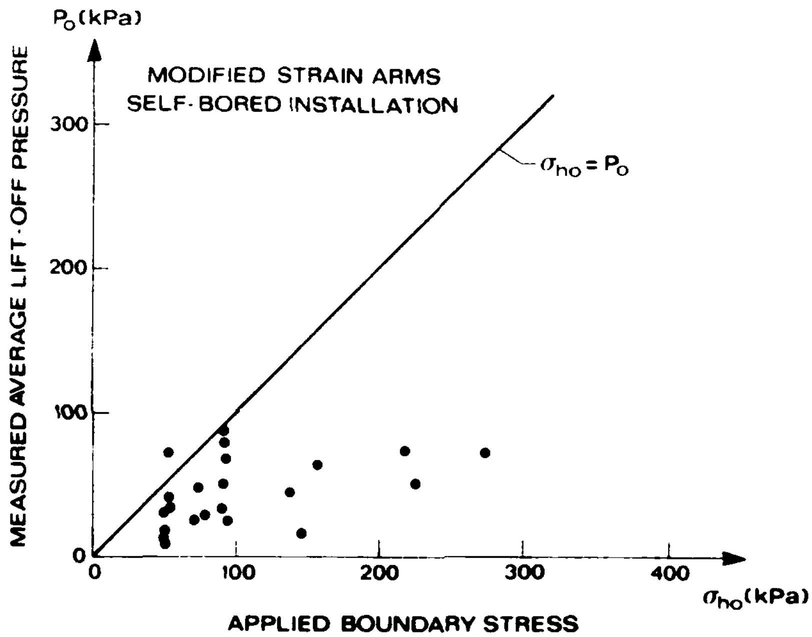

FIG. 16: COMPARISON BETWEEN MEASURED AVERAGE LIFT-OFF PRESSURES AND APPLIED STRESSES FOR SELF-BORED INSTALLATION

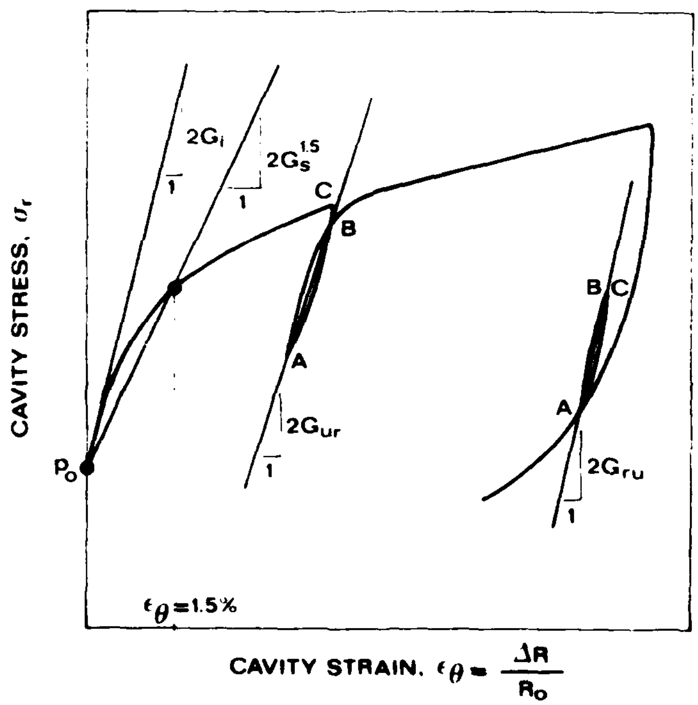

FIG.17: SCHEMATIC OF SHEAR MODULI FROM SBP TESTS

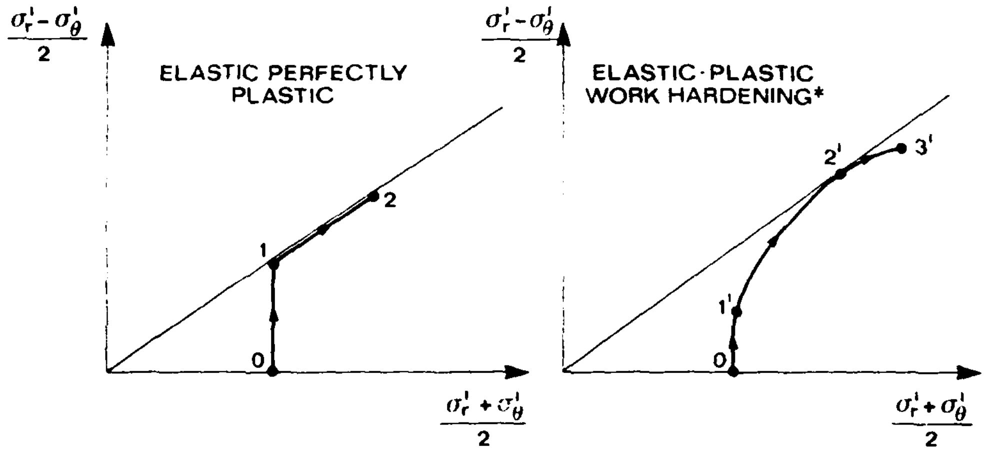

$\overline{0,1}$ → LINEAR ELASTIC

$\overline{1,2}$ → PERFECTLY PLASTIC

$\overline{0,1'}$ → ELASTIC

$\overline{1',2'}$ → ELASTO-PLASTIC STRAIN HARDENING

2' → $\frac{\sigma_r'}{\sigma_\theta'}$ = MAXIMUM

$\overline{2',3'}$ → ELASTO-PLASTIC STRAIN SOFTENING

(*) ACCORDING MANASSERO (1987)

FIG. 18: SCHEMATIC OF EFFECTIVE STRESS PATH OF SOIL ELEMENT ADJACENT TO AN EXPANDING PRESSUREMETER

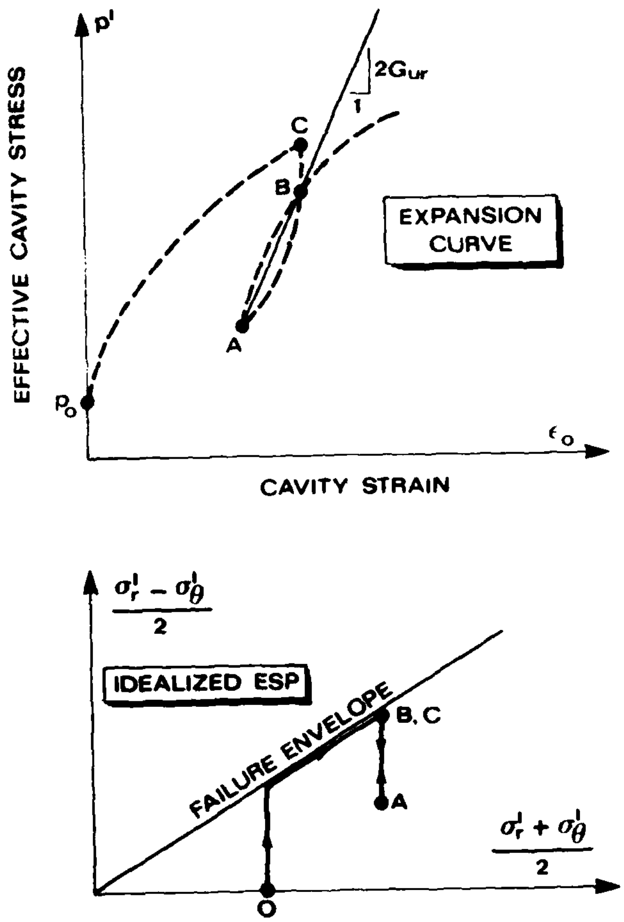

FIG. 19: SCHEMATIC OF UNLOADING-RELOADING CYCLE DURING SBPT IN SAND

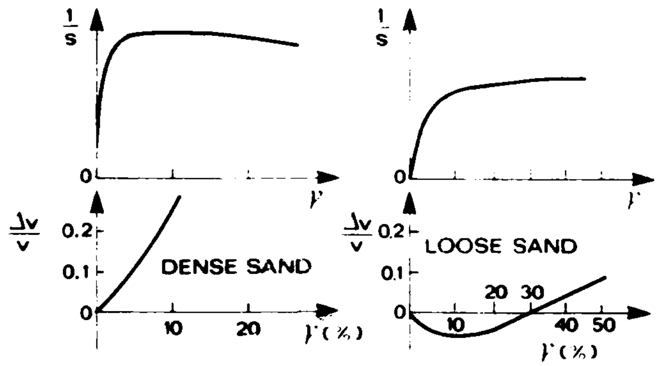

a) RESULTS OF SIMPLE SHEAR TEST (AFTER STROUD 1971)

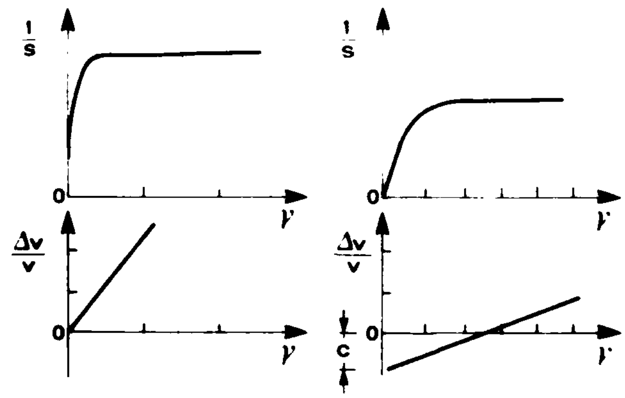

b) SIMPLIFIED MODEL ASSUMED BY HUDGES ET AL (1977)

FIG 20 : STRESS-STRAIN AND VOLUMETRIC STRAIN-SHEAR STRAIN CURVES FOR a) SIMPLE SHEAR TEST RESULTS (STROUD, 1971), b) IDEALIZED BY HUGES ET AL (1977)

FIG.21: Stress / strain relationships from test N 222 (D_R =46.2 %)

MANASSERO (1987)

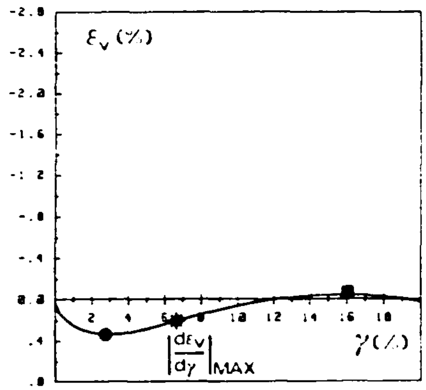

a) Volumetric strain vs shear strain

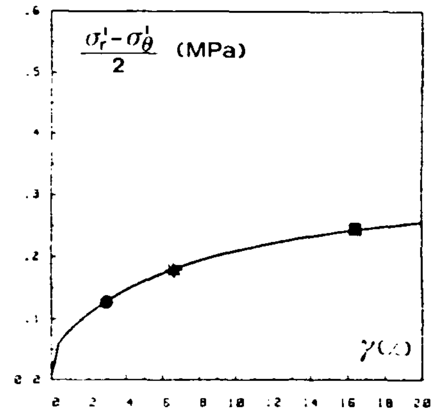

b) Shear stress vs shear strain

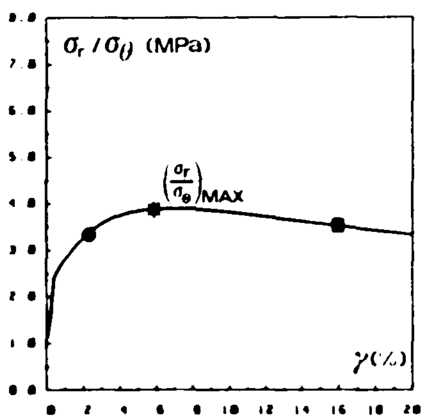

c) Stress ratio vs shear strain

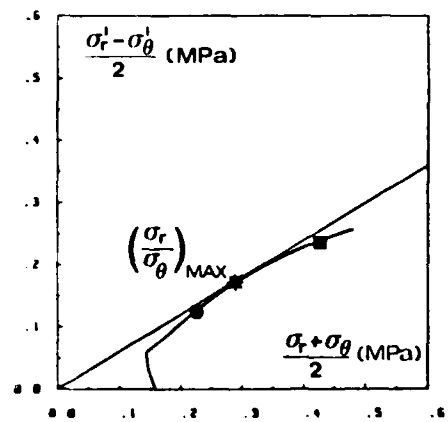

d) Shear stress vs mean normal stress

FIG.22 Stress / strain relationships from test N. 228 (D_R = 77.0 %)

MANASSERO (1987)

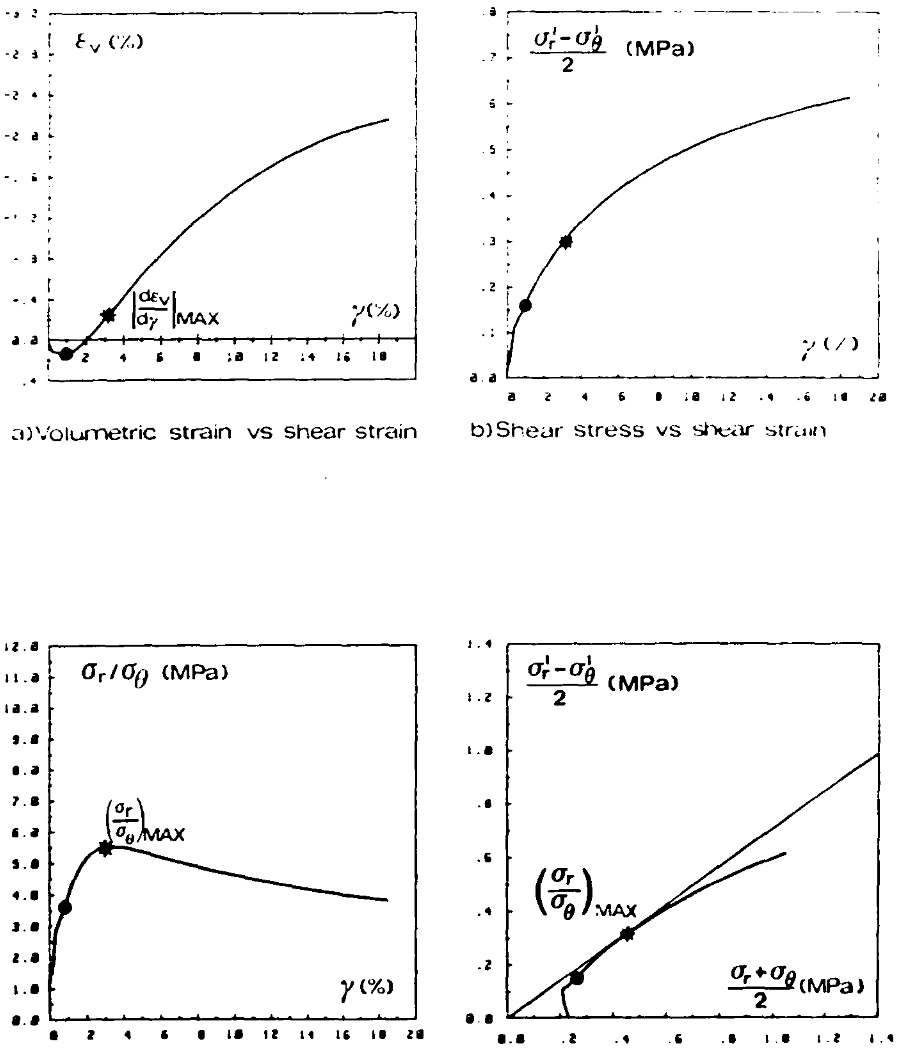

a) Volumetric strain vs shear strain

b) Shear stress vs shear strain

c) Stress ratio vs shear strain

d) Shear stress vs mean normal stress

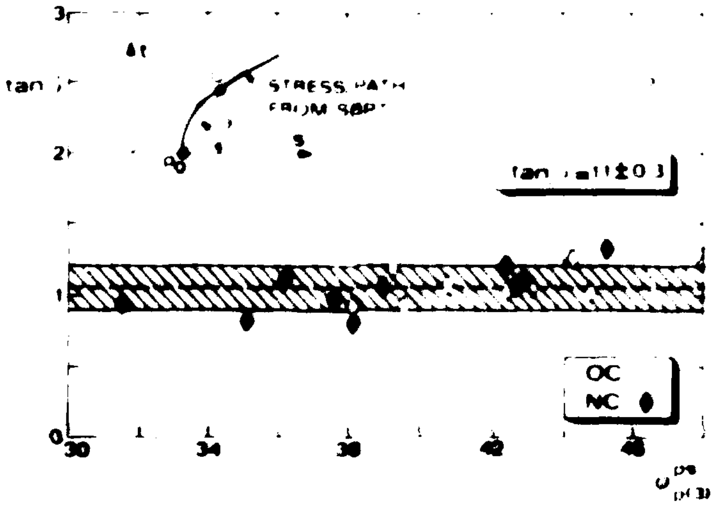

FIG. 23 ANGLE β. DEVIATION OF THE ESP FROM ISOTROPIC ELASTIC BEHAVIOUR (FOR WHICH β = 90°)

MANASSERO (1987)

FIG. 24: φ_{cv} OF SANDS USED IN CC TEST

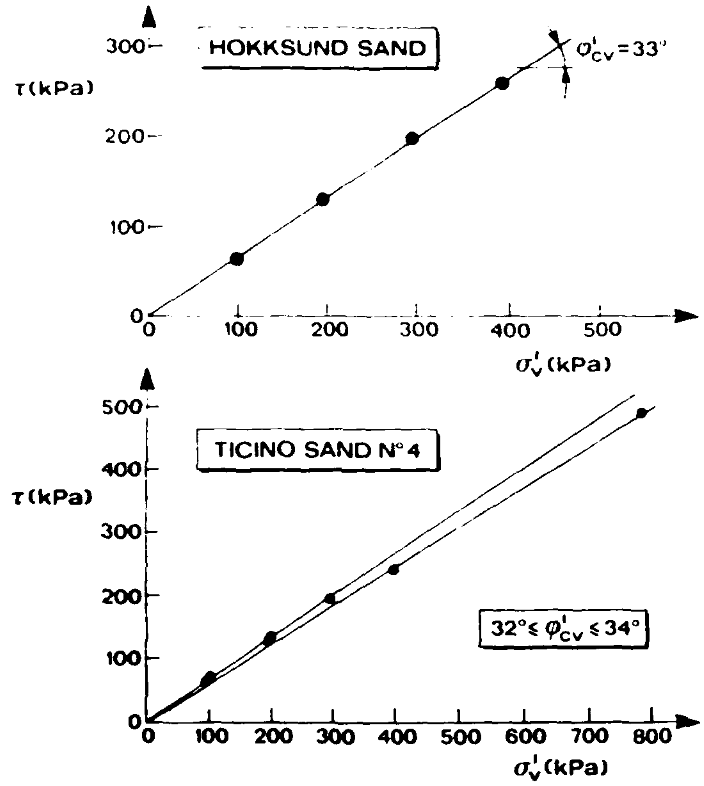

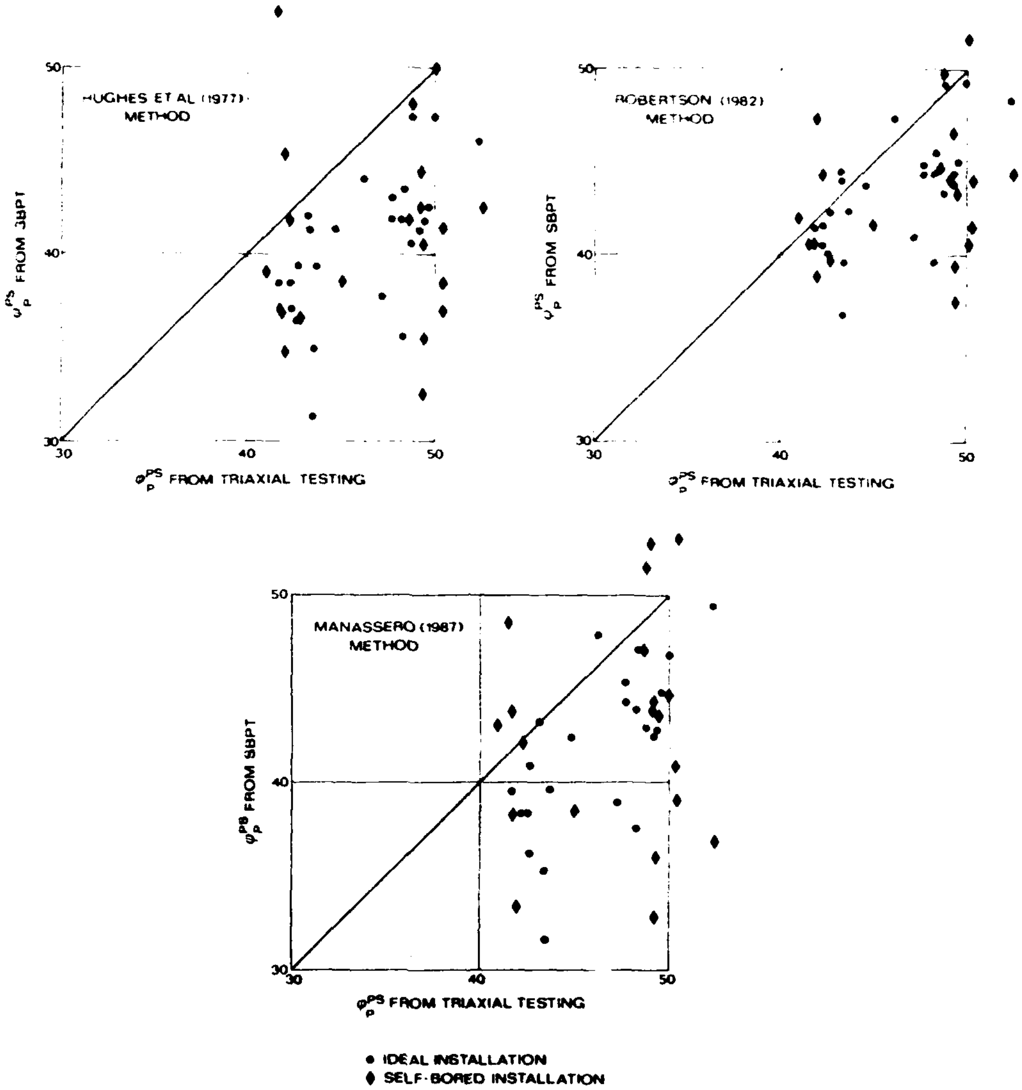

FIG. 25: COMPARISON OF CALCULATED φ_p^{PS} FROM SBPT AND EQUIVALENT φ_p^{PS} FROM TRIAXIAL TESTS

APPENDIX I

EXAMPLE OF COMPUTER GENERATED PLOTS

FOR TYPICAL SBPT RESULT

ENEL-CRIS OF MILAN AND TECHNICAL UNIVERSITY OF TURIN
CC TEST N 234 - SBP
TICINO SAND TS-4; Dr=76.1%; OCR=5.34
PRESSUREMETER TEST, BCI
(All data referred to the average strain of the three strain arms)

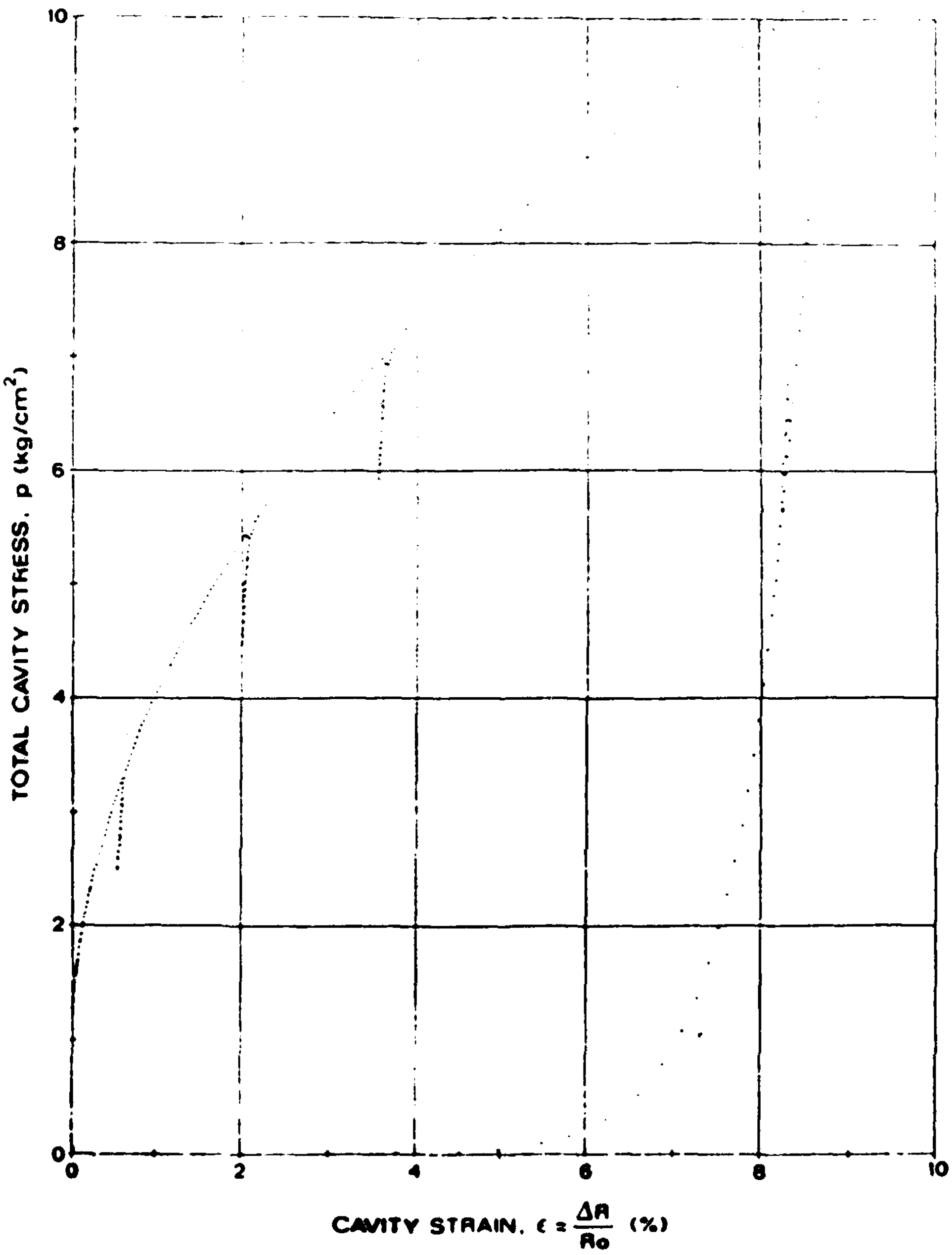

ENEL-CRIS OF MILAN AND TECHNICAL UNIVERSITY OF TURIN
CC TEST N.234 - SBP
TICINO SAND TS-4; Dr=76.1%, OCR=5.34
PRESSUREMETER TEST, 301
(All data referred to the average strain of the three strain arms)

LOOP N°1 UR

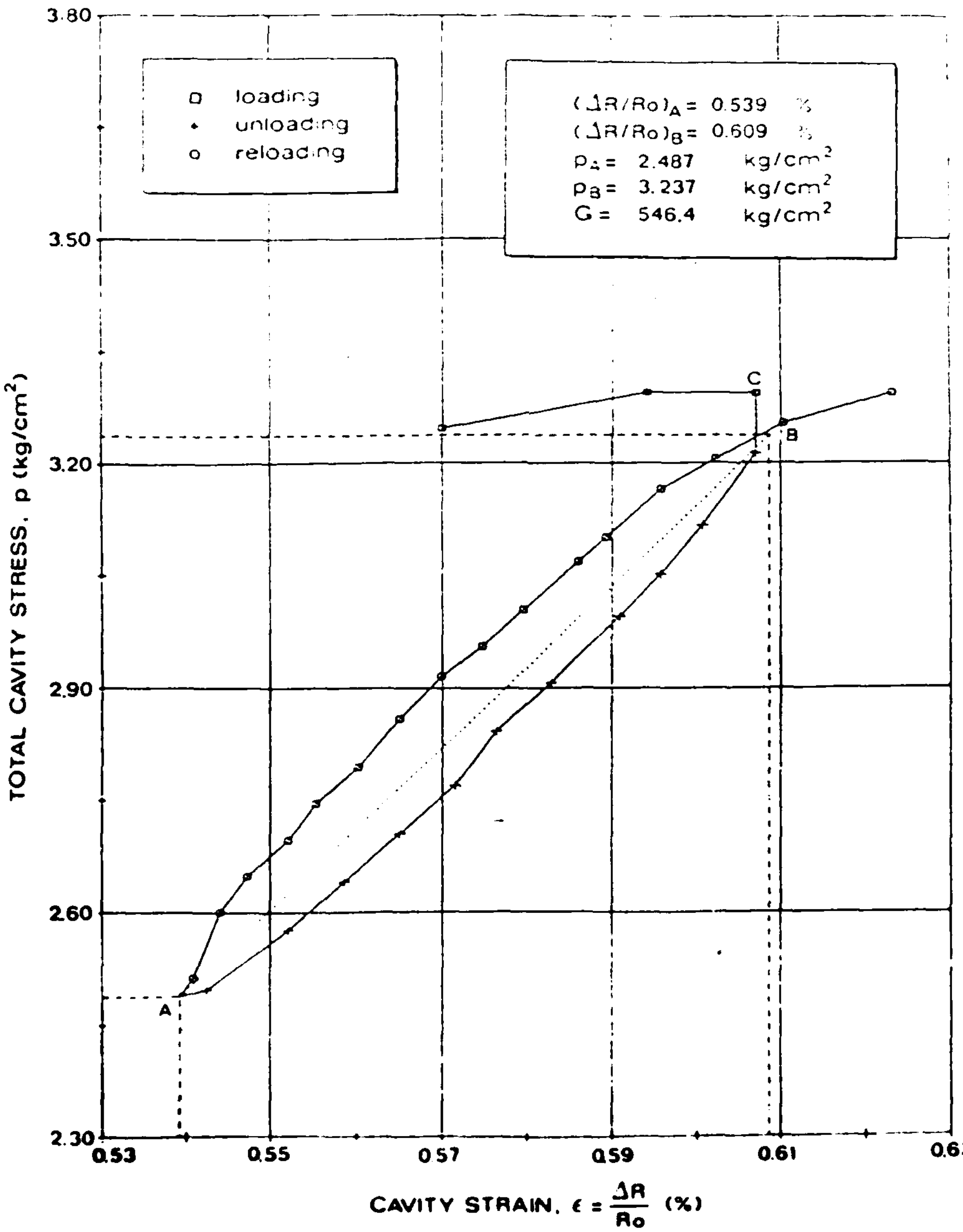

ENEL CRIS F MILAN AND TECHNICAL UNIVERSITY OF TURIN
CC TEST N 234 - SBP
TICINO SAND TS-4; Dr=76 1%; OCR=5 3
PRESSUREMETER TEST, BC1
(All data referred to the average strain of the three strain arms)

LOOP N° 2 UR

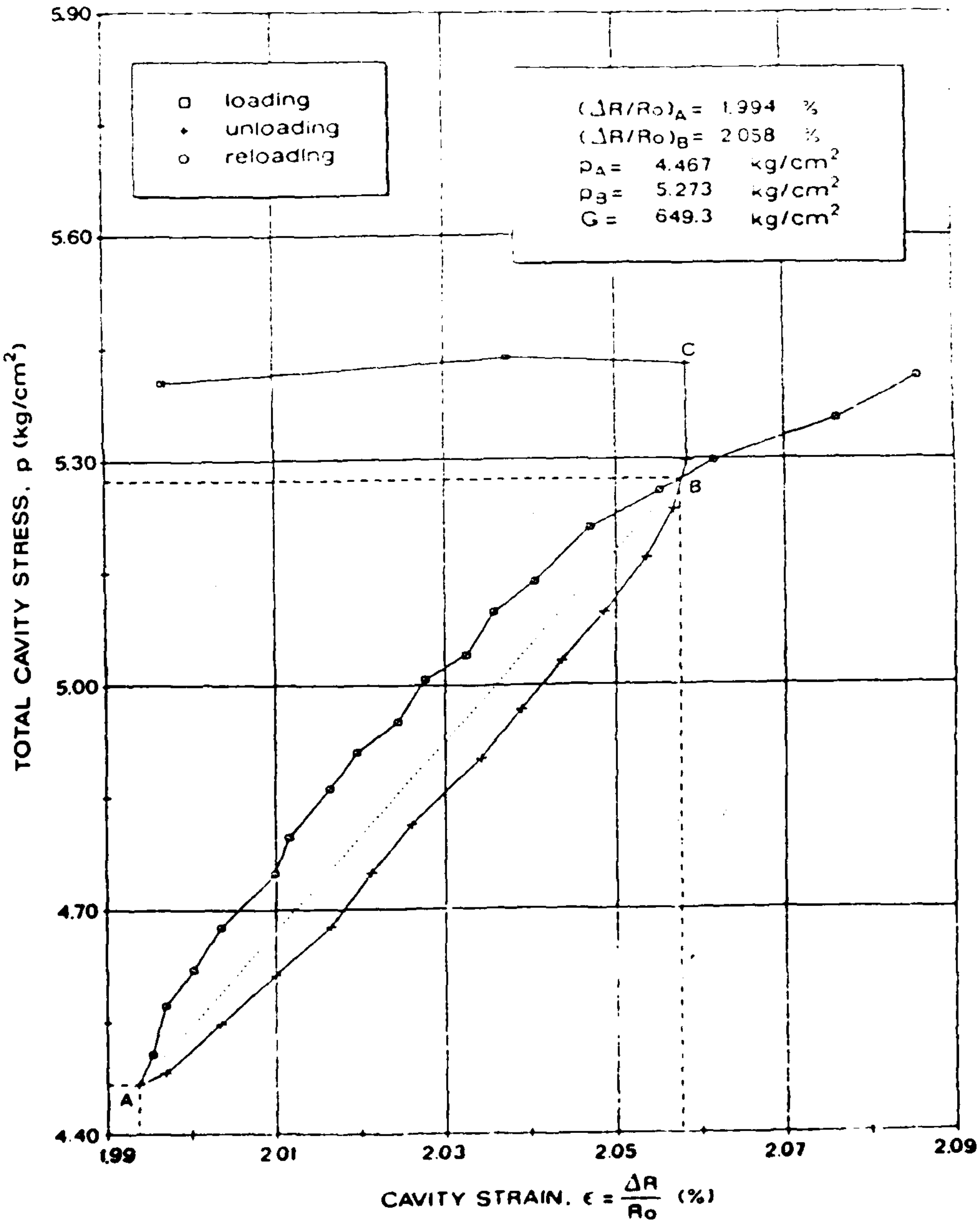

ENEL CRIS OF MILAN AND TECHNICAL UNIVERSITY OF TURIN
CC TEST N 234 - SBP
TICINO SAND TS-4, Dr=76 1%, OCR=5 3%
PRESSUREMETER TEST, BC1
(All data referred to the average strain of the three strain arms)

LOOP N° 3 UR

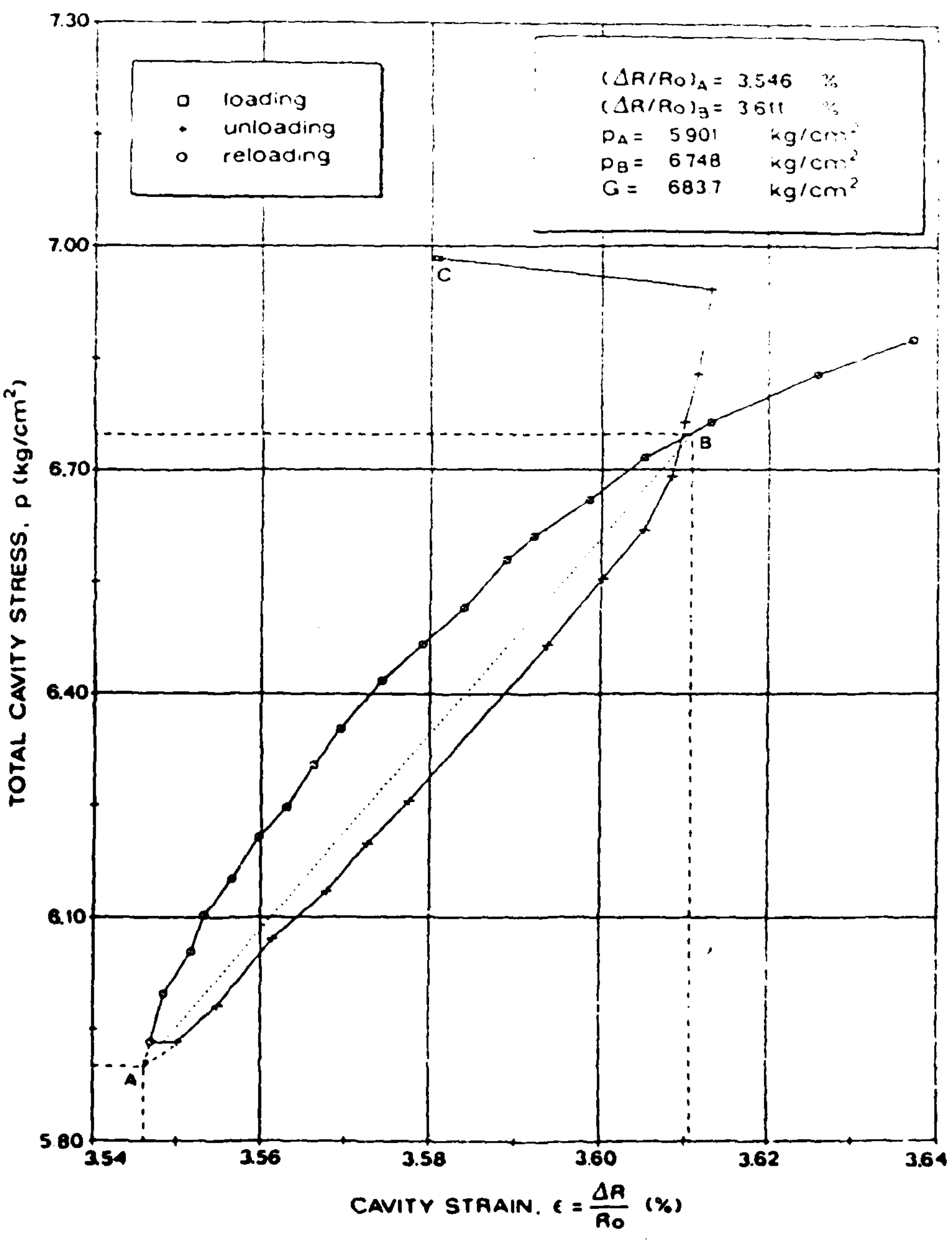

ENEL CRIS OF MILAN AND TECHNICAL UNIVERSITY OF TURIN
CC TEST N 2?. SBP
TICINO SAND TS 4, Dr=76 1%, ...
PRESSUREMETER TEST, BC1
(All data referred to the average strain of the three strain arm

LOOP N° 4 RU

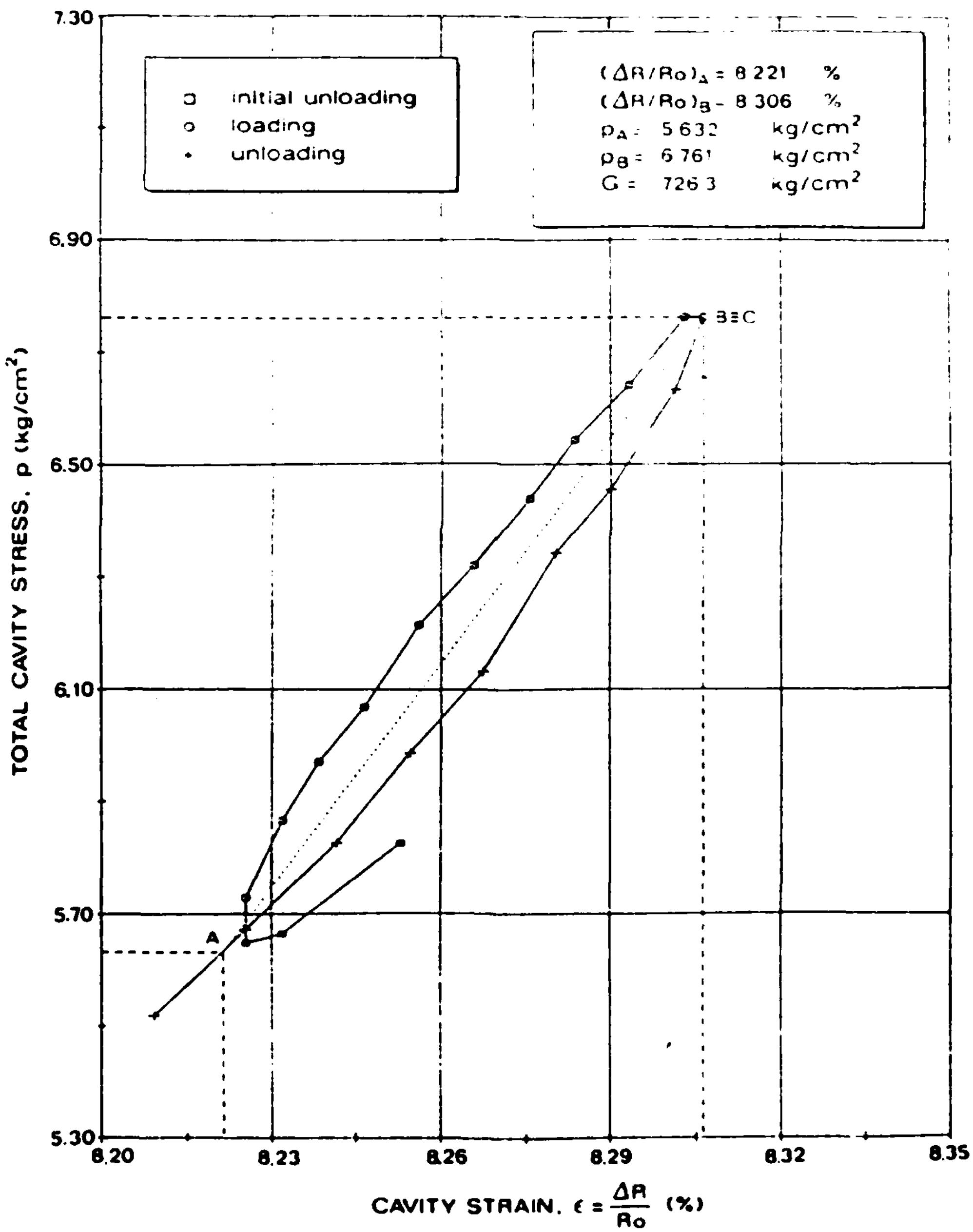

ENEL-CRIS OF MILAN AND TECHNICAL UNIVERSITY OF TURIN
CC TEST N.234 - SBP
TICINO SAND TS-4; Dr=76.1%; OCR=5.34
PRESSUREMETER TEST, BC1
(All data referred to the average strain of the three strain arms)

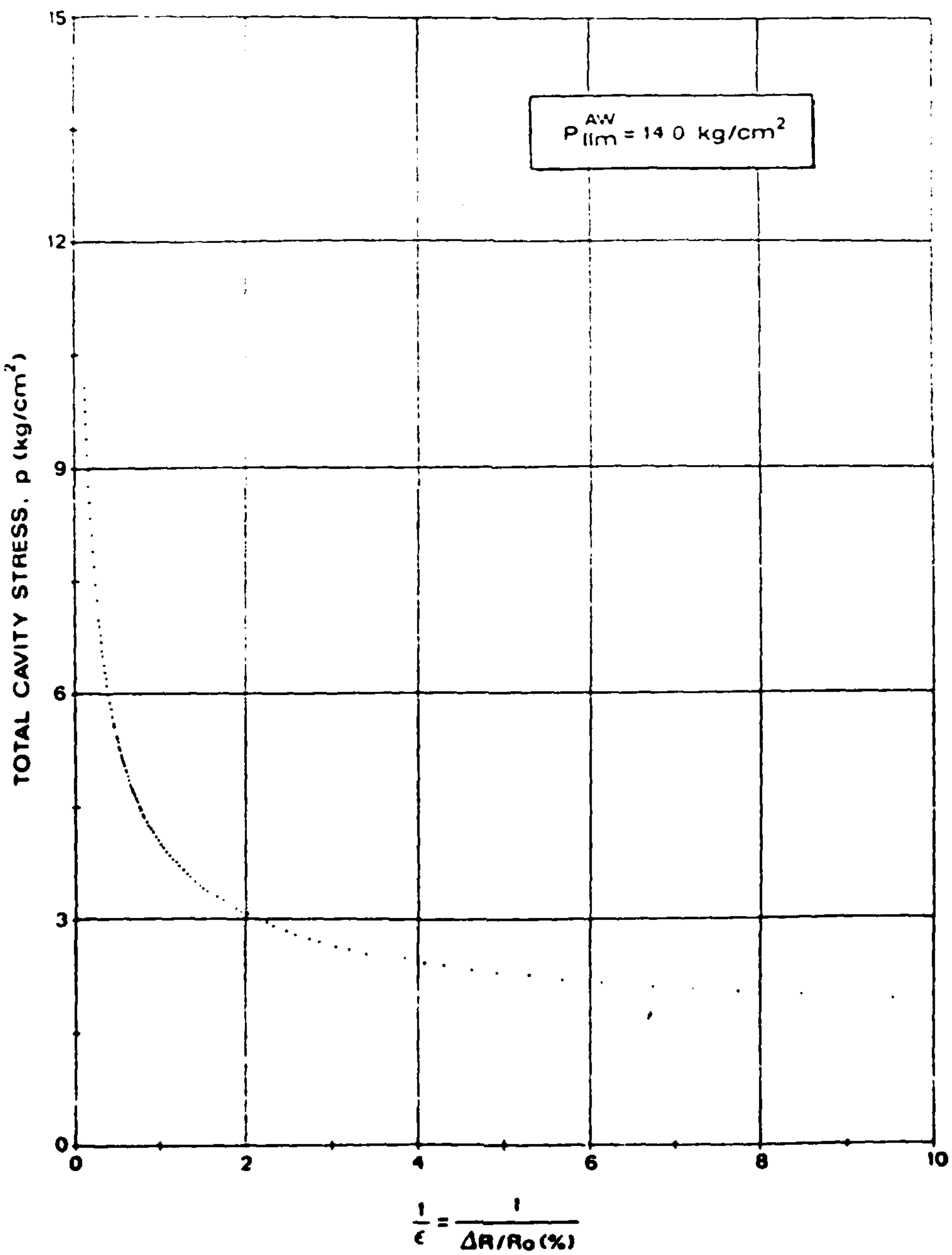

ENEL-CRIS OF MILAN AND TECHNICAL UNIVERSITY OF TURIN
CC TEST N.234 - SBP
TICINO SAND TS-4; Dr=76.1%, OCR=5.34
PRESSUREMETER TEST, BC1
(All data referred to the average strain of the three strain arms)

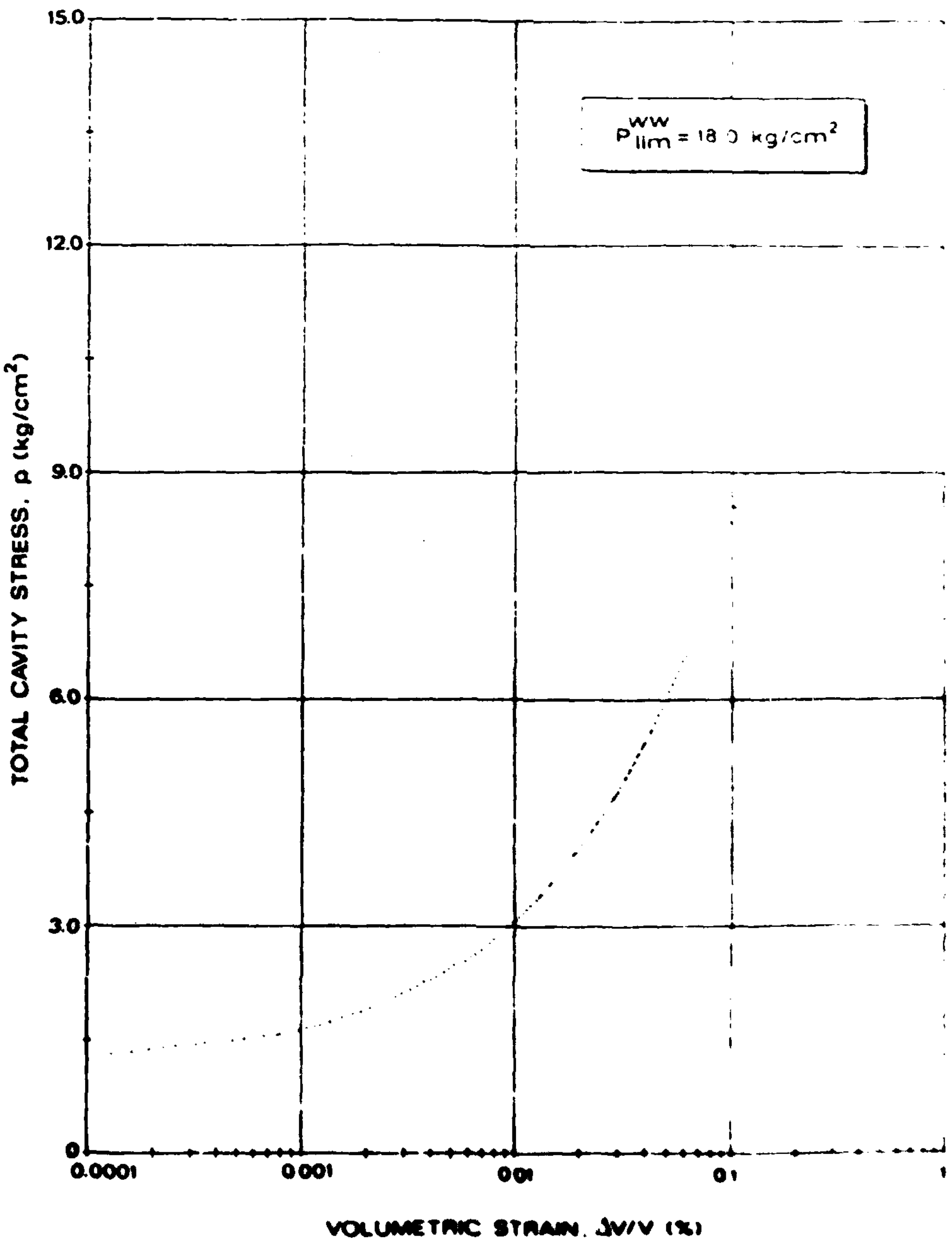

ENEL-CRIS OF MILAN AND TECHNICAL UNIVERSITY OF TURIN
CC TEST N 234 SBP
TICINO SAND TS-4, Dr=76 14, OCR=5 34
PRESSUREMETER TEST, BC1
(All data referred to the average strain of the three strain arms)

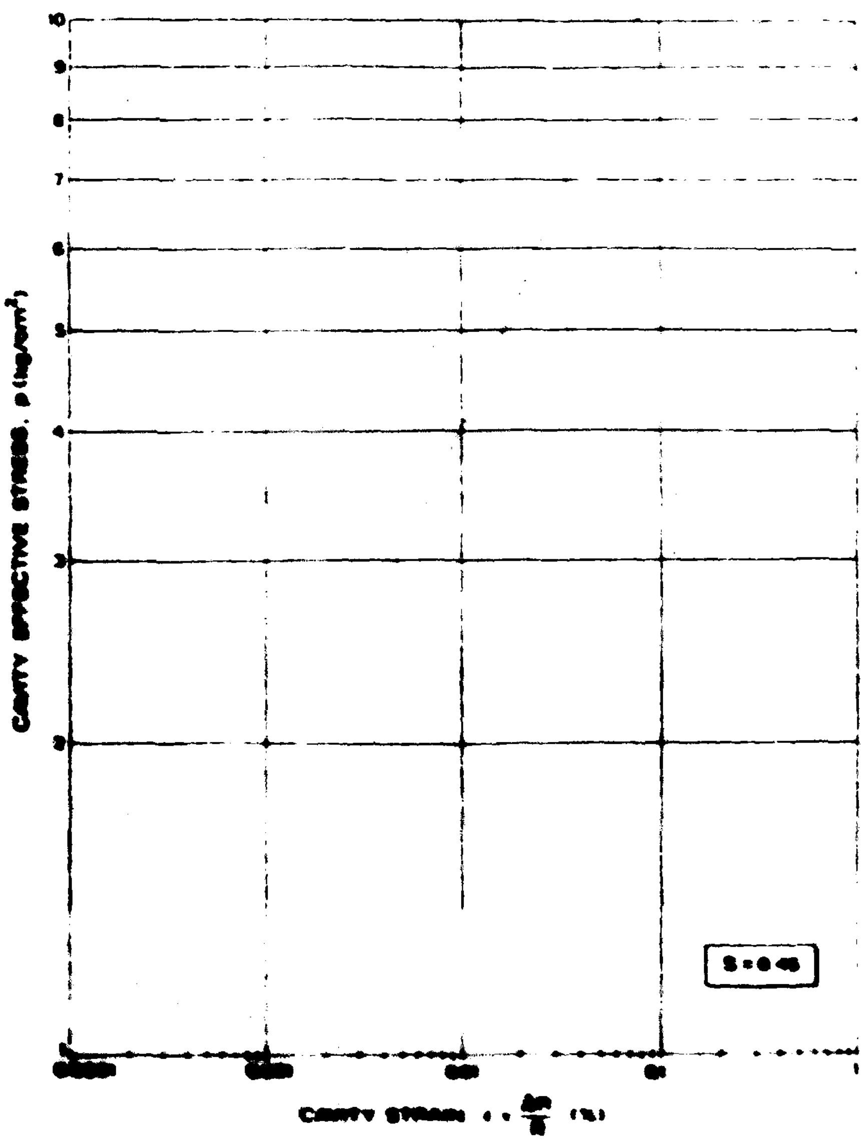

APPENDIX II

COMPLETE LISTING FOR EACH

SBPT RESULTS

APPENDIX III

CALCULATION OF AVERAGE STRESS ON HORIZONTAL PLANE IN PLASTIC ZONE AROUND EXPANDING CAVITY

AVERAGE STRESS ON HORIZONTAL PLANE IN PLASTIC ZONE

$$s = \frac{\sigma'_r + \sigma'_\theta}{2} = \frac{p'_c}{1 + \sin \phi'_{PS}} \left(\frac{R}{r} \right)^{1-K_a} \qquad \ldots (1)$$

where:

σ'_r = radial effective stress at a generic radial distance $r \leq R_p$

σ'_θ = circumferential effective stress at a generic radial distance $r \leq R_p$

p'_c = effective cavity stress at which unloading-reloading loop starts

r = radial distance

R_p = radius of plastic zone

R = current cavity radius

$$K_a = \frac{1-\sin \phi'_{PS}}{1+\sin \phi'_{PS}}$$

$$p'_{AV} = \frac{\int_R^{R_p} s \, dr}{\int_R^{R_p} dr} \qquad \ldots (2a)$$

or:

$$p'_{AV} = \frac{\int_R^{R_p} s \cdot 2\pi r \cdot dr}{\int_R^{R_p} 2\pi r \cdot dr} \qquad \ldots (2b)$$

Due to the tentative and preliminary nature of the proposed approach, the more simple solution ... (2a) integrating s along the radius r is the only method considered here.

Introducing the value of s from equation ... (1) into equation ... (2a) one obtains:

$$p'_{AV} = \frac{p'_c}{1 + \sin \phi'_{PS}} \left(R \right)^{1-K_a} \frac{\int_R^{R_p} \left(r \right)^{K_a - 1} dr}{R_p - R}$$

$$p'_{AV} = \frac{p'_c}{1 - \sin \phi'_{PS}} \cdot \frac{\left(\frac{R_p}{R} \right)^{K_a} - 1}{\frac{R_p}{R} - 1} \qquad \ldots (3)$$

Also:

$$\frac{R_p}{R} = \left[\frac{\dfrac{p_c'}{\sigma_{ho}'}}{1 + \sin \phi_{PS}'} \right]^{\frac{1}{1-K_a}} \qquad \ldots (4)$$

Introducing the ratio $\frac{R_p}{R}$ from equation ... (4) into equation ... (3) one obtains:

$$\frac{p_{AV}'}{\sigma_{ho}'} = \frac{p_c'}{\sigma_{ho}' \ (1-\sin \phi_{PS}')} \cdot \frac{\left[\dfrac{p_c'}{\sigma_{ho}' \ (1+\sin \phi_{PS}')}\right]^{\omega_1} - 1}{\left[\dfrac{p_c'}{\sigma_{ho}' \ (1+\sin \phi_{PS}')}\right]^{\omega_2} - 1} \qquad \ldots (5)$$

where:

$$\omega_1 = \frac{K_a}{1-K_a} = \frac{1 - \sin \phi_{PS}'}{2 \sin \phi_{PS}'}$$

$$\omega_2 = \frac{1}{1-K_a} = \frac{2 \sin \phi_{PS}'}{1 + \sin \phi_{PS}'}$$

From equation ... (5) the following two formulae allows the evaluation of p_{AV}' in the plastic zone around the expanding cavity

$$p_{AV}' = \sigma_{ho}' + \alpha \left(p_c' - \sigma_{ho}'\right) \qquad \ldots (6a)$$

or:

$$p_{AV}' = \chi \ p_c' \qquad \ldots (6b)$$

where:

$$\chi = \frac{1}{(1-\sin \phi_{PS}')} \cdot \frac{\left[\dfrac{p_c'}{\sigma_{ho}' \ (1+\sin \phi_{PS}')}\right]^{\omega_1} - 1}{\left[\dfrac{p_c'}{\sigma_{ho}' \ (1+\sin \phi_{PS}')}\right]^{\omega_2} - 1} \qquad \ldots (7)$$

$$\alpha = \frac{\dfrac{p_c'}{\sigma_{ho}' \ (1-\sin \phi_{PS}')} \cdot \dfrac{\left[\dfrac{p_c'}{\sigma_{ho}' \ (1+\sin \phi_{PS}')}\right]^{\omega_1} - 1}{\left[\dfrac{p_c'}{\sigma_{ho}' \ (1+\sin \phi_{PS}')}\right]^{\omega_2} - 1}}{\dfrac{p_c'}{\sigma_{ho}'} - 1} \qquad \ldots (8)$$

Equations (6a) and (6b) are valid only if a plastic zone exists which means:

$$p'_c > \sigma'_{ho}(1 + \sin \phi'_{PS}) \qquad \ldots (9)$$

Otherwise one has to assume $p'_{AV} = \sigma'_{ho} = p'_o$

APPENDIX IV

DETAILS ON MANASSERO (1987) METHOD

FOR DETERMINATION OF φ FROM SBPT IN SAND

STRESS-STRAIN RELATIONSHIPS
FROM DRAINED SELF BORING PRESSUREMETER TESTS IN SAND

by

MARIO MANASSERO

DIPARTIMENTO DI INGEGNERIA STRUTTURALE DEL POLITECNICO DI TORINO

ATTO N° 6675910

ABSTRACT

A numerical method is presented in order to obtain the complete stresses and strains path during a self boring pressuremeter test (SBPT) in sand.
Plane strain conditions and a material behaviour according to Rowe's /23/24/ dilatancy theory are assumed.
The obtained results have been checked using a large number of SBPT in sand performed in a calibration chamber (CC).

RIASSUNTO

Viene illustrato un procedimento di calcolo numerico che permette di ottenere gli andamenti completi delle componenti di tensione e deformazione durante una prova di espansione eseguita con il pressiometro autoperforante (SBPT) in sabbia.
Si ipotizzano condizioni di deformazione piane ed un comportamento del materiale in accordo con la teoria della dilatanza di Rowe /23/24/.
I risultati ottenuti sono stati controllati usando numerosi SBPT in sabbia, eseguiti in camera di calibrazione (CC).

1. INTRODUCTION

The first closed form solution of an expanding cavity problem has been obtained considering a linear elastic material and small deformations (Lamé /18/).
By using this solution it is possible to find the elastic shear modulus G both from the first part of the SBPT and from an unload-reload cycle.
Solutions for a linear elastic-perfectly plastic material have been presented later by Bishop et al. /6/ for a pure cohesive soil, and by Hill /11/, Menard /19/ /20/, Cassan /8/, Salençon /25/ and Vesic /26/ for a frictional and cohesive soil.
On the basis of the above mentioned solutions, Gibson et al. /10/, Ladanyi /13/14/15/16/, Palmer /21/, Baguelin et al. /[illegible]/, Wroth et al. /27/, Hughes et al. /12/ and Robertson /22/ have presented procedures for the interpretation of pressuremeter tests, allowing the derivation of the stress-strain relationships of a soil element at the inner boundary of the expanding cavity.
The interpretation method for a pure frictional material presented in this paper is closely related to Wroth's et al. /27/ and Hughes's et al. /12/ analyses and it is based on Rowe's /23/24 dilatancy theory.

2. BASIC ASSUMPTION

The basic assumptions, used in the here presented approach, are briefly summarized in the following points

a) The particulate material surrounding the infinitely long expanding cavity deforms in plane strain conditions, i.e. the vertical strain $\varepsilon_z = 0$.

b) The principal stresses $\sigma_1, \sigma_2, \sigma_3$ are coincident with radial, vertical, hoop stresses around the cavity, $\sigma_r, \sigma_z, \sigma_\Theta$, the same applies to the strains $\varepsilon_1, \varepsilon_2, \varepsilon_3$ and $\varepsilon_r, \varepsilon_z, \varepsilon_\Theta$. In the following either subscript notations can be used.

c) Stresses and strains are positive in compression.

d) All stresses and strength parameters are in terms of effective stress.

e) The strains are considered to be completely plastic. Elastic strains are not considered.

f) Only frictional forces act at the contact points of particles (sand grains).

g) Strains due to particle crushing or plastic yield at contact points are supposed not affecting the soil behaviour in the case of the contemplated sand.

h) The hypothesis of small strains is adopted.

3. CONSTITUTIVE RELATIONSHIP

According to Rowe's /23/24/ theory, the behaviour of a particulate medium may be described by the following equation:

$$\frac{\sigma_1 d\varepsilon_1}{(\sigma_2 d\varepsilon_2 + \sigma_3 d\varepsilon_3)} = - K_p^{cv} \tag{1}$$

where:

$K_p^{cv} = \dfrac{1+\sin\phi_{cv}}{1-\sin\phi_{cv}}$: constant volume principal stress ratio coefficient;

ϕ_{cv} = constant volume friction angle

Taking into account for plain strain conditions ($d\varepsilon_2 = 0$) the eq. (1) reduces to:

$$\frac{\sigma_1}{\sigma_3} = - K_p^{cv} \frac{d\varepsilon_3}{d\varepsilon_1} \qquad (2)$$

Shear (γ) and volumetric (ε_v) strains are defined by the following:

$$\gamma = \varepsilon_1 - \varepsilon_3 \qquad (3)$$

$$\varepsilon_v = \varepsilon_1 + \varepsilon_3 \qquad (4)$$

Using this last set of equations the stress ratio (σ_1/σ_3) can be expressed also as follows

$$\frac{\sigma_1}{\sigma_3} = K_p^{cv} \frac{1 - \frac{d\varepsilon_v}{d\gamma}}{1 + \frac{d\varepsilon_v}{d\gamma}} \qquad (5)$$

The introduced relationships of the adopted constitutive model are qualitatively shown in Fig. 1.

4. CAVITY EXPANSION RELATIONSHIPS

The equations of equilibrium and compatibility of strains all around the cavity are: (see also Fig.2)

$$\frac{d\sigma_r}{dr} = \frac{\sigma_\theta - \sigma_r}{r} \qquad (6)$$

$$\frac{d\varepsilon_\theta}{dr} = \frac{\varepsilon_r - \varepsilon_\theta}{r} \qquad (7)$$

where:

σ_r, σ_θ: principal stresses (MAX and min) around the cavity (corresponding to σ_1 and σ_3)

$\varepsilon_r, \varepsilon_\theta$: principal strains around the cavity (corresponding to ε_1 and ε_3)

r : radial distance.

This last set of equations with eq. (2) described in chapter 2 allows to obtain the solution of the expanding cylindrical cavity problem (See 5th Sect.).

5. PROPOSED METHOD

Expressing the equations (6) and (7) as function of $\frac{r}{dr}$ and referring them to a generic radius r around the expanding cavity, one can write:

$$\frac{\sigma_\theta - \sigma_r}{d\sigma_r} = \frac{\varepsilon_r - \varepsilon_\theta}{d\varepsilon_\theta} \qquad (8)$$

Introducing into eq. (8):

$$\sigma_\theta = - \frac{\sigma_r}{K_p^{cv}} \frac{d\varepsilon_r}{d\varepsilon_\theta}$$

given by eq. (2) and rearranging it, one gets

$$\frac{d\sigma_r}{d\varepsilon_\theta} = - \frac{\sigma_r \left(1 + K_a^{cv} \frac{d\varepsilon_r}{d\varepsilon_\theta}\right)}{\varepsilon_r - \varepsilon_\theta} \qquad (9)$$

being : $K_a^{cv} = \frac{1}{K_p^{cv}}$

This equation of general validity can be solved for a soil element at the cavity wall where the $\sigma_r = p$ and $\varepsilon_\theta = \varepsilon$ are measured. To do this analitically, a relationship $\varepsilon_r = f(\varepsilon_\theta)$ is required (see Hughes et al. /12/), nevertheless knowing $p = F(\varepsilon)$ one can solve eq. (9) using numerical techniques, like finite difference.

6. NUMERICAL ANALYSIS

With the aim to assess the ε_r at the cavity wall through a numerical procedure, the following equations at the points (i) and (i-1) can be setup (see also Fig. 3).

$$\frac{dp}{d\varepsilon} = \frac{p(i) - p\,(i-1)}{\varepsilon(i) - \varepsilon\,(i-1)} \qquad (10)$$

$$\frac{d\varepsilon_r}{d\varepsilon} = \frac{\varepsilon_r(i) - \varepsilon_r(i-1)}{\varepsilon(i) - \varepsilon\,(i-1)} \qquad (11)$$

Introducing eqs. (10) and (11) into eq. (9), using ave rage criteria between forward and backwards interpolations tecniques and making appropriate arrangements it is obtained:

$$\varepsilon_r(i) = \frac{p(i)\left[\varepsilon(i-1)+K_a^{cv}\,\varepsilon_r(i-1)\right] - p(i-1)\,\varepsilon(i)}{2\left[p(i)\,(1+K_a^{cv}) - p\,(i-1)\right]} +$$

$$+ \frac{p(i)\left[\varepsilon(i-1)-\varepsilon_r(i-1)\right] + p(i-1)\left[\varepsilon_r(i-1)\,(1+K_a^{cv})-\varepsilon(i)\right]}{2\,K_a^{cv}\,p\,(i-1)} \qquad (12)$$

Moreover knowing that $\varepsilon_r(0)=0$, equation (12) allows to compute step by step the unknown values $\varepsilon_r(i)$ from $i = 1$ to $i = n$.

Once $\varepsilon_r(i)$, $\varepsilon(i)$, $p(i)$ and $\sigma_0(0) = p(0)$ are known, one can compute from eqs. (3) and (4) the deformation components $\gamma(i)$, $\varepsilon_v(i)$ and solving equation (2) or (5), once more with finite difference technique, the complete stress-strain curve and stress-path for the soil element at the cavity wall can be assessed.

AKNOWLEDGEMENTS

The author wishes to aknowledge Dr.P.Bertacchi and ... lotti of ENEL-CRIS - Milan, who made available the results ... SBPT's performed in the CC, used to validate the interp... method exposed in the paper.

REFERENCES

/1/ BAGUELIN, F., JÉZÉQUEL, J.F. ... "Expansion of Cylindrical Probes in Cohesive Soils", Journal of the Soil Mechanics and Foundations ... American Society of Civil Engineers, Vol. ..., No. ..., Proc. Paper 9377, (1972) November, pp. ...

/2/ BAGUELIN, F., JÉZÉQUEL, J.F. and SHIELD, ...,"The pressuremeter and foundation engineering", Series on ... and Rock Mechanics, Vol. 2, No.4, Trans Tech Publications, (1978).

/3/ BALIGH, M.M., "Cavity Expansion in Sand with Curved Envelopes", Journ. Geot. Eng. Div. ASCE, GT. 11, (1976).

/4/ BALDI ET AL., "Laboratory Validation of in-Situ Tests", Published by A.G.I. on the occasion of the ISSMFE Golden Jubilee, (1985a).

/5/ BELLOTTI,R.,BRUZZI G. and GHIONNA V.,"Design, Construction and Use of a Calibration Chamber", Proc. ESOPT II, Amsterdam, Vol. 2, (1982), pp. 439-446.

/6/ BISHOP, R.F., HILL, R.,and MOTT, N.F., "Theory of indentation and hardness tests", Proc. Phys. Soc. 57, 147, (1945).

/7/ CARTER, J.P., BOOKER, J.R.andYEUNG., S.K., "Cavity expansion in cohesive frictional soils", Geotechnique 36,No.3, (1986), pp. 349-358

[illegible] Travaux [illegible] de Belgique, Bruxelles, [illegible]

/14/ LADANYI, B., "Evaluation of Pressuremeter Tests in Granular Soils", Proceedings of the Second Pan American Conference on Soil Mechanics and Foundation Engineering, Brasil, Vol. I, (1963), pp. 3-20.

/15/ LADANYI, B., "Expansion of a Cavity in a Saturated Clay Medium", Journal of the Soil Mechanics and Foundation Division, Proceedings of the American Society of Civil Engineers, Vol. 90, No SM4, Proc. Paper 3577, (1963), July, pp. 127-161.

/16/ LADANYI, B., "In Situ Determination of Undrained Stress-Strain Behavior of Sensitive Clays with the Pressuremeter", Canadian Geotechnical Journal, Vol. 9, (1972).

/17/ LADE, P.V. and LEE, K.L. "Engineering Properties of Soils", Report, UCLA-ENG-7652, (1976), pp.145.

/18/ LAMÉ, G., "Leçons sur la théorie mathématique de l'elasticité des corps solides", Bachelier, Paris, France, (1852).

/19/ MÉNARD, L., "Mesure in situ des proprietés physiques des sols", Annales des Ponts et Chaussées, Paris, No. 14, (1957), Mai-Juin, pp. 357-377.

/20/ MÉNARD, L., "An Apparatus for Measuring the Strength of Soils in Place", Thesis, University of Illinois, (1957).

/21/ PALMER, A.C.,"Undrained plane-strain expansion of a cylindrical cavity in clay: a simple interpretation of the pressuremeter test", *Géotechnique* 22, No. 3, (1972), pp. 451-457.

/22/ ROBERTSON, P.K., "In Situ Testing of Soil with emphasis on its application to liquefaction assessment", PhD Thesis Department of Civil Engineering,Vancouver (Canada), (1982).

/23/ ROWE, P.W., "The stress-dilatancy relation for static equilibrium of an assembly of particles in contact", Proc. Royal Soc., Vol. 269, (1962), pp. 500-527.

/24/ ROWE, P.W., "Stress-Strain Relationship for Particulate Materials at equilibrium", *Proc. of the specialty* Conference on Performance of Earth and Earth-supported Structures. Purdue University, Lafayette (Indiana). Published by ASCE, (1972).

/25/ SALENÇON, J., "Expansion quasi-statique d'une cavité à symétrie *sphérique ou cylindrique dans* un milieu élasto plastique", Annales des Ponts et Chaussées, Paris, Vol. III, (1966), pp. 175-187.

/26/ VESIC, A.S., "Expansion of cavities in infinite soil mass.", J. Soil Mech. Fdns Div. Am.Soc. Civ. Engrs 98, SM3, (1972), pp. 265-290.

/27/ WROTH, C.P. and WINDLE, D., "Analysis of the pressuremeter test allowing for volume change", Technical Note, Geotechnique 25, (1975), pp. 598-610.

AD-A188 792 SELF-BORING PRESSUREMETER IN PLUVIALLY DEPOSITED SANDS 2/2
(U) CENTRO DI RICERCA IDRAULICA E STRUTTURALE MILAN
(ITALY) R BELLOTTI ET AL. JUN 87 DAJA45-84-C-0034

UNCLASSIFIED F/G 14/2 NL

END
DATE
FILMED

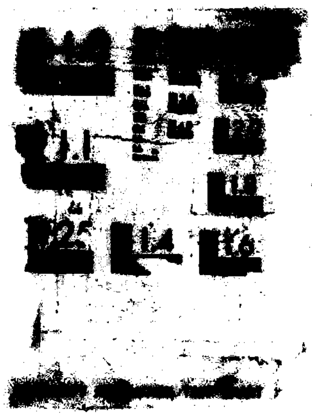

TAB. 1 - TESTED SAND SHEAR STRENGTH

TICINO SAND			
D_R (%)	ϕ_o^{TX} (°)	α (°)	R^2 (-)
45	38.2	4.2	0.67
65	40.2	6.5	0.78
85	42.9	8.1	0.89

ϕ_o^{TX}, α: parameters describing the curved strength envelopes (Baligh/3/) (*)

R^2 = correlation coefficient

D_R = average relative density of the tested specimens, at the end of consolidation

$$(*)\ \mathrm{tg}\,\phi_p^{TX} = \frac{\tau_{ff}}{\sigma_{ff}} = \left[\mathrm{tg}\,\phi_o^{TX} + \mathrm{tg}\,\alpha\left(\frac{1}{2.3} - \log_{10}\frac{\sigma_{ff}}{\sigma_o}\right)\right]$$

where:

ϕ_p^{TX} : secant peak friction angle from laboratory triaxial compression test

τ_{ff} = shear stress on the failure surface at failure

σ_{ff} = effective normal stress on the failure surface at failure

σ_o = reference stress, assumed equal to 1 Kg/cm^2 = 98.2 KPa

ϕ_o^{TX} = secant friction angle from laboratory triaxial compression test at $\sigma_{ff} = 2.72\ \sigma_o$

α = angle which describes the curvature of the failure envelope.

TAB. 2 : Experimental readings from Test N. 228

R_d N.	$-\varepsilon$ [%]	p [MPa]	R_d N.	$-\varepsilon$ [%]	p [MPa]	R_d N.	$-\varepsilon$ [%]	p [MPa]
1	0.22200	.2080	40	.34645	.4124	79	2.11714	.8243
2	.20350	.2131	41	.36219	.4164	80	2.24836	.8462
3	.20700	.2181	42	.37794	.4202	81	2.38134	.8672
4	.21225	.2232	43	.39134	.4266	82	2.51781	.8891
5	.21575	.2282	44	.42594	.4312	83	2.65953	.9118
6	.22100	.2343	45	.42168	.4349	84	2.80826	.9337
7	.22625	.2383	46	.43393	.4395	85	2.88174	.9446
8	.22974	.2444	47	.45143	.4462	86	3.03221	.9674
9	.23849	.2524	48	.45893	.4506	87	3.19143	.9901
10	.24199	.2555	49	.48117	.4543	88	3.35055	1.0139
11	.24724	.2606	50	.54591	.4709	89	3.51336	1.0319
12	.25424	.2656	51	.55991	.4755	90	3.67958	1.0558
13	.05124	.2716	52	.57216	.4801	91	3.84929	1.0777
14	.26649	.2757	53	.58366	.4847	92	4.02950	1.0996
15	.07174	.2807	54	.62130	.4893	93	4.21146	1.1216
16	.28049	.2877	55	.62115	.4948	94	4.39517	1.1444
17	.23099	.2927	56	.63690	.4994	95	4.58588	1.1664
18	.09798	.2969	57	.65440	.5050	96	4.78184	1.1883
19	.12673	.3019	58	.67189	.5096	97	4.98129	1.2111
20	.11548	.3079	59	.68939	.5133	98	5.18425	1.2339
21	.12598	.3139	60	.71039	.5206	99	5.39595	1.2558
22	.13473	.3179	61	.72613	.5234	100	5.61289	1.2795
23	.14348	.3229	62	.76453	.5335	101	5.83684	1.3032
24	.15398	.3280	63	.80312	.5437	102	6.05904	1.3241
25	.16622	.3351	64	.84511	.5556	103	6.28823	1.3468
26	.17672	.3390	65	.95884	.5804	104	6.52617	1.3686
27	.18722	.3451	66	1.00084	.5905	105	6.76586	1.3923
28	.19597	.3491	67	1.04109	.6006	106	7.01430	1.4140
29	.20997	.3562	68	1.08132	.6108	107	7.27498	1.4377
30	.22047	.3602	69	1.12507	.6209	108	7.53216	1.4584
31	.23096	.3652	70	1.16881	.6310	109	7.80334	1.4821
32	.24321	.3713	71	1.21255	.6411	110	8.07802	1.5056
33	.25546	.3763	72	1.25804	.6502	111	8.36144	1.5282
34	.26596	.3803	73	1.43301	.6888	112	8.65186	1.5499
35	.27996	.3884	74	1.53099	.7127	113	8.95103	1.5715
36	.29395	.3924	75	1.63773	.7337	114	9.26594	1.5950
37	.30795	.3984	76	1.74971	.7566	115	9.58785	1.6156
38	.32020	.4034	77	1.85593	.7795	116	9.91325	1.6391
39	.33420	.4084	78	1.98765	.8015	117	10.25265	1.6605

R_d : number of the experimental reading

ε : hoop strain at the cavity wall

p : radial stress at the cavity wall

FIG.1: Stress – strain relationships for plane strain conditions

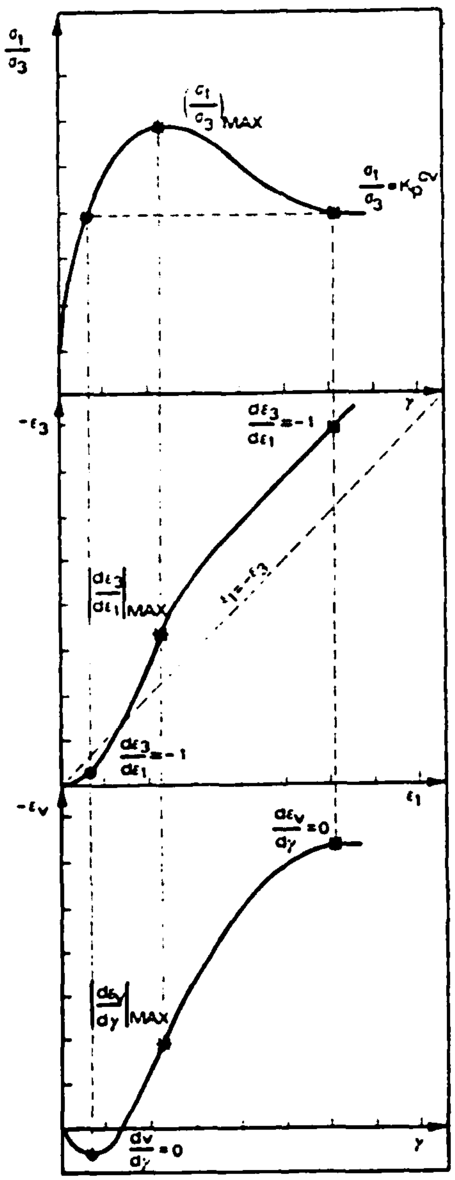

FIG.2 : Stresses and strains around the expanding cavity

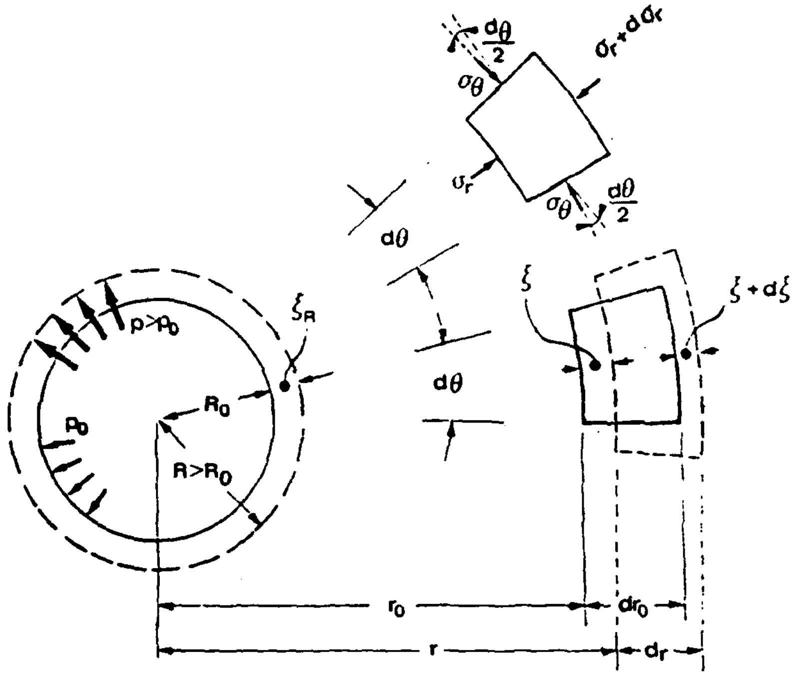

Compatibility equations

$$\begin{cases} \varepsilon_r & \text{(radial strain)} = -d\xi / d_r \\ \varepsilon_\theta & \text{(hoop strain)} = -\xi / r \end{cases}$$

At the cavity wall $\quad \varepsilon \quad$ ("cavity strain") $= -\xi_R / R_0$

Equilibrium equation

$$\frac{d\sigma_r}{dr} = \frac{\sigma_\theta - \sigma_r}{r}$$

FIG. 3: Use of pressuremeter curve for numerical analysis

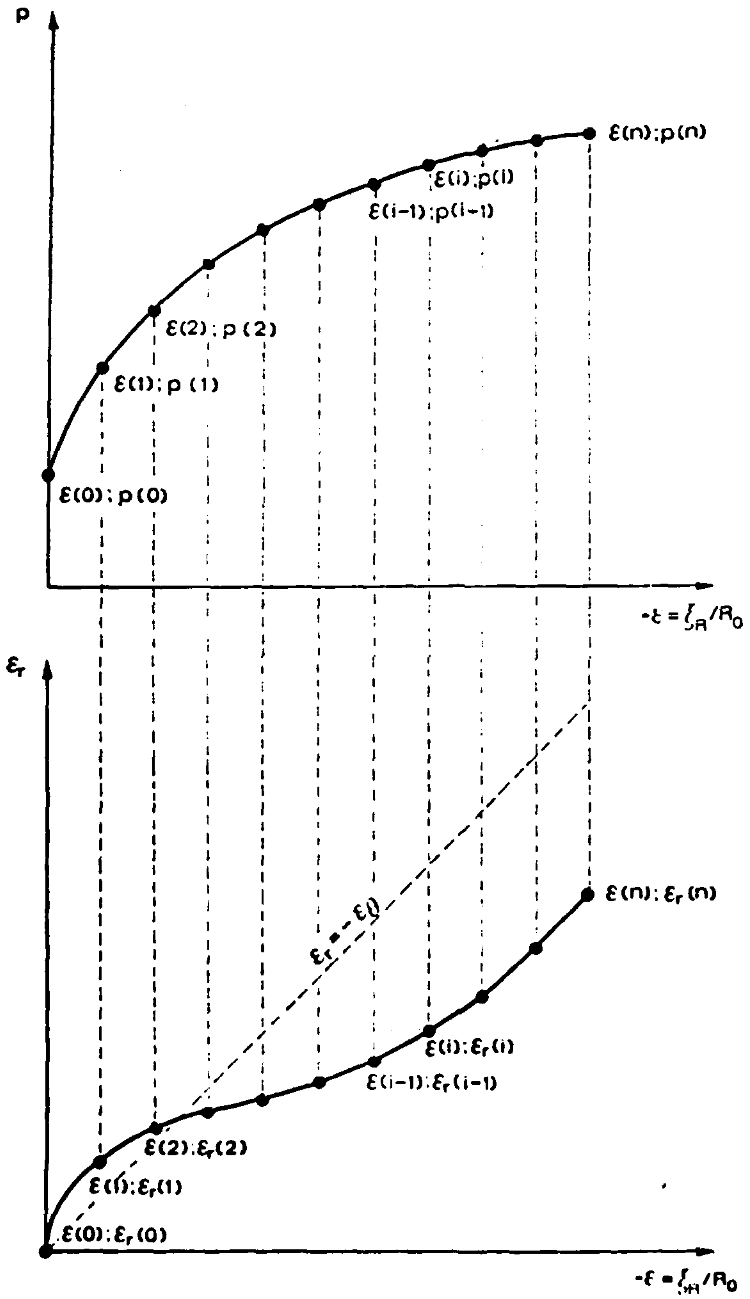

FIG. 4 : Characteristics of the tested sand

SAND	1.2-TICINO
DOMINANT MINERAL	QUARTZ(30)
ANGULARITY (LEE'S CHART)	8÷9
MICA	~5%
γ_{max} (t/m^3)	1] 1.705 2] 1.700
γ_{min} (t/m^3)	1] 1.398 2] 1.391

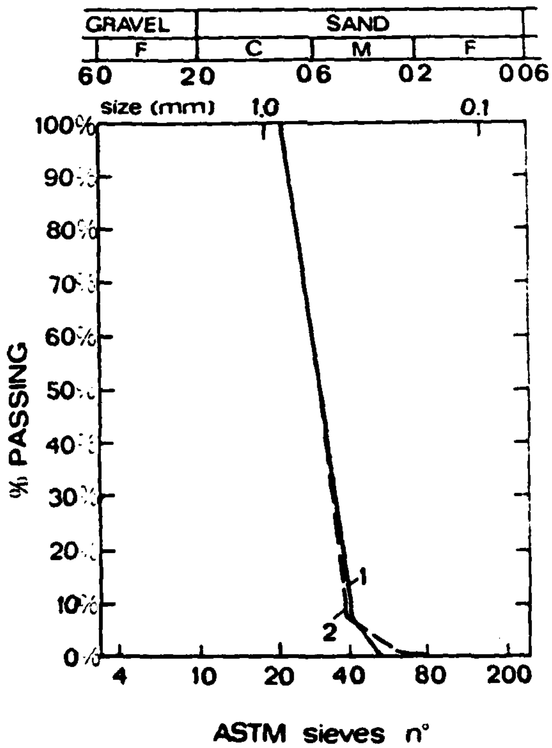

FIG.5: Stress / strain relationships using the experimental readings from test N: 228 (D_R = 77.0 %)

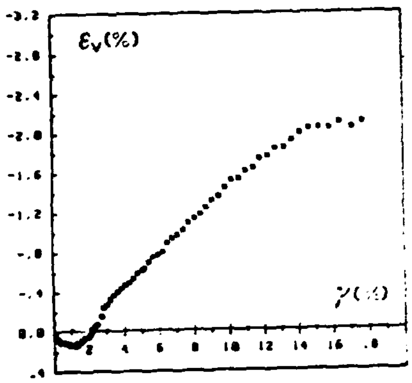

a) Volumetric strain vs shear strain

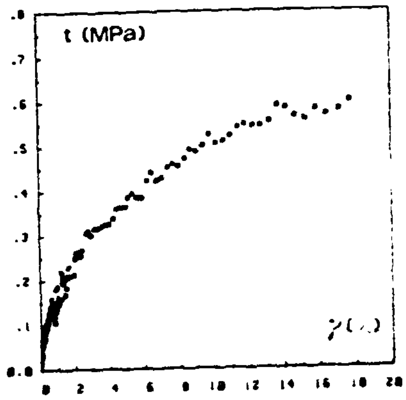

b) Shear stress vs shear strain

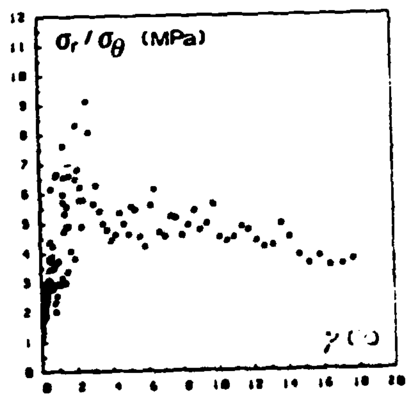

c) Stress ratio vs shear strain

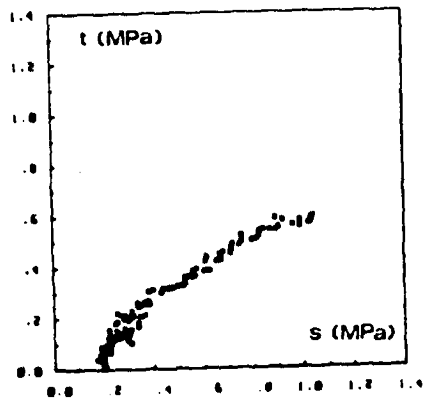

d) Shear stress vs mean normal stess

FIG. 6 : Curve fitting results with 7th polynomial degree in original p vs ε plot

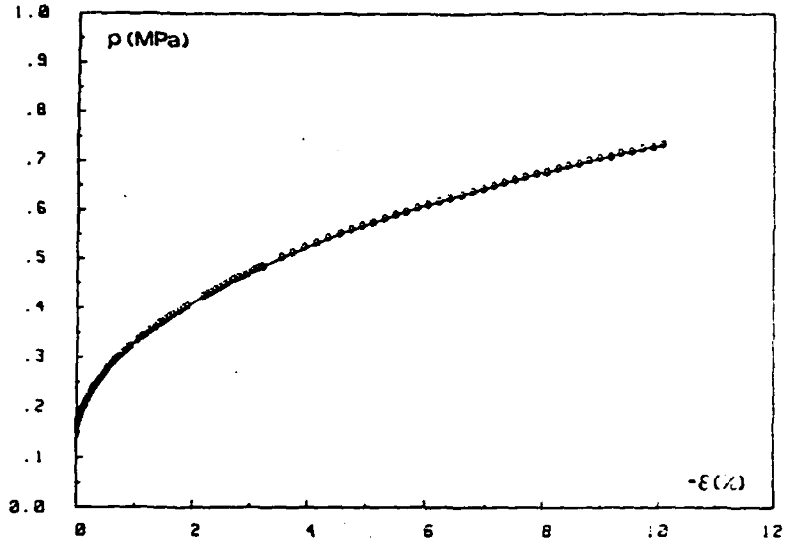

a) Test N. 222

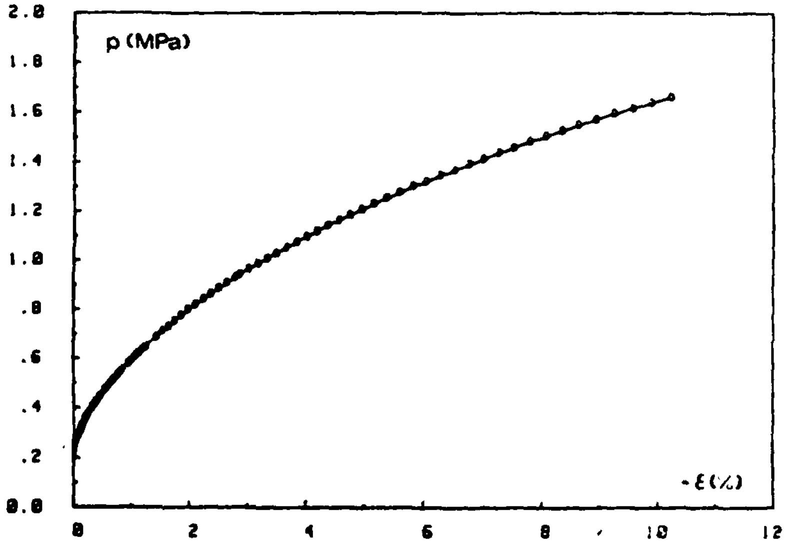

b) Test N. 228

FIG.7 : Stress ratio - strain curve for 5th, 7th and 9th degree polynomials (Test N. 228)

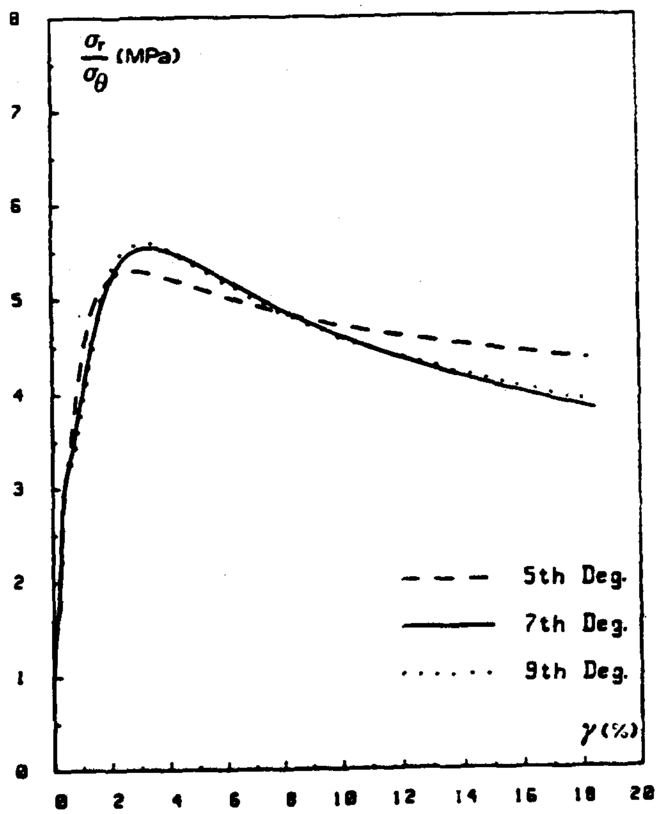

FIG.8 : Stress / strain relationships from test N°222 (D_R = 46.2%)

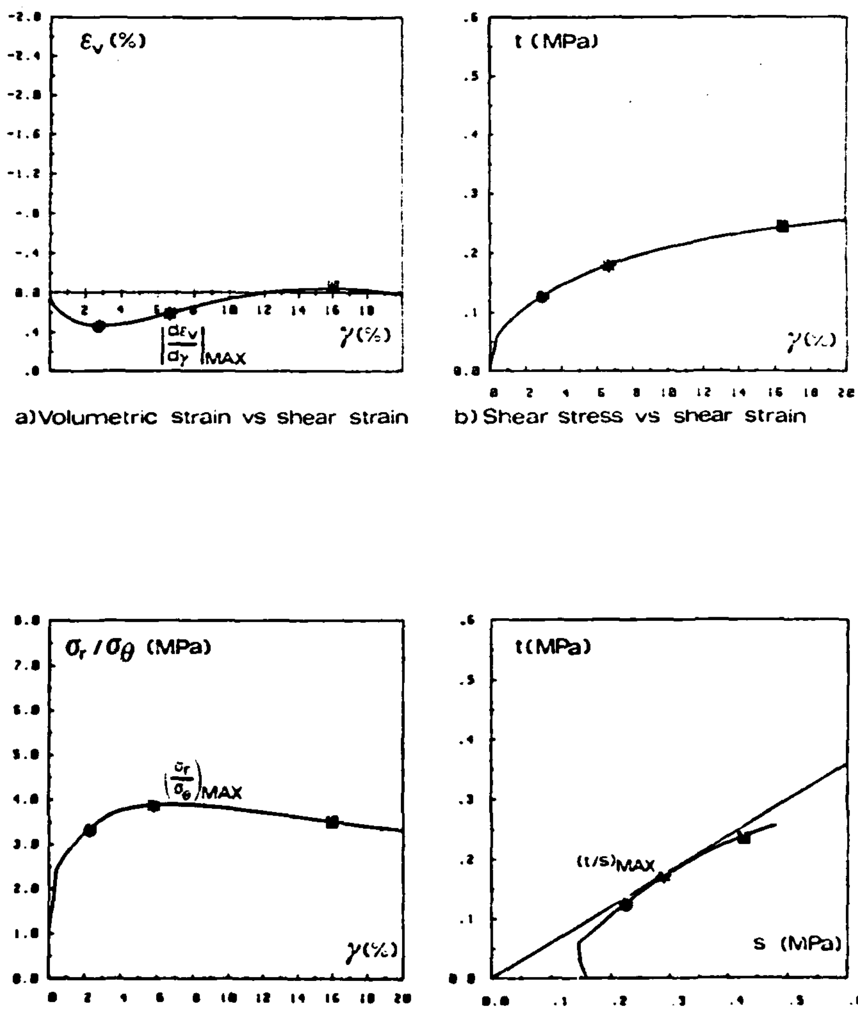

a) Volumetric strain vs shear strain

b) Shear stress vs shear strain

c) Stress ratio vs shear strain

d) Shear stress vs mean normal stress

FIG.9 : Stress / strain relationships from test N. 228 (D_R = 77.0 %)

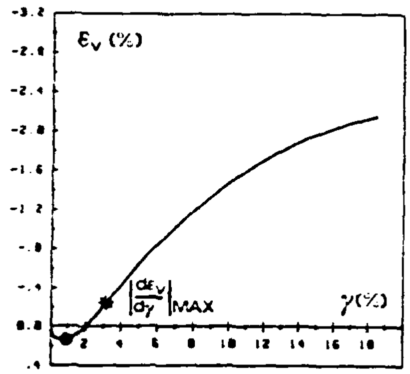

a) Volumetric strain vs shear strain

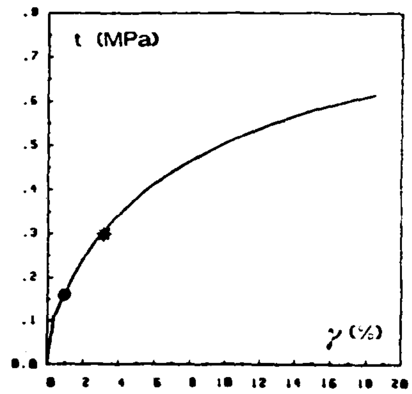

b) Shear stress vs shear strain

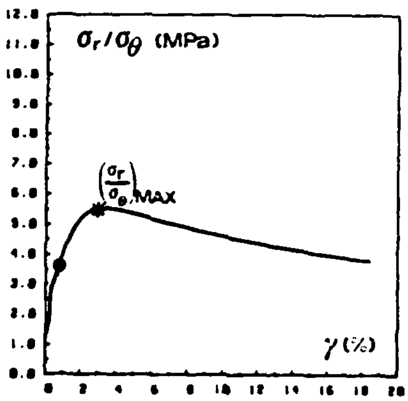

c) Stress ratio vs shear strain

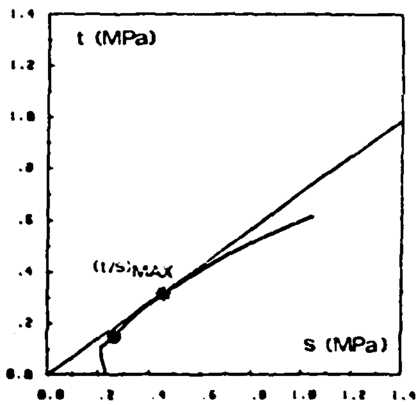

d) Shear stress vs mean normal stress

END

DATE

FILMED

3 88